ISSN 2461-4254

EUREKA:

PHYSICS AND ENGINEERING

- Chemical Engineering
- Chemistry
- Computer Science
- Earth and Planetary Sciences
- Energy
- Engineering
- Materials Science
- Mathematics
- Physics and Astronomy

Volume 2(21)
2019

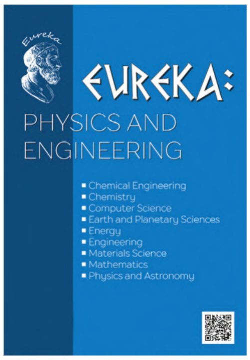

SCIENTIFIC JOURNAL

EUREKA: Physics and Engineering – scientific journal whose main aim is to publish materials allowed to see ***new discoveries at the intersection of sciences.***

- Chemical Engineering
- Chemistry
- Computer Science
- Earth and Planetary Sciences
- Energy
- Engineering
- Material Science
- Mathematics
- Physics and Astronomy
- Technology Transfer

EUREKA: Physics and Engineering
publishes
4 types of materials:
– review article,
– progress reports,
– original Research Article
– reports on research projects

PUBLISHER OÜ «Scientific Route»
European Union
Editorial office
«EUREKA: Physical Sciences and Engineering»
Narva mnt 7-634, Tallinn, Eesti
Harju maakond, 10117
Tel. + 372 602-7570
e-mail: info@eu-jr.eu
Website: http://eu-jr.eu

CONTENT

Original Research Article: full paper

(2019), «EUREKA: Physics and Engineering»
Number 2

MODELING OF THE INTELLECTUAL SYSTEM'S WORK FOR SUPPORTING DECISIONS MAKING ON TECHNICAL REGULATION IN BUILDING UNDER UNCERTAINTY CONDITIONS

Dmytro Isaienko
Confederation of Builders of Ukraine
4 Bekhterevsky lane, Kyiv, Ukraine, 04053
d.isaenko@ukr.net

Volodymyr Scochko
Department of Architectural Structures
Kyiv National University of Construction and Architecture
31 Povitroflotsky ave., Kyiv, Ukraine, 03037
vladimir.and.friends@gmail.com

Abstract

The main aim of the work is to elaborate algorithms and structure of data of the intellectual system of decisions making, able to provide functioning of the organizational-technical system of technical regulation in building under uncertainty conditions. The ability of intellectual systems to function under uncertainty conditions of different types is provided by using methods of indistinct mathematics and organization of a data structure, formed for revealing uncertainty automatically. The main attention in the article is paid to forming a data structure and algorithm for revealing uncertainty, caused by excessive information. The material of the research is information, contained in normative documents, according to which the technical regulation of the Ukrainian building branch is realized. It is especially urgent to reveal conflicts of parameters and rules, connected with reformation of the legislation in a part, related to the technical regulation of the branch. The automatic revelation of uncertainty that results in a discordance or conflict of parameters and rules, essentially facilitates elaboration of project documents and realization of expert evaluations at stages of building and exploitation of unique objects. But introduction of such intellectual systems allows to raise a speed and reliability of the work of other systems of the documents' circulation under transformation conditions essentially. The scientific novelty of the work is in using models of indistinct mathematics at formalizing norms and rules of the technical regulation in building and elaborating methods of their processing by the intellectual system of making decisions. The results of the work are demonstrated on the example of determination of a technical regulation parameter at excessive information, manifested in the presence of more than one normative document with instructions for determination of one regulation parameter. The probation and adaptation of norms and rules are realized in the legislative regulation of the activity in the Ukrainian building branch under conditions of changes, directed on improving the city-planning activity according to world standards.

Keywords: building branch, conflict of rules, data processing, organizational-technical system, technical regulation.

DOI: 10.21303/2461-4262.2019.00866

1. Introduction

One of most urgent problems in the branch of technical regulation in building and architecture is the presence of conflicts in instructions and principles of determining calculating regulation parameters. Such problem appears at transforming the organizational-technical system of technical regulation, connected with the transfer from a prescribing method of standardization to a parametric one. The accumulation of problems, connected with changes in standardization and regulation of licensing-conciliatory procedures in building according to world standards, favors [1, 2]:

– the growth of the demand for unique buildings and edifices;

– the change of requirements to influences on the external environment and priorities at forming the living environment;

– the introduction of changes to some legislative acts;

– the change of the raw material base for building materials;

– the development of designing and building technologies.

At that different types of uncertainty appear that result in a necessity to create additional normative documents for explaining an order of actions in a case of uncertainty. Their accumulation complicates the process of technical regulation in whole and may cause conflicts of parameters and rules in the building branch.

2. Aim of research

It is modeling of the work of the intellectual system for supporting decisions making, able to provide functioning of the organizational-technical system of technical regulation under uncertainly conditions, caused by excessive information.

3. Materials and methods of research

The material of the research is information, contained in normative documents, according to which the technical regulation of the building branch is realized.

The analysis of the modern condition of the organizational-technical scheme of technical regulation in the Ukrainian building branch has demonstrated that the system of existent norms and rules of this branch contains different types of uncertainty [2, 3]. Causes of appearing, mathematical models and methods, which algorithms of the work of supporting systems for decisions making are based on, may be different and depend on an uncertainty type.

The classification of uncertainty of norms and rules for the technical regulation in the building branch by the type of existent information is demonstrated on **Fig. 1**.

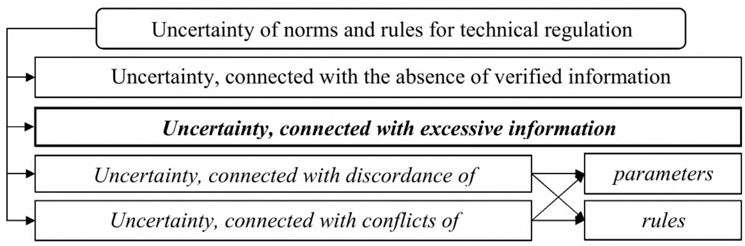

Fig. 1. Classification of uncertainty by the type of existent information

Uncertainty, connected with excessive information is in the absence of instructions for determining some regulation parameters or realization principles of procedures and operations in different normative documents.

The elaboration of methods and algorithms of the automatic revelation of conflict norms and rules at forming project documents, maintenance of building and exploitation of objects needs a correspondent understanding, systematization and structurization of documents.

Models and methods of indistinct mathematics are used in the work for solving the problem of the adequate presentation of norms and rules [4, 5].

In the first turn each element of the set of documents, destined for the technical regulation of a certain direction of the building branch's activity, is formalized as the vector:

$$\{A\}^T = \{A_j\} = \{A_1, A_2, ..., A_n\}. \tag{1}$$

Each coordinate A_j (j=1,…, n) of which corresponds to one normative document, n – number of documents; T – transposition operation.

After that the set of conflict norms and rules, in further subjected to decomposition and comparison, is taken from the set of formalized documents [3]. But work [3] pays the main attention to the problem of overcoming uncertainty, connected with rules that have identical conditions and different conclusions.

This work is devoted to the processing of uncertainty, connected with the presence of procedures and operations for determining one parameter in more than one normative document. For realizing the procedure of selection of the set of uncoordinated or conflict norms and rules, the regulation parameters are given as the vector {B}:

$$\{B\}^T = \{B_i\} = \{B_1, B_2, ..., B_m\}, \quad (2)$$

where m – number of correspondent parameters.

Each element of the vector {B} corresponds to one calculating value or one rule of the technical regulation.

For realizing fast algorithms for searching for information in the set of documents {A}, according to which {B} parameters are determined, data (1), (2) are structured in **Table 1** [6–8].

Table 1

Fragment of the data structure of the technical regulation system

D	A_1	A_1	…	A_n
B_1	$B_1 \vee 0$	$B_1 \vee 0$	…	$B_1 \vee 0$
B_2	$B_2 \vee 0$	$B_2 \vee 0$	…	$B_2 \vee 0$
…	…	…	…	…
B_m	$B_m \vee 0$	$B_m \vee 0$	…	$B_m \vee 0$

Each line of **Table 1** contains one parameter B_i of the certain direction, each column A_j corresponds to the normative document that includes the set of parameters B_i, and symbol «∨» means the operation of disjunction – «or».

The systematization of information is realized according to the priority PA_j of the determining rule or calculating method of the parameter B_i in documents A_j, established based on ranging results [9]:

$$PA_{i,1} < \dots < PA_{i,a-1} < PA_{i,a}$$

or

$$PA_{i,1} > PA_{i,2} > \dots > PA_{i,a}. \quad (3)$$

If documents have the same priority at that:

$$PA_{i,1} < \dots < PA_{i,a-1} = PA_{i,a}$$

or

$$PA_{i,1} = PA_{i,2} > \dots > PA_{i,a}. \quad (4)$$

Ranging results are subjected to the expert thought.

The information, contained in **Table 1** may be represented as the matrix [K], each element of which is found according to [9]:

$$K_{i,j} = \begin{cases} 1 \to D_{i,j} = B_j \\ 0 \to D_{i,j} = 0 \end{cases} \quad (i = 1, 2, ..., m; j = 1, 2, ..., n). \quad (5)$$

That is:

– «1» – if the element $D_{i,j}$ in the matrix D equals B_i;

– «0» – if the element $D_{i,j}$ in the matrix D equals null.

The symbol «→» means implication (logic conclusion).

If the normative base, responsible for the technical regulation, is perfect, the matrix [K]:

$$K = \begin{pmatrix} K_{1,1} & \cdots & K_{1,n} \\ \vdots & \ddots & \vdots \\ K_{m,1} & \cdots & K_{m,n} \end{pmatrix} = \begin{pmatrix} 1 \vee 0 & \cdots & 1 \vee 0 \\ \vdots & \ddots & \vdots \\ 1 \vee 0 & \cdots & 1 \vee 0 \end{pmatrix}. \quad (6)$$

Must correspond to conditions [9]:

1. The sum of elements of each line of the matrix [K] doesn't exceed 1:

$$a = \sum_{j=1}^{n} K_{i,j} \le 1, \ (i = 1, 2, \cdots m). \quad (7)$$

2. The sum of the elements of each column of the matrix [K] doesn't exceed the number of the technical regulation parameters m:

$$b = \sum_{i=1}^{m} K_{i,j} \le m, \ (i = 1, 2, \cdots m). \quad (8)$$

3. The sum of all elements of the matrix [K] doesn't exceed the number of the technical regulation parameters m:

$$c = \sum_{i=1}^{m} \sum_{j=1}^{n} K_{i,j} \le m. \quad (9)$$

If one of conditions (7)–(9) is not satisfied, the set of normative documents contains conflicts that may cause problems and mistakes at solving problems of the technical and juridical type [10, 11].

3. 1. Calculating experiments

One of main indicators of uncertainty, connected with excessive information is breaking of condition (7). Just this condition indicates the presence of several independent methods of fixing or calculation of a technical regulation parameter, determined by more than one normative document. Such situation complicates the work of the system and may cause a conflict of parameters or rules.

The problem is solved by revealing and excluding excessive information or coordinating conflict one and provides realization of the algorithm:

1) to establish the priority of documents A_j, according to which the parameter B_i is found;
2) to involve experts, if documents with the same priority are present that is reflected by (4);
3) to reflect the priority of the parameters as the dependence:

$$B_i = f(B_1, B_2, \ldots B_{j-1}, B_j, B_{j+1} \ldots, B_r), (j \ne i; j = 1, 2, \ldots r_{i,j}).$$

1. To structure the data as **Fig. 2**.

PD	A_1	A_2	A_3	
B_1	B_1=const$_1$	0	0	
B_2	$B_2=f(B_1)$	0	0	
B_3	0	0	$B_3=f(B_1,B_2,B_4)$	
B_4	0	B_4=const$_4$	0	
B_5	B_5=const$_5$	0	$B_5=f(B_1,B_2,B_3,B_4)$	Conflict!

Fig. 2. Example of the table of the ranging priority reflection

2. To replace determination procedures of the conflict parameter or rule by a reference to more priority document.

Fig. 2 demonstrates the example of the ranging documents' priority refection (PD), determined in p. 1 by rule (3), and cursors show the determination succession of the technical regulation parameters and the conflict of rules for determining the parameter B_5.

The scheme of revelation of excessive information and solution of conflicts of parameters and rules in documents, according to which the technical regulation in the building branch is realized, is presented on **Fig. 3.**

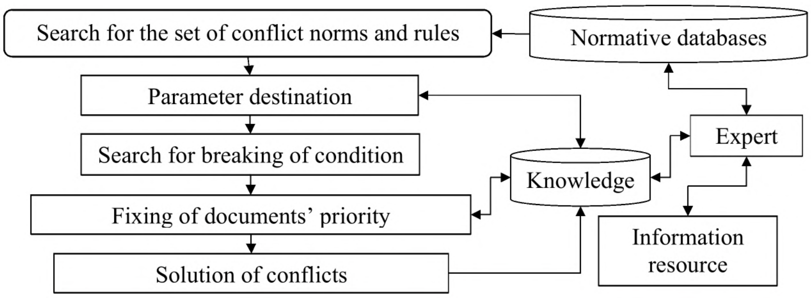

Fig. 3. Scheme of revelation of excessive information and solution of conflicts

At solving a conflict for determining a parameter, the most priority document is selected.

4. Results

The logic of the system of decisions making that functions at the presence of excessive information by the described algorithm is presented on the example, reflected on **Fig. 2**. The last line of the table doesn't satisfy condition (7). It means that there is a necessity to correct one of the normative documents A_1 or A_3. At that it must be understood what corrections must be introduced in the technical regulation system for determining or calculating the parameter B_5.

It is logical to exclude the parameter B_5 from the document A_1, because in the document A_3 this parameter is determined based on the functional dependence on all 4 other parameters of technical regulation B_1, B_2, B_3 and B_4, whereas in the document A_1 this parameter is determined forcedly. But logical considerations are insufficient in such cases.

The numerical analysis of the technical regulation parameters with a possibility to compare the correspondent parameters is based on the processed matrix [L]:

$$L=\begin{pmatrix} L_{1,1} & \dots & L_{1,n} \\ \vdots & \ddots & \vdots \\ L_{m,1} & \dots & L_{m,n} \end{pmatrix}=\begin{pmatrix} (r_{1,1})\vee 1\vee 0 & \dots & (r_{1,n})\vee 1\vee 0 \\ \vdots & \ddots & \vdots \\ (r_{m,1})\vee 1\vee 0 & \dots & (r_{m,n})\vee 1\vee 0 \end{pmatrix}. \tag{10}$$

The elements of the matrix [L] are determined as following:

$$L_{i,j}=\begin{cases} 1, & \rightarrow \quad D_{i,j}=\mathrm{const}_i, \\ r_{i,j}+1, & \rightarrow \quad D_{i,j}=f(B_1,B_2,\dots B_{k1},B_k,B_{k+1}\dots,B_r)_i, \\ 0, & \rightarrow \quad D_{i,j}=0, \end{cases} \begin{pmatrix} i=1,2,\cdots m; \\ j=1,2,\cdots n; \\ i\neq k=1,2,\cdots r_{i,j} \end{pmatrix}. \tag{11}$$

For the example from **Fig. 2**, the values $r_{i,j}$, are:

1) $r_{1,1}=1$, because $B_1=\mathrm{const}_1$;
2) $r_{2,1}=1+1=2$, because $B_2=f(B_1)$;
3) $r_{5,1}=1$, because $B_5=\mathrm{const}_5$;
4) $r_{4,2}=1$, because $B_4=\mathrm{const}_4$;
5) $r_{3,3}=3+1=4$, because B3=$f(B_1, B_2, B_4)$;
6) $r_{5,3}=4+1=5$, because $B_5=f(B_1, B_2, B_3, B_4)$.

After the substitution and exclusion from data, excessive as to the parameter B_5 with the priority $r_{5,1}$=1 ($r_{5,1}$<$r_{5,3}$) the matrix [L] looks as:

$$L=\begin{pmatrix}1&0&0\\2&0&0\\0&0&0\\0&0&4\\0&1&0\\1&0&5\end{pmatrix}=\begin{pmatrix}1&0&0\\2&0&0\\0&0&4\\0&1&0\\0&0&5\end{pmatrix}=[L'], \qquad (12)$$

where $[L']$ – corrected matrix, each element of which forms by the principle:

$$L'_{i,j}=\begin{cases}L_{i,j}, & \to \quad L_{i,j}>L_{i,k},\, j\neq k=1,2,\ldots j-1, j-1,\ldots n;\\ 0, & \to \quad L_{i,j}<L_{i,k},\, j\neq k=1,2,\ldots j-1, j-1,\ldots n;\end{cases}\begin{pmatrix}i=1,2,\cdots m;\\ j=1,2,\cdots n\end{pmatrix}, \qquad (13)$$

Now the matrix $[L']$, in general looks as:

$$[L']=\begin{pmatrix}L'_{1,1}&\ldots&L'_{1,n}\\ \vdots&\ddots&\vdots\\ L'_{m,1}&\ldots&L'_{m,n}\end{pmatrix}=\begin{pmatrix}L_{1,1}\vee 0&\ldots&L_{1,n}\vee 0\\ \vdots&\ddots&\vdots\\ L_{m,1}\vee 0&\ldots&L_{m,n}\vee 0\end{pmatrix}. \qquad (14)$$

Form (14) may be used for determining the global priority of the technical regulation parameters. For that it is necessary to calculate the sums of the lines of the matrix $[L']$, and to form the priority vector {PB}:

$$\{PB\}^T=\{PB_1 \quad PB_2 \quad \cdots \quad PB_m\}, \qquad (15)$$

where

$$PB_i=\sum_{j=1}^{n}L'_{i,j},\,(i=1,2,\cdots m). \qquad (16)$$

Especially, for matrix (12) the vector {PB} looks as:

$$\{PB\}^T=\{1 \quad 2 \quad 4 \quad 1 \quad 5\}. \qquad (17)$$

After forming the vector {PB} and sorting the elements of the matrixes [K] and $[L']$, it becomes possible to range the technical regulation parameters.

The result of the described transformations is the vector {PB*} and matrixes [K*] and [L*]:

$$\begin{matrix}PB^*_1 & & PB^*_{m-1} & & PB^*_m, & & PB^*_1 & & PB^*_2 & & & & PB^*_m,\\ \{K^*\}_1 & <\cdots< & \{K^*\}_{m-1} & < & \{K^*\}_m, & \text{or} & \{K^*\}_1 & > & \{K^*\}_2 & >\cdots> & & & \{K^*\}_m,\\ \{L^*\}_1 & & \{L^*\}_{m-1} & & \{L^*\}_m, & & \{L^*\}_1 & & \{L^*\}_2 & & & & \{L^*\}_m.\end{matrix} \qquad (18)$$

At that functional connections of the "bottom-up" type will not appear in the tables "D" and "PD".

After sorting by growth, formulas (17) and (12) look as:

$$\{PB^*\}^T=\{1 \quad 1 \quad 2 \quad 4 \quad 5\} \qquad (19)$$

and

$$L^{*}=\begin{pmatrix}1&0&0\\0&1&0\\2&0&0\\0&0&4\\0&0&5\end{pmatrix}. \qquad (20)$$

It must be noted, that at excluding some conflict technical regulation parameter from one document, it is necessary to analyze conditions and recommendations, present in less priority one. Such analysis prevents the unreasonable shift of instructions to more priority document that may result in losing a content or distinctness of information. At that the correction of both conflict documents may result in contradictions jut in more priority document.

Just that is why step 5 of the algorithm of the revelation and exclusion of excessive information of coordination of conflict one are left for experts at this stage of elaborating the system.

5. Conclusions

1. The use of models and methods of indistinct mathematics at formalizing documents gives a possibility to improve the work of the organizational-technical system of technical regulation at the expanse of automation of text information processing.

2. The offered matrix data structure facilitates the procedure of searching for excessive information in documents on technical regulation in the building branch.

3. The algorithm of revelation and solution of conflicts is grounded on comparison of the documents' priority. Just that is why further researches are planned to be devoted to the analysis of algorithms for searching and sorting text information.

References

[1] Regulation (EU) No 305/2011 of the European Parliament and of the Council of 9 March 2011 laying down harmonised conditions for the marketing of construction products and repealing Council Directive 89/106/EEC Text with EEA relevance.

[2] Isayenko, D. V. (2017). Zakonodavche rehulyuvannya diyal'nosti v budivel'niy haluzi. Osoblyvosti svitovoho dosvidu ta Yevropeys'koho pidkhodu dlya vyznachennya priorytetiv pry formuvanni zhyttyevoho. Budivel'ne vyrobnytstvo, 63, 11–15.

[3] Isaienko, D., Ploskyi, V., Terenchuk, S. (2018). Formation of the fuzzy knowledge of the knowledge support system for decision-making technical regulation of construction activity. Management of Development of Complex Systems, 35, 168–174.

[4] Terenchuk, S., Pashko, A., Yeremenko, B., Kartavykh, S., Ershova, N. (2018). Modeling an intelligent system for the estimation of technical state of construction structures. Eastern-European Journal of Enterprise Technologies, 3 (2 (93)), 47–53. doi: http://doi.org/10.15587/1729-4061.2018.132587

[5] Kulikov, P., Ploskiy, V., Skochko, V. (2014). The Principles of Discrete Modeling of Rod Constructions of Architectural Objects. Motrol, 16 (8), 3–10.

[6] Thomas, H., Leiserson, C. E., Rivest, R. L., Stein, C. (2003). Introduction to Algorithms. Cambridge: MIT Press.

[7] Graybill, F. A. (1969). Introduction to matrices with applications in statistics. Belmont: Wrels Worth Publishing Company, Inc., 372.

[8] Skochko, V., Ploskyi, V. (2018). Morphogenesis and adjustment of flat rod structures. USEFUL Online Journal, 2 (2), 8–26. doi: http://doi.org/10.32557/useful-2-2-2018-0002

[9] Kuprenas, J. A. (2003). Implementation and performance of a matrix organization structure. International Journal of Project Management, 21 (1), 51–62. doi: http://doi.org/10.1016/s0263-7863(01)00065-5

[10] Skochko, V. (2018). Determination of support reactions of rod constructions obtained by morphogenesis. USEFUL Online Journal, 2 (3), 29–42. doi: http://doi.org/10.32557/useful-2-3-2018-0005

[11] Laslo, Z., Goldberg, A. I. (2008). Resource allocation under uncertainty in a multi-project matrix environment: Is organizational conflict inevitable? International Journal of Project Management, 26 (8), 773–788. doi: http://doi.org/10.1016/j.ijproman.2007.10.003

Original Research Article: full paper

(2019), «EUREKA: Physics and Engineering» Number 2

INTRODUCTION OF CLUSTERIZATION PRINCIPLES IN THE SOLUTION OF PROBLEMS OF ENERGY EFFICIENCY AND ECOLOGICAL SAFETY OF THE EXISTENT BUILDING FUND

Serhii Kozhedub
Department of Architectural Constructions
Kyiv National University of Construction and Architecture
31 Povitroflotsky ave., Kyiv, Ukraine, 03037

Maksym Mykytas
Department of Architectural Constructions
Kyiv National University of Construction and Architecture
31 Povitroflotsky ave., Kyiv, Ukraine, 03037

Vitalii Ploskyi
Department of Architectural Constructions
Kyiv National University of Construction and Architecture
31 Povitroflotsky ave., Kyiv, Ukraine, 03037

Bohdan Yeremenko
Department of Information Technology Design and Applied Mathematics
Kyiv National University of Construction and Architecture
31 Povitroflotsky ave., Kyiv, Ukraine, 03037

Abstract

The aim of the work is to introduce clusterization principles in the solution of problems of energy efficiency and ecological safety of the existent building fund. The material of the research is the process of modeling of energetically effective architecture-building clusters. In this sense it is topical and expedient to elaborate technologies and schemes, able to support making decisions as to the formation of energetically effective architecture-building clusters. The main attention is paid to the solution of infrastructure problems of energy saving of the architecture-building branch, connected with the absence of universal models, distinct algorithms of the formation of energy efficiency clusters and reliable instruments of their activity optimization. But realization of advantages of energy efficiency clusters is possible only at introducing effective mechanisms of the formation of a structure, able to provide a result, optimal by an energy efficiency criterion. The work offers a scheme of the formation process of such structure. The synthesis of models of energetically effective architecture-building clusters is based on principles of the systemic construction of geometric models and provides the imitative modeling of different development scenarios of synthesized clusters. At this stage of the research a function of making decisions as to the real cluster formation is left for experts. But an algorithm of the synthesis of models provides the formation of a knowledge base that will be in further a base of an "internal model" of the intellectual system of supporting decisions making, elaborated for modeling cluster structures. The scientific novelty of the work is in the elaboration of theoretical bases of the technology of coordinating the structure with object properties.

Keywords: energy effective architecture-building cluster, energy- reconstruction, energy saving.

DOI: 10.21303/2461-4262.2019.00865

1. Introduction

The increase of energy efficiency of existent buildings and introduction of arrangements of energy saving, effective use of fuel-energetic resources, renewable energy sources and alternative fuel types are main priorities of any state. But as opposite to innovative solutions, introduced in new building or capital reconstruction of buildings, projects on local energy-reconstruction have a partial effect. Element by element energy-reconstruction, thermo-modernization or other arrangements of raising the energy efficiency to integral property complexes, placed at a separate territory, provided with autonomous engineer communications and energy supply, is not rational [1–3].

Such complexes as architecture-building clusters are complicated systems. System properties of cluster structures determine their additional potential, but often become a cause of inadequacy of developed models, for prospective planning and elaboration of a development strategy for clusters [4, 5].

Just that is why, the elaboration of methods and means of modeling clusters and scientific substantiation of choosing a structure of energetically effective architecture-building clusters remain an urgent scientific problem, which solution has an essential economic and scientific potential [6, 7].

2. Aim of research

The aim of the work is to introduce clusterization principles in the solution of problems of energy efficiency and ecological safety of the existent building fund by elaborating means and methods of the synthesis of models of energetically effective architecture-building clusters.

3. Research materials and methods

The classic approach to the synthesis (construction) of a model of any system provides the transfer from setting an "aim" to making "functions" and determining a "structure" that contains a final set of functional units and relations between them [8].

The material of the research is the process of modeling of energetically effective architecture-building clusters (EABC). An energetically effective architecture-building cluster consists of target objects and target organizations.

Target objects in this work are considered as complexes of buildings and edifices of different organizations that plan the formation of an energetically effective cluster on the base of the existent building fund by energy-reconstruction.

Such target objects are complicated systems that usually:

– Consist of buildings of different functional destinations;

– Buildings of one functional destination are erected in different times of different building materials and belong to different construction types;

– Compactly placed at limited territories;

– Function under different conditions.

The aim of clusterization (target function) of such objects is to decrease volumes of consumed energy at the expanse of saving energy resources. The target function may be achieved by optimizing the distribution of energy resources, thermo-modernization and other energetically effective arrangements, which realization is provided by different target organizations.

Thus, requirements to the structure of energetically effective architecture-building clusters depend on many factors. Additional conditions and limitations are set at forming a database and are usually connected with:

– Location at historical zones of cities, which are a historical heritage;

– A schedule of functioning of bureaucratic institutions that influences building works planning.

Earlier [8, 9] studied methods of forming a database of criteria, system signs, structural and functional connections between clusterization subjects, and also requirements that must be satisfied by energetically effective cluster structures of the building branch [9, 10] described in detail the process of elaborating mathematical instruments for modeling a cluster structure, optimal by energy efficiency parameters. This work is devoted to the transfer from the conceptual modeling to the elaboration of an intellectual system of supporting decisions making as to the formation of a real cluster structure.

Fig. 1 demonstrates the conceptual scheme of the elaboration of methodological principles of the introduction of energetically effective clusters' models in the building branch with a list of the model and methods, expedient to be used at different elaboration stages. At that the following abbreviations are accepted: GM – geometrical modeling; EE – expert evaluation; EM – evolution modeling; EMM – economic-mathematical modeling; NM – non-distinct models; SA – system analysis; SD – system dynamics; SC – system construction; ANN – artificial neuron networks.

The algorithm of EABC modeling (**Fig. 1**) is based on the methods of system geometric modeling. These methods form by the inductive-reductive scenario as a result of the counter comparison of data about subsystems of an object, the system of ideas about a modeling object and purpose-oriented construction of methods of geometric modeling (GM). The method and set of operations, used at realizing the algorithm are described in [11, 12].

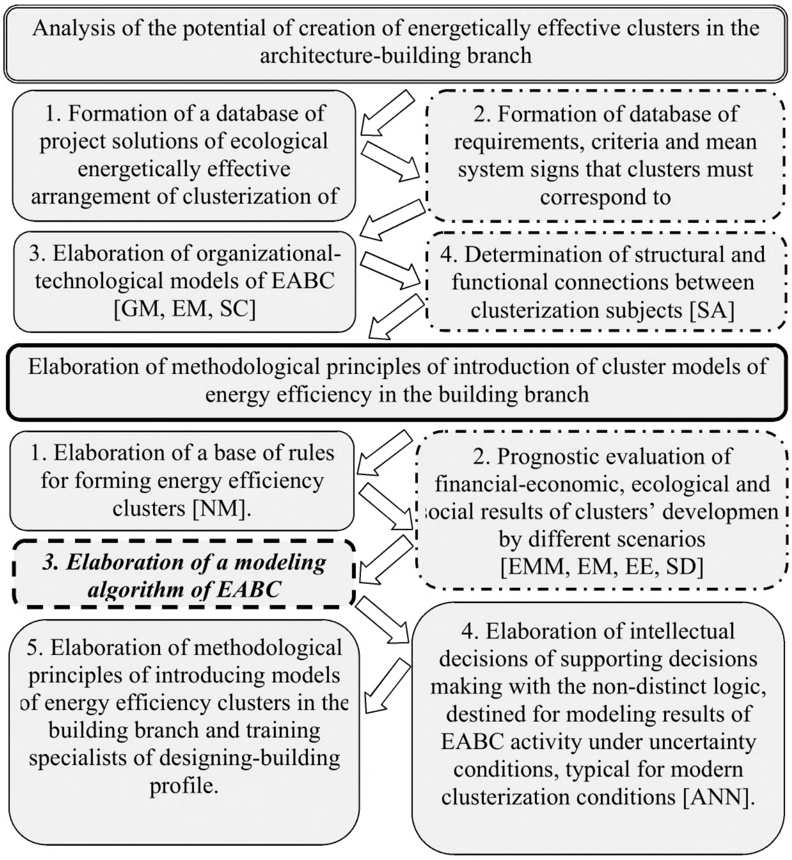

Fig. 1. Conceptual scheme of elaboration of methodological principles of introduction of energetically effective clusters' models in the building branch

Then there is offered the system of energetically effective architecture-building clusters' formation, according to which the cluster structure forms as a result of the criteria selection of candidates, able to provide the coordinated realization of set functions under given conditions, from the set.

3. 1. Calculating experiments

The system construction (synthesis) and decisions as to organizational clusterization are offered to be realized based on the system analysis and expert evaluation of results of calculating experiments with energetically effective architecture-building clusters' models.

Fig. 2 demonstrates the scheme, according to which the synthesis algorithm of energetically effective architecture-building clusters' models is elaborated.

According to the scheme on **Fig. 2**, the synthesis of models is a result of comparing a set of practical problems on the one side and one of their solutions, on the other one. Sets of connections form as a result of realizing certain operations on geometric modeling methods [12].

Each synthesized EABC model undergoes calculating experiments for evaluating its activity results under different conditions by different scenarios. Calculating experiments are realized by scenarios of the inductive destination, elaborated by the principle "from practical requirements to a geometric model" [12]. Principles are based on including essential properties of form creation in the structure of the geometric modeling method, used for solving variation problems.

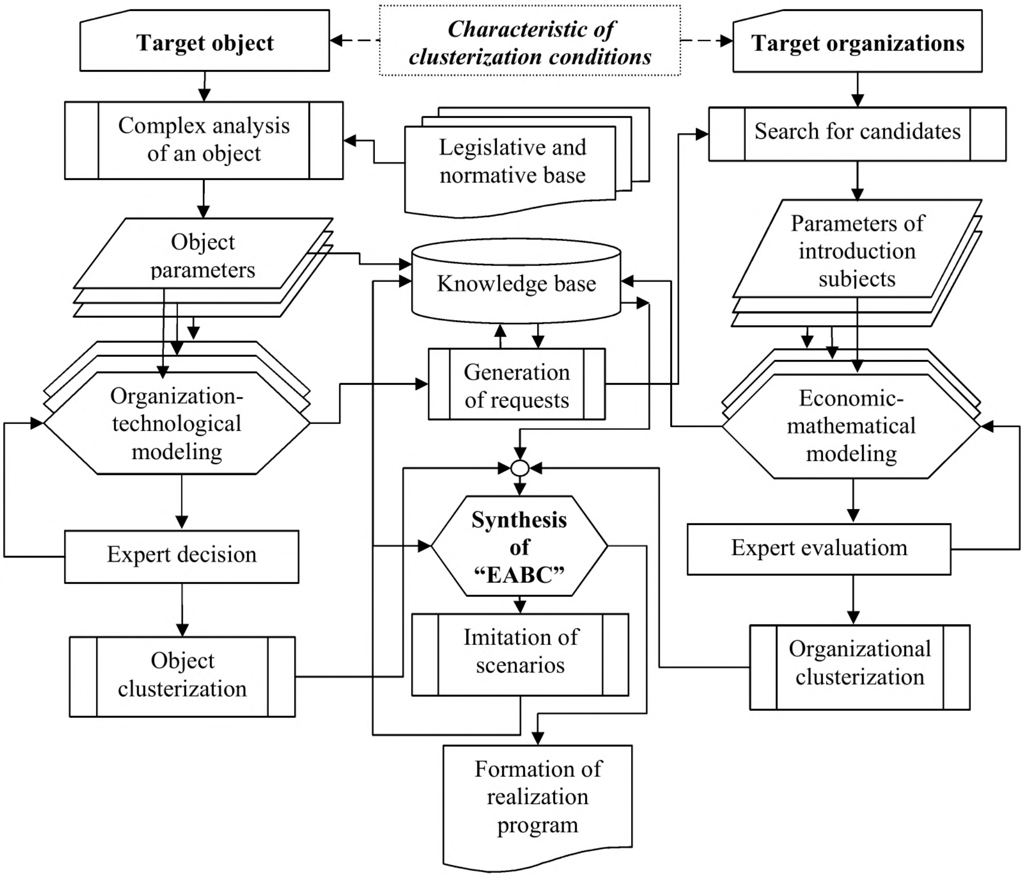

Fig. 2. Scheme of the formation process of energetically effective architecture-building clusters

At this approach clusters' models are synthesized as a result of the superposition of target objects and subjects of introduction, based on the criteria selection of introduction subjects, able to provide the coordinated realization of set functions under given conditions, from the set of target organizations.

The complex analysis of a target object, potential of creation of energetically effective clusters on its base, selection of candidates from the set of target organizations, set of probable changes in the external environment and influence degree of system properties on the adaptation mechanism of synthesized clusters, are determined and evaluated by experts.

A decision as to organizational clusterization at this stage is also accepted based on expert evaluations of parameters of introduction subjects and economic-mathematical modeling results. But the algorithm of EABC modeling, organization and realization of calculating experiments provide the formation of a knowledge base of the intellectual system of decisions making, elaborated for modeling cluster structures.

In further the generalized experience of experts is planned to be used for training artificial neuron networks, able to play the role of experts in such systems.

4. Results

Today such methods as stochastic limit analysis [1] and non-parametric one [2, 3] are widely used for determining cluster structures, most acceptable for combining. But none of them allows to determine a structure, most suitable for realizing the set aim under given conditions, unambiguously. It is connected with a fact that none of them solves the problem of multi-factor optimization and cannot prognosticate system properties of clusters.

[5, 6] describes properties of the cluster organization and management, but an analysis of system properties of clusters, necessary to be taken into account at elaborating models for prospective planning and development strategy of cluster structures, is absent.

Works [13, 14]:

– Present formalized, generalized and descriptive recommendations as to creation of territorial clusters for providing the competitiveness of the regional economy and sustainable regional development;

– Describe cluster strategies of state-private partnership, criteria and statements of the state policy of economy clusterization;

– Elaborate conceptual models of clusters of renewable energetics.

But these works don't present concrete formation aspects and optimization instruments of cluster structures sufficiently.

The expected practical importance of results of this study is in:

1) the use of geometric modeling methods gives a possibility to automate the process of purpose-oriented synthesis of cluster models;

2) the analysis of results of calculating experiments with synthesized models provides the scientifically grounded support of making decisions as to forming real clusters taking into account peculiarities of target objects and characteristics of clusterization conditions;

3) based on imitation modeling of the system of key parameters of energy efficiency, there appears a possibility to optimize the use of fuel-energetic resources, renewable energy sources, alternative fuel types and to manage the flow distribution of combined resources of a cluster.

5. Conclusions

1. For realizing the conception of creation of the energetically effective, eco-safe, comfort architecture environment, there has been formed the conceptual scheme of elaboration of methodological principles of introducing models of energetically effective architecture-building clusters. The elaborated principles may be used at realizing arrangements, directed on reducing thermal losses of heat-supplying systems by their optimization at reconstruction.

2. The methodology of introducing models of cluster structures in the building branch needs elaborating program means for realizing the purpose-oriented synthesis of models. The work of the algorithm, elaborated for synthesizing models of energetically effective architecture-building clusters, is offered to be based on geometric modeling methods.

3. At this stage of the research a function of making decisions as to the real cluster formation is left for experts. But the algorithm of EABC modeling provides the formation of the knowledge base that will be in further a base of an "internal model" of the intellectual system of supporting making decisions with the non-distinct logic.

References

[1] Lundgren, T., Marklund, P.-O., Zhang, S. (2016). Industrial energy demand and energy efficiency – Evidence from Sweden. Resource and Energy Economics, 43, 130–152. doi: http://doi.org/10.1016/j.reseneeco.2016.01.003

[2] Shi, G.-M., Bi, J., Wang, J.-N. (2010). Chinese regional industrial energy efficiency evaluation based on a DEA model of fixing non-energy inputs. Energy Policy, 38 (10), 6172–6179. doi: http://doi.org/10.1016/j.enpol.2010.06.003

[3] Özkara, Y., Atak, M. (2015). Regional total-factor energy efficiency and electricity saving potential of manufacturing industry in Turkey. Energy, 93, 495–510. doi: http://doi.org/10.1016/j.energy.2015.09.036

[4] Sölvell, Ö., Lindqvist, G., Ketels, C. (2003). The Cluster Initiative Greenbook. Stockholm: Ivory Tower, 92.

[5] The Role of Clusters in Smart Specialisation Strategies (2013). Luxembourg: Publications Office of the European Union, 59.

[6] Smart guide to cluster policy (2016). Belgium, 60.

[7] Mykytas, M. V., Ploskyi, V. O. (2017). Stalyi rozvytok mist: stan doslidzhen, mizhnarodnyi ta ukrainskyi dosvid. Enerhoefektyvnist v budivnytstvi ta arkhitekturi, 9, 168–173.

[8] Mykytas, M. V., Ploskyi, V. O., Kozhedub, S. A. (2018). Doslidzhennia systemnykh oznak enerhoefektyvnykh klasternykh orhanizatsiinykh struktur arkhitekturno-budivelnoi haluzi. Upravlinnia rozvytkom skladnykh system, 35, 68–75.

[9] Mykytas, M., Terenchuk, S., Zhuravska, N. (2018). Models, Methods and Tools of Optimizing Costs for Development of Clusterized Organizational Structures in Construction Industry. International Journal of Engineering & Technology, 7 (3.2), 250. doi: http://doi.org/10.14419/ijet.v7i3.2.14414

[10] Kulikov, P., Mykytas, M., Terenchuk, S., Chupryna, Y. (2018). Development of a methodology for creating adaptive energy efficiency clusters of the architecture and construction industry. Technology Audit and Production Reserves, 6 (5 (44)), 11–16. doi: http://doi.org/10.15587/2312-8372.2018.150879

[11] Klir, Dzh. (1990). Sistemologiya. Avtomatizatsiya resheniya sistemnykh zadach. Moscow: Radio i svyaz’, 544.

[12] Ploskiy, V. A. (1996). Operatsii na mnozhestve metodov geometricheskogo modelirovaniya kak element ikh sistemnogo issledovaniya. Prikladnaya geometriya i inzhenernaya grafika, 60, 79–83.

[13] Prokip, A. V., Dudiuk, V. S., Kolisnyk, R. B. (2015). Orhanizatsiini ta ekoloho-ekonomichni zasady vykorystannia vidnovliuvanykh enerhoresursiv. Lviv: ZUKTs, 338.

[14] Mamonova, V. V., Kuts, Yu. O., Makarenko, O. M. et. al. (2013). Formuvannia terytorialnykh klasteriv yak instrumentu rehionalnoho rozvytku. Kyiv: NADU, 36.

EXPERIMENTAL INVESTIGATIONS OF THE METHOD OF DETERMINATION OF OPTIMAL CONTROLLER SETTINGS

Maryna Loriia
Department of Electronic Devices
East Ukrainian National University named after Vladimir Dal
59a Central ave., Severodonetsk, Ukraine, 93400
atp01@ukr.net

Abstract

A method for finding the optimal PID controller settings is proposed, which takes into account all the shortcomings of the most common engineering methods for finding controller settings. The method is characterized by: simplicity and versatility, which allows determining the optimal controller settings for one iteration; highly accurate identification of the control object, taking into account its nonlinearity, does not require an active experiment, provides improved dynamic properties of systems.

Tuning parameters of controllers are found by the proposed method of finding the optimal settings of the controller and the most common engineering methods for finding the settings of controllers for ACS control objects in the production of nitric acid. In addition to the examples given, a number of control objects with varying degrees of oscillation and inertia are investigated. A comparative analysis of the proposed method with the most common engineering methods for finding controller settings for ACS control objects in the production of nitric acid is performed. The analysis shows that the controller parameters found by the proposed method significantly improve the dynamic properties of the system (the overshoot decreased by 10 times, the regulation time decreased by about 30 %, the static and dynamic errors decreased by 2–3 times).

Keywords: second order link, controller settings, regulation time, identification algorithm, transient process, delay time.

DOI: 10.21303/2461-4262.2019.00864

1. Introduction

Market globalization is becoming comprehensive and this means that in order to stay in business, manufacturing industries need to pay more attention to quality and efficiency issues. In turn, this focuses on the development of advanced control systems so that the processes flow better. In particular, improved management is the key to improving technology. This provides: improved product quality, minimizing losses, protecting the environment, increasing productivity for installed capacity, increasing production, postponing costly upgrades to management facilities and higher safety margins.

However, in most cases, when changing the characteristics of the object and require reconfiguration of systems. Such cases include various kinds of switching, changes in the characteristics of raw materials and materials, incoming changes caused by the variable mode of operation of objects, the properties of actuators and regulatory bodies, the interdependence of the circuits in multidimensional systems.

At present, operational personnel do not have methods suitable for industrial conditions necessary for recalculating controller settings. Under operating conditions, the only way out is weakening the controller settings, thus achieving a reduction in the mutual influence of the circuits, ensuring the necessary stability margin under any possible object operation modes. The quality of the systems is obviously much worse, and the profits are much lower than those achievable with the settings corresponding to the characteristics of the object.

Many of the quality improvement methods that are proposed by management theory are practically unsuitable for industrial environments. So the methods associated with increasing the order of control devices, providing an increase in quality, reduce the region of stability in the parameter space of the object model.

As a result, we have such a difficult situation (typical statistics for most enterprises):
– 10–90 % of the contours are in manual mode;
– 30 % control valves with serious problems;
– 30 % of ACS set up completely wrong;

– 40 % of contours with fluctuations; 30 % unsuitable regulation organization; 85 % non-optimal settings;

– 75 % of controllers only increase instability.

The overwhelming majority of ACSs operating in enterprises have enormous untapped potential. This potential can be "raised" at the expense of not technological measures, but at the expense of increasing the operation efficiency of these systems, optimal tuning, the main ACS devices, and controllers.

Therefore, today the task is very relevant, the development of reliable methods for finding the optimal controller settings, which would significantly improve the ACS quality.

2. Materials and methods

The results obtained in [1, 2] are experimentally confirmed. The object of research is the production of nitric acid. The subject of research is the elements of the production management system of nitric acid. The study of ACS control objects and settings PID-controllers are carried out theoretically using a computer and experimentally; using the theory of mathematical modeling and the theory of optimal control for the development and study of mathematical models of control objects and the optimal controller settings; using the methods of mathematical statistics in the processing of experimental results. The study of mathematical models and systems of automatic control of control objects in the production of nitric acid is carried out using modern software: TRACE MODE 6.08 SCADA-systems, MS Excel 2013 Maple 17, MathCAD 15.

3. Investigation of the method for finding the optimal controller settings

The distributed control system was implemented in the TRACE MODE SCADA system, the executive modules of which ensured the real-time operation of the system. The system can be used in the union, consisting of several process ACS located in different sites. Internet channels, industrial buses, serial interfaces, radio networks and dial-up telephone lines, as well as support for workplaces of mobile employees (for example, service personnel) working out of the office were used as data transmission channels. Employees can exchange data via GSM operators through pocket computers, laptops, the web, or even through a simple cell phone. TRACE MODE also allows to use GSM networks and for remote control and data collection of geographically distributed oil production facilities, for example, using GSM modems, it is possible to reach remote field facilities.

A distributed control system for the production of nitric acid (**Fig. 1**) has been developed, which, due to the implementation of the method for finding optimal controller settings (OCS) at the middle level, has ensured the ACS optimal operation. To ensure optimal ACS operation of distributed control system, a method for finding an OCS was implemented at an average level [3].

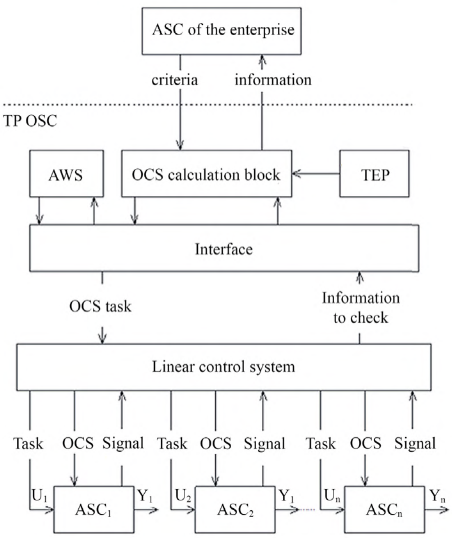

Fig. 1. Structurally-functional diagram of distributed control systems

The main requirements for calculating the settings of the controller are simplicity, reliability, versatility, accuracy. The obtained optimal settings of the controller, which are not subject to further adjustment, should provide the ACS with such properties as accuracy, stability margin and proper speed. In many cases, known methods of searching for controller settings do not satisfy such requirements and, despite their simplicity, they have a number of significant drawbacks, namely:

– finding the MM of the control object and further determining the settings of the controller by conducting an active experiment on the object itself can lead to loss of quality of the finished product, damage to raw materials, catalysts, and even to emergencies, including fires, explosions, emissions of harmful substances to the environment;

– the control object is described by polynomials, do not take into account their nonlinearity;

– to the formulas for finding the settings of the controllers that do not include optimization indicators, that is, it is impossible to say in advance what system of optimality criteria the transition process to meet with given controller settings;

– the absence in the design formulas of the quality indicators of the transition process leads to the fact that in practice it is necessary to manually change the controller settings obtained by this or that method so that the transition process meets the control standards for a particular technological process;

– lack of universality of existing methods. The application of a specific method becomes impossible if its main calculated indicator is missing and is applied only for certain types of controllers and control objects.

Without taking into account these features of the methods, it is impossible to further improve the methods for determining the optimal controller settings for systems and objects of various types, and to improve their dynamic properties.

All these drawbacks are taken into account by the proposed method for finding the optimal controller settings [4], which combines two algorithms: an algorithm for identifying model parameters using global extrema of dynamic characteristics [4] and an algorithm for finding optimal controller settings using a quadratic optimization function [5, 6]:

– to identify the control objects and further determine the optimal settings of the controller, a passive experiment is conducted in an open loop, since in this case there is no possibility of taking the system out of stability;

– non-linearity of the control object is taken into account, depending on the type of the transition process, by the corresponding equation of the transition function of the second-order link [7]. In this case, the approximation of the transition function of the control object is performed using the dynamics of the transition process, described by such parameters as speed, acceleration, acceleration speed, etc., which are derived from the output signal with respect to time;

– to enter optimization indicators and quality indicators into formulas for finding optimal controller settings, we use the formula of a quadratic integral criterion, which is unimodal function for most processes and, as a single numerical value, gives a generalized estimate of the attenuation rate and the deviation value of the controlled variable. This integral determines the square of the plane between the task and the transition curve, and also depends on the controller tuning parameters;

– the versatility of this method lies in the fact that the optimal ACS settings are found for any types of transient processes of control objects and controllers, and there is no such thing as a calculated indicator in it.

The method is based on the fact that the acceleration curve of the control object is analyzed, its character is determined for approximating the transition function of the system by a second-order link with a delay time at characteristic points using the nonlinear least squares method. The equations found in this way are then used to find the optimal controller settings by quadratic integral criterion. The search for optimal controller settings is to find such controller parameters for which the quadratic integral criterion (the square of the dynamic error) would be minimal. To search for the extremum of the optimization function, let's use the conjugate gradient method. The values found in this way will be the optimal controller settings [9, 10].

To illustrate the work, a comparative analysis (**Fig. 2–5, *b–d***) of the proposed method for finding the optimal controller settings (in the figure under 1) and widely used in engineering practice of the triangle method (in the figure under 2), Ziegler-Nichols method (Z–N) (in the figure under 4) and the CHR method (in the figure under 3). The P, PI, and PID controllers of single-circuit ACS for aperiodic control objects are calculated using the example of the acceleration curves of the purge column in the production of nitric acid through the channel consumption of nitric acid → level in the column (**Fig. 2, *a***) [8].

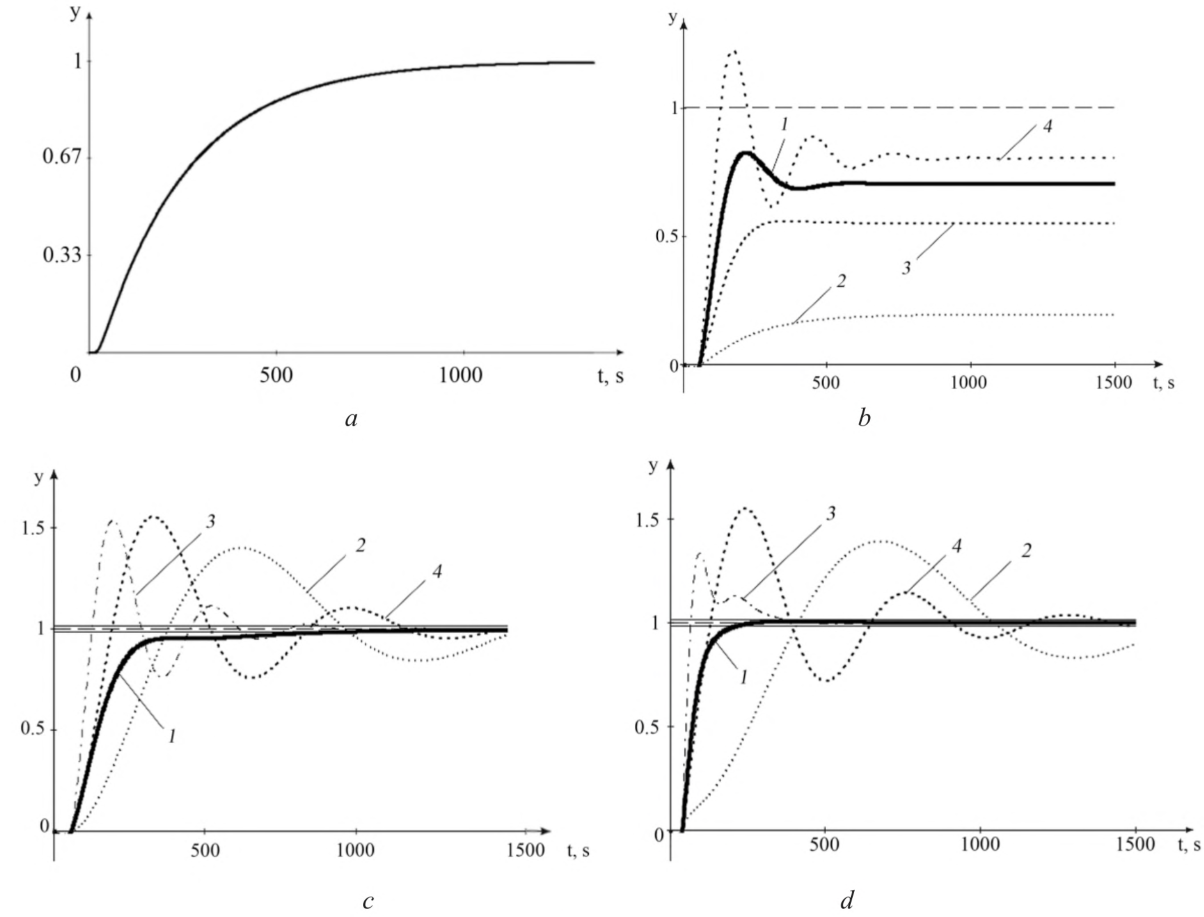

Fig. 2. ACS TP of the purge column:
a – CO AC; *b* – ACS TP with P controller;
c – ACS TP with PI controller; *d* – ACS TP with PID controller

The quality indicators of ACS transients (overshoot σ, regulation time Tc, static Δ_{st} and dynamic J errors), in which the controller settings were calculated using the proposed method for finding the optimal controller settings, as well as by the triangle method, the Z-N method and the CHR method are given in comparative **Tables 1, 2**.

From the analysis of the research results (**Fig. 2, *b–d*** and **Tables 1, 2**), it is possible to state the improvement of the dynamic properties of the system when using the optimal controller settings calculated by the proposed method compared to the most common engineering methods of searching the controller settings for ACS with aperiodic and oscillatory parameters control objects (reduction of overshoot by an order of magnitude, regulation time and dynamic error, reduction of the static system error by 2–3 times).

Table 1
Comparative table of the ACS operation quality for aperiodic CO

Method for finding controller settings	Regulation law	Control object	Controller settings			Regulation quality indicators			
			Kp	Ti	Td	σ	Δ_{st}	Tp	J
Proposed method	P controller	Purge column	2.39	∞	0.00	17.26	29.52	465.45	148.04
Triangle method			0.24	∞	0.00	0.00	80.39	816.34	665.90
Z – N methods		Purge column Gas reactor	4.12	∞	0.00	52.36	19.52	765.26	130.18
CHR methods			1.24	∞	0.00	1.31	44.70	202.83	273.18
Proposed method	P controller PI controller		1.14	∞	0.00	45.90	46.72	27.09	13.69
Triangle method			0.57	∞	0.00	25.77	63.79	18.33	14.60
Z – N methods		Gas reactor Purge column	1.78	∞	0.00	83.71	35.93	69.26	17.04
CHR methods			0.53	∞	0.00	15.47	65.15	18.28	12.97
Proposed method			1.62	187.95	0.00	0.00	0.00	959.79	124.97
Triangle method			0.29	135.56	0.00	40.09	0.00	2564.73	247.94
Z – N methods		Purge column Gas reactor	3.71	60.28	0.00	53.47	0.00	895.26	122.30
CHR methods			1.44	56.36	0.00	55.50	0.00	1709.88	176.51
Proposed method	PI controller PID controller		0.66	7.57	0.00	0.00	0.00	32.45	5.24
Triangle method			0.68	6.07	0.00	5.66	0.00	24.05	5.01
Z – N methods		Gas reactor Purge column	1.60	6.24	0.00	37.87	0.00	60.54	5.66
CHR methods			0.62	5.84	0.00	8.46	0.00	24.53	5.11
Proposed method			3.07	85.01	95.58	0.00	0.00	219.48	73.98
Triangle method			0.20	135.56	30.12	39.12	0.00	2805.33	241.60
Z – N methods		Purge column Gas reactor	4.95	27.40	167.68	33.43	0.00	372.91	80.15
CHR methods			2.47	27.40	83.84	54.81	0.00	1598.62	129.71
Proposed method	PID controller		0.68	5.88	0.89	0.48	0.00	15.78	4.30
Triangle method			0.47	6.07	1.35	5.64	0.00	31.55	4.61
Z – N methods		Gas reactor	2.14	2.84	3.25	60.73	0.00	30.37	4.62
CHR methods			1.07	2.84	1.62	14.14	0.00	23.71	3.48

Table 2
Comparative table of the ACS operation quality for oscillatory CO oscillatory

Method for finding controller settings	Regulation law	Control object	Controller settings			Regulation quality indicators			
			Kp	Ti	Td	σ	Δst	Tp	J
Proposed method	P controller	Nitrogen oxide absorber	1.01	∞	0.00	66.44	49.76	119.00	55.61
Triangle method			0.60	∞	0.00	42.74	62.56	81.22	51.60
Z – N methods			1.76	∞	0.00	106.29	36.21	5500.00	760.42
CHR methods			0.53	∞	0.00	38.77	65.42	53.08	47.23
Proposed method		Purge column	1.01	∞	0.00	56.43	49.78	57.73	22.97
Triangle method			0.61	∞	0.00	33.14	62.08	31.33	16.06
Z – N methods			1.72	∞	0.00	87.54	36.79	150.81	33.01
CHR methods			0.52	∞	0.00	28.61	65.99	31.57	19.88
Proposed method	PI controller	Nitrogen oxide absorber	0.30	25.35	0.00	0.00	0.00	102.45	15.46
Triangle method			0.72	12.60	0.00	24.94	0.00	116.58	11.73
Z – N methods			1.59	13.11	0.00	Unstable process			
CHR methods			0.62	12.26	0.00	24.98	0.00	125.07	11.82
Proposed method		Purge column	0.34	13.76	0.00	0.00	0.00	56.72	8.34
Triangle method			0.73	7.02	0.00	16.96	0.00	51.79	5.88
Z – N methods			1.55	7.49	0.00	42.97	0.00	180.33	9.69
CHR methods			0.60	7.01	0.00	15.95	0.00	46.83	6.07
Proposed method	PID controller	Nitrogen oxide absorber	0.56	10.82	3.23	2.31	0.00	47.88	8.14
Triangle method			0.50	12.60	2.80	1.07	0.00	34.37	8.89
Z – N methods			2.11	5.96	6.66	71.93	0.00	200.23	16.42
CHR methods			1.06	5.96	3.33	38.71	0.00	71.03	8.71
Proposed method		Purge column	0.64	5.88	1.90	1.99	0.00	26.18	4.37
Triangle method			0.51	7.02	1.56	1.85	0.00	28.89	4.94
Z – N methods			2.06	3.41	3.62	45.87	0.00	38.54	4.37
CHR methods			1.03	3.41	1.81	26.97	0.00	31.62	4.20

4. Discussion of the results of an experimental research of the method for finding the optimal controller settings

As a result, it is found the optimal settings of the PID controllers for the ACS control objects in the production of nitric acid using the developed experimental-theoretical method of finding the optimal settings of the PID controller. Simplicity and versatility allows to determine the optimal settings for the PID controller in one iteration. The method is characterized by a high accuracy of identification of control objects with regard to their nonlinearities, and also does not require an active experimen: improved dynamic properties of ACS (reduction of overshoot by an order of magnitude, regulation time and dynamic error, reduction of the static system error by 2–3 times) as a result of which safer process management.

The developed method of finding the optimal settings of the PID controller can also be applied when finding the optimal settings of the PID controller for other ACSs, in which control objects can be identified by a second-order link with a delay.

5. Conclusions

A distributed control system for the production of nitric acid is developed, due to the implementation in it at an average level of the method of finding OSC, has ensured optimal ACS operation.

A method for finding the optimal PID controller settings is proposed, which takes into account all the shortcomings of the most common engineering methods for finding controller settings. It is characterized by: simplicity and versatility, which allows to determine the optimal controller settings for one iteration; highly accurate identification of the control object, taking into account its nonlinearity, does not require an active experiment, provides improved dynamic properties of systems.

Regulation parameters of controllers are found by the proposed method of finding the optimal controller settings and the most common engineering methods for finding the settings of controllers for ACS of control objects in the production of nitric acid. In addition to the examples given, a number of control objects with varying degrees of oscillation and inertia are investigated.

A comparative analysis of the proposed method with the most common engineering methods for finding controller settings for ACS control objects in the production of nitric acid is performed. It shows that the controller parameters found by the proposed method significantly improved the dynamic properties of the system (overshoot decreased by 10 times, regulation time decreased by about 30 %, static and dynamic errors decreased by 2–3 times).

References

[1] Ananiev, M. V., Tselishchev, O. B., Loriya, M. H., Yelisieiev, P. Y. (2010). Optymalne nastroiuvannia rehuliatora za kvadratychnoiu optymizatsiynoiu funktsieiu. Visnyk Skhidnoukrainskoho natsionalnoho universytetu imeni Volodymyra Dalia, 6, 134–141.

[2] Ananiev, M. V., Tselishchev, O. B., Loriya, M. H., Yelisieiev, P. Y., Yerokhina, O. V. (2010). Identyfikatsiya obiektiv keruvannia. Vymiriuvalna ta obchysliuvalna tekhnika v tekhnolohichnykh protsesakh, 2 (36), 178–181.

[3] Ananiev, M. V., Tselishchev, O. B., Loriya, M. H., Yelisieiev, P. Y. (2011). Aproksymatsiya perekhidnoi funktsiyi obiekta keruvannia lankoiu druhoho poriadku. Vymiriuvalna ta obchysliuvalna tekhnika v tekhnolohichnykh protsesakh, 2, 209–213.

[4] Karakawa, K., Abe, N., Ichihara, H. (2002). Joint design method of closed-loop identification and IMC structure for temperature control system with time delay. Proceedings of the 41st SICE Annual Conference. SICE 2002. doi: https://doi.org/10.1109/sice.2002.1196548

[5] Soderstrom, T., Stoica, P. (2002). Instrumental variable methods for system identification. Circuits, Systems, and Signal Processing, 21 (1), 1–9. doi: https://doi.org/10.1007/bf01211647

[6] Astrom, K. J., Hang, C. C., Lim, B. C. (1994). A new Smith predictor for controlling a process with an integrator and long dead-time. IEEE Transactions on Automatic Control, 39 (2), 343–345. doi: https://doi.org/10.1109/9.272329

[7] Hongdong, Z., Ruixia, L., Huihe, S. (2004). Control for integrating processes based on new modified smith predictor. Control 2004, University of Bath.

[8] Kealy, T., O'Dwyer, A. (2002). Comparison of Open- and Closed-loop Process Identification Techniques In The Time-Domain. Proceedings of the 3rd Wismarer Automatisierungssymposium. Wismar.

[9] Mamat, R., Fleming, P. J. (1995). Method for on-line identification of a first order plus dead-time process model. Electronics Letters, 31 (15), 1297–1298. doi: https://doi.org/10.1049/el:19950865

[10] Verhaegen, M., Verdult, V. (2012). Filtering and System Identification: A Least Squares Approach. Cambridge University Press, 422.

ASSESSMENT OF SURFACE DOWNWELLING SHORTWAVE RADIATION IN 2021–2050 IN LAAYOUNE − SAKIA EL HAMRA REGION, MOROCCO

Youssef El Hadri
Department of Agrometeorology and Agroecology
Odessa State Environmental University
15 Lvivska str., Odessa, Ukraine, 65016
magribinetsm@gmail.com

Valeriy Khokhlov
Department of Meteorology and Climatology
Odessa State Environmental University
15 Lvivska str., Odessa, Ukraine, 65016
khokhlov.valeriy@gmail.com

Mariia Slizhe
Department of Meteorology and Climatology
Odessa State Environmental University
15 Lvivska str., Odessa, Ukraine, 65016
magribinets@ukr.net

Kateryna Sernytska
Department of Environmental Economics
Odessa State Environmental University
15 Lvivska str., Odessa, Ukraine, 65016
katris@i.ua

Kateryna Stepanova
Department of Economics and International Economic Relations
International Humanitarian University
33 Fountain Road str., Odessa, Ukraine, 65009
Katstep2013@gmail.com

Abstract

Morocco's energy system is highly dependent on external energy markets. According to the Ministry Energy, Mines and Sustainable Development today more than 93 % of energy resources are imported to Morocco. In 2008 the Moroccan Government has developed a National Energy Strategy, and one of its priority areas is to increase the share of renewable technologies in the country's energy sector. Morocco is rich in solar energy resources. Studies on the assessment of the Morocco's solar energy potential indicate, among other benefits, low additional costs when using solar installations compared to losses associated with the solution of future climate problems and lack of resources. The plan envisages the commissioning of solar power plants in Ouarzazate, Ain Ben Mathar, Boujdour, Tarfaya and Laayoune by 2020.

The aim of this research is determination of the characteristics of the distribution of Surface Downwelling Shortwave Radiation in the area of the solar power Boujdour, Tarfaya and Laayoune, located in the Laayoune − Sakia El Hamra region in 2021−2050. The data from regional climate modeling with high spatial resolution of the CORDEX-Africa project are used in this research. The RCM modeling is carried out for the region of Africa, in a rectangular coordinate system with a spatial resolution of ~44 km. Then, from the modeling data, values are highlighted for the territory of Laayoune − Sakia El Hamra region. Model calculation is performed taking into account the greenhouse gas concentration trajectory of RCP 4.5 calculated using 11 regional climate models. As a result of the simulation for the period 2021−2050, average monthly values of the Surface Downwelling Shortwave Radiation "RSDS" (W/m2) are derived, on the basis of which the mean values for the period of time are calculated. For more detailed information, average monthly total cloud cover values "TC" (%) for the period under study are calculated.

Analysis of the change in RSDS in 2021–2050 relative to the recent climatic period is shown that in the Laayoune − Sakia El Hamra region we can expect an increase or retention of its values. The annual run of the RSDS has one maximum in June and one minimum in December.

In the future, the distribution of RSDS in the Laayoune − Sakia El Hamra region will have a significant impact on proximity to the Atlantic Ocean, where an increased amount of total cloud cover significantly reduces the amount of incoming radiation.

In the location of solar power plants in the near future, the current RSDS values are expected to be maintained, which creates favorable conditions for the further development of the renewable energy industry in this area and increasing its productivity.

Keywords: CORDEX-Africa, Surface downwelling shortwave radiation, RCM, solar energy, Morocco.

DOI: 10.21303/2461-4262.2019.00863

1. Introduction

Morocco's energy system is highly dependent on external energy markets. According to the Ministry of Energy, Mines and Sustainable Development today more than 93 % of energy is imported to Morocco. The state purchases coal for its power plants and petroleum products on the international energy markets. Natural gas is imported from Algeria as compensation for the transit of Algerian gas through Morocco to the south of Spain. From 14 to 20 % of electricity consumed annually in Morocco is imported from Spain via the Strait of Gibraltar [1]. Dependence on international energy markets is a burden on the balance of payments and poses risks to the country's energy security. The growing demand for energy increases the pressure on the Moroccan economy, making the use of alternative energy sources to become the only way out of the current situation.

In 2008 the Moroccan Government has developed a National Energy Strategy, and one of its priority areas is to increase the share of renewable technologies in the country's energy sector. In addition, Morocco launched the renewable energy development program [2], which aims to achieve a total installed capacity of 2000 MW from wind power, 2000 MW from solar energy and an increase in the capacity of hydropower to 2000 MW by 2020 [3].

Morocco is rich in solar energy resources. Studies on the assessment of the Morocco's solar energy potential indicate, among other benefits, low additional costs when using solar installations compared to losses associated with the solution upcoming future climate problems and lack of resources. As part of National Energy Strategy has been developed Moroccan Solar Plan, the main strategic objectives of which are [3]:

– diversification of energy supply;
– preservation of environment;
– exploitation of domestic renewable energy resources;
– reduction of energy dependency.

The plan envisages the commissioning of solar power plants in Ouarzazate, Ain Ben Mathar, Boujdour, Tarfaya and Laayoune by 2020 [4].

In [5] presents the results of assessing the solar potential of Morocco in the current climatic conditions carried out within the framework of the Moroccan Solar Plan. The study used data sets HelioClim 3, HelioClim 1 (average monthly values for the period 1985−2004), and the average values of solar radiation in the period 1981−2000, on the basis of which the calculation of technical and economic indicators for the selection and Substantiation of areas for the placement of Photovoltaic (PV) and Concentrated solar power (CSP) plants on the territory of Morocco.

Concentrated solar power plants usually use parabolic cylindrical reflectors or special tracking mirrors (heliostats) to focus sunlight on a tube or a collector tower, where the heat carrier (liquid or gas) is heated to a very high temperature. Such stations are little dependent on wavelength, and focus direct radiation incoming in the visible, UV and IR ranges, and on cloudy days they can use long-wave radiation of the atmosphere and clouds.

Traditional photovoltaic semiconductor materials, based on which electricity is produced by Photovoltaic power plants, are mainly sensitive to radiation with a wavelength of about 0.4 to

1.1 μm, which is a shortwave part of the spectrum [6–8]. The conversion of solar energy into electric energy, with the help of semiconductor solar cells, is currently the most scientifically and practically developed method.

Regional climate models (RCMs) are the main source of forecasts for possible future climate changes and allow obtaining information with a high spatial resolution for specific regions [9]. In the models, the calculation of the radiation balance at the top of the atmosphere (TOA) and on the underlying surface takes into account the cloud cover, cloud water content, and the size of cloud particles. The observed differences in the results of model calculations and satellite observations are due to the fact that in the models the hydrometeors are provided in a suspended state. excessive surface downwelling shortwave radiation (RSDS) estimates in the calculations of global climate models are caused by underestimates of cloud water content due to the fact that models of the convective cloud core are not taken into account [10]. Thus, total cloud cover is a key component affecting the incoming radiation [11]. Patterns in the change of monthly sum of total radiation under actual cloud conditions are caused mainly by the characteristics of the annual cycle of total radiation and cloud cover [12].

The aim of research is determination of the distribution characteristics of surface downwelling shortwave radiation in the area of the solar power Boujdour, Tarfaya and Laayoune, located in the Laayoune − Sakia El Hamra region in 2021–2050.

2. Materials and methods of research

2. 1. Description of the investigated area

The Laayoune − Sakia El Hamra region is located in the southern part of Morocco, at a latitude from 25 to 28 North latitude, in the west it is washed by the Atlantic Ocean, in the east it borders with Mauritania. The relief in this region is a plain that passes from the accumulative coastal lowlands on the Atlantic coast to the elevated basement plains in the east. In the North-Eastern part of the area penetrate spurs stepped of Draa plateau, much of the territory is covered with sand and dunes of the Sahara desert. The climate in this area is tropical desert, hot in the interior and milder on the coast.

On the territory of the Laayoune − Sakia El Hamra region is one of the richest deposits of phosphates Bou Craa, which reserves exceed 10 billion tons, deposits of uranium, oil and gas. On the coast there are port facilities, industrial plants for the enrichment and desalination of phosphates. The operation and maintenance of these facilities, as well as the development and construction of new ones, require an uninterrupted supply of electricity.

In rural areas, where there are relatively small distant settlements, the creation of centralized energy systems is impractical. In such areas, it is necessary to create autonomous power installations of low power based on the use of renewable energy sources. Currently, one of the main tasks of the Moroccan Government is solving the problem of supplying residents of the Laayoune − Sakia El Hamra region with electricity, hot water, heat or cold supply on the basis of alternative energy sources [13].

The Boujdour, Tarfaya and Laayoune solar power plants are located on the Atlantic coast and have the following characteristics (**Table 1**).

Table 1

Description of sites for solar power plants [5]

Site	Coordinates		Elevation, m	Location	Installed capacity, MW
	φ, °	λ, °			
Boujdour	26.10	–14.47	55	4 km to the north of Boujdour	100
Tarfaya	27.15	–13.20	69	south of the city of Tarfaya	500
Laayoune	27.93	–12.93	7	south of Foum El Oued	500

The population of the Laayoune − Sakia El Hamra region is 256 152 inhabitants, approximately 200 000 habitants lives in Laayoune, 41 178 in Boujdour, and 8 027 inhabitants in Tarfaya.

2. 2. Data and methods

In this study, data from regional climate modeling with high spatial resolution of the CORDEX-Africa project [14, 15] are used. The RCM modeling is carried out for the region of Africa, in a rectangular coordinate system with a spatial resolution of ~ 44 km. Then, from the modeling data, values are highlighted for the territory of Laayoune − Sakia El Hamra region. Model calculation is performed taking into account the greenhouse gas concentration trajectory of RCP 4.5. 11 climate models developed in research institutes and meteorological centers around the world are used for the calculation (**Table 2**). Further, RCM calculations are performed using an ensemble of models to increase the success of reproduction of average climatic characteristics. This is due to the fact that the systematic errors inherent in each model separately are often random in relation to the ensemble of models and are mutually compensated when averaged by the ensemble [16].

Table 2
Regional climate models characteristics

No. of model	Model name	The atmospheric general circulation model	Data centre
M1	KNMI-ICHEC-EC-EARTH	IFS	CNRM, France
M2	CanESM2	CanCM4	CCCMA, Canada
M3	CNRM-CM5	ARPEGE	CNRM / CERFACS, France
M4	SMHI-ICHEC-EC-EARTH	IFS	CNRM, France
M5	CSIRO Mark 3.6	Mk3 AGCM	CSIRO, Australia
M6	IPSL-CM5A-MR	LMDZ	IPSL, France
M7	MIROC5	AGCM CCSR	AORI/NIES/JAME S&T, Japan
M8	HadGEM2-ES	HadGEM2-A	Hadley Center, UK
M9	MPI-ESM-LR	ECHAM6	MPI, Germany
M10	NorESM1	CAM4-Oslo	NCC, Norway
M11	GFDL-ESM2M	AM3	GFDL, USA

As a result of the simulation for the period 2021-2050, average monthly values of the surface downwelling shortwave radiation "RSDS" (W/m^2) are derived, on the basis of which the mean values for the period of time are calculated. For more detailed information, average monthly total cloud cover values "TC" (%) for the period within the study are calculated. The CERES_EBAF-Surface_Ed4.0 data for the 2005–2015 [17] is used as the base values to estimate the change in the amount of surface downwelling shortwave radiation.

3. Experimental researches

The results of the RCMs calculations showed that in 2021–2050 average RSDS value (**Fig. 1**) in Tarfaya will be 235 W/m^2, in Laayoune and Boujdour 242 and 240 W/m^2, respectively. The nature of the distribution of RSDS has a deviation from latitudinal on the Atlantic coast, which is not surprising, since the amount of incoming radiation is significantly affected by cloudiness. As noted [18], the increased amount of total cloud cover on the Atlantic coast of Morocco is caused by the transfer to the continent of clouds formed above the ocean surface. Above the cold waters of the Canary Current, which flows near the coast, favorable conditions are created for the condensation of wet sea air, the formation of fog and low stratus clouds.

Analysis of changes in the incoming RSDS in 2021-2050 relative to the recent climatic period (**Fig. 2**), showed that in the Laayoune − Sakia El Hamra region we can expect an increase or retention of its values. The most interesting is the Atlantic coast, where are located solar power plants and the main objects of economic activity in the region. In the areas of power plants location, the models predict the preservation of the number of RSDSs, and when moving deeper into the region at 70 km, about 10 W/m^2 and more.

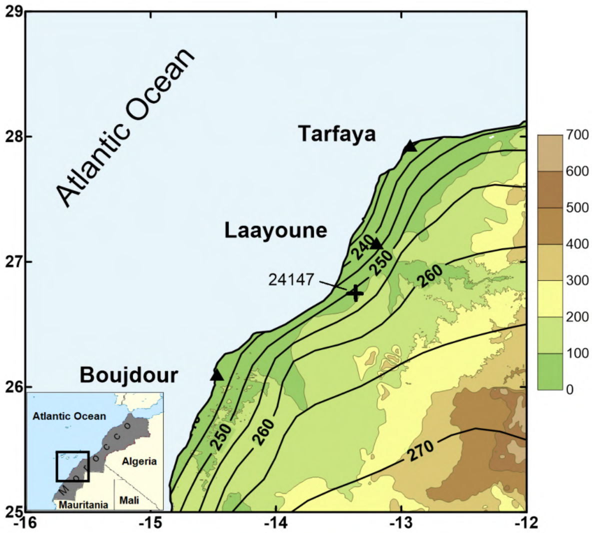

Fig. 1. The location of solar power plants (triangles) and the distribution of the RSDS (W/m^2) in 2021–2050

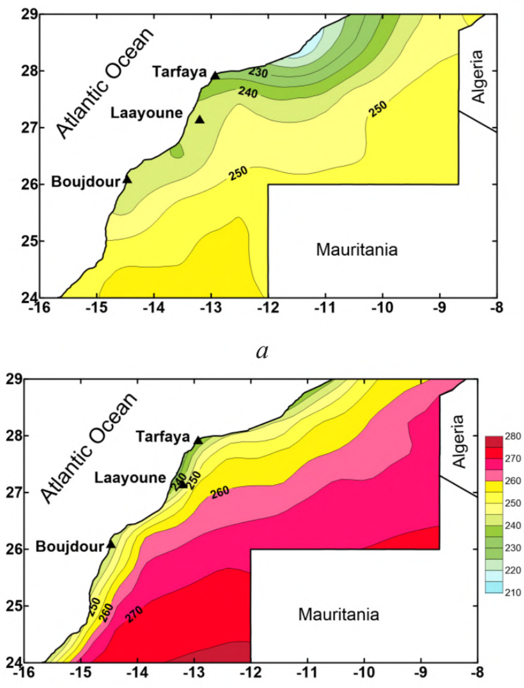

a

b

Fig. 2. Average value RSDS (W/m^2): *a* – 2005–2015; *b* – 2021–2050

The largest increase in RSDS is expected in the areas adjacent to the border with Mauritania (up to 20 W/m^2), but the remote location and sparse population makes these areas unsuitable for installing solar installations.

The annual run of the RSDS is affected by the course of solar radiation, due to astronomical factors and the annual run of the total cloud cover. In the extratropical latitudes of the Northern Hemisphere, the annual course of insolation has one maximum in June and one minimum in December [19]. The amplitude of the seasonal variations of insolation increases with increasing latitude.

The analysis of the predicted RCM annual run of short-wave radiation is carried out on the basis of calculations of monthly average RSDS values in the 24147 model grid node, located 47 km south of Laayoune (**Fig. 3**). As can be seen from the figure, the expected maximum RSDS falls on the month of June and will be 320 W/m^2.

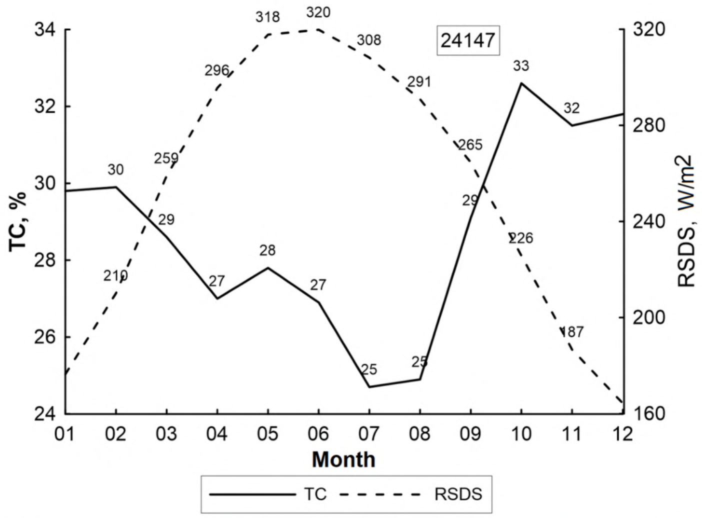

Fig. 3. Annual run of TC (%), and RSDS (W/m^2) in grid node 24147

The average monthly total cloud cover calculated by the RCM in the summer months ranges from 25–27 %, which reduces the amount of incoming radiation.

4. Conclusions

The proximity of the Atlantic Ocean has a significant impact on the distribution of RSDS in the Laayoune – Sakia El Hamra region, where an increased amount of total cloud cover significantly reduces the amount of incoming radiation.

In the location of solar power plants in the near future, the current RSDS values are expected to be maintained, which creates favorable conditions for the further development of the renewable energy industry in this area and increasing its productivity. The projected increase in RSDS is expected in the interior of the region, the remote location of which creates additional costs for the transmission of electricity, which significantly increases its cost and makes these areas less promising from the point of view of solar energy.

References

[1] Nfaoui, H., Sayigh, A. A. M. (2015). Contribution of Renewable Energy to Morocco's Energy Independence. ISESCO Journal of Science and Technology, 11 (19), 90–96.

[2] Borodkina, N. (2015). French renewable energy policy in Morocco in the early 21st Century. Vestnik of Northern (Arctic) Federal University. Series "Humanitarian and Social Sciences", 3, 5–10. doi: https://doi.org/10.17238/issn2227-6564.2015.3.5

[3] Jamae, E. M. (2015). Renewable Energy Transition in Morocco. Renewable Energy Transitions in Jordan and the MENA Region, 23–31.

[4] Moroccan Agency for Solar Energy Projects. Available at: https://www.masen.ma/en/masen/

[5] Richts, C. (2012). The Moroccan Solar Plan – a comparative analysis of CSP and PV utilization until 2020. Available at: https://www.uni-kassel.de/eecs/fileadmin/datas/fb16/remena/theses/batch2/Master-Thesis_Christoph_Richts.pdf

[6] Andreev, V. M., Grilihes, V. A., Rumyancev, V. D. (1989). Fotoelektricheskoe preobrazovanie koncentrirovannogo solnechnogo izlucheniya. Leningrad: Nauka, 310.

[7] Timchenko, S. L., Dementieva, O. J., Zadorozhnyi, N. A. (2015). The Influence on Radiation Spectrum Characteristic Curves of the Solar Battery. Physical education in universities, 21 (1), 3–13.

[8] Bazyomo, S. D. Y. B., Agnidé Lawin, E., Coulibaly, O., Ouedraogo, A. (2016). Forecasted Changes in West Africa Photovoltaic Energy Output by 2045. Climate, 4 (4), 53. doi: https://doi.org/10.3390/cli4040053

[9] Feser, F., Rockel, B., von Storch, H., Winterfeldt, J., Zahn, M. (2011). Regional Climate Models Add Value to Global Model Data: A Review and Selected Examples. Bulletin of the American Meteorological Society, 92 (9), 1181–1192. doi: https://doi.org/10.1175/2011bams3061.1

[10] Li, J.-L. F., Waliser, D. E., Stephens, G., Lee, S., L'Ecuyer, T., Kato, S. et. al. (2013). Characterizing and understanding radiation budget biases in CMIP3/CMIP5 GCMs, contemporary GCM, and reanalysis. Journal of Geophysical Research: Atmospheres, 118 (15), 8166–8184. doi: https://doi.org/10.1002/jgrd.50378

[11] Katragkou, E., García-Díez, M., Vautard, R., Sobolowski, S., Zanis, P., Alexandri, G. et. al. (2015). Regional climate hindcast simulations within EURO-CORDEX: evaluation of a WRF multi-physics ensemble. Geoscientific Model Development, 8 (3), 603–618. doi: https://doi.org/10.5194/gmd-8-603-2015

[12] Shakirov, V. A., Artemyev, A. Y. (2014). Technique for considering the influence of cloudiness on the solar radiation flux according to the archives of meteorological stations. Systems Methods Technology, 4 (24), 79–83.

[13] Mohamed Fadel' Ali Salem (2010). Zapadnaya Sahara: resursniy potencial i politicheskie realii. Sankt-Peterburg: Roza mira, 107.

[14] Climate impact portal. Available at: https://climate4impact.eu/

[15] Kim, J., Waliser, D. E., Mattmann, C. A., Goodale, C. E., Hart, A. F., Zimdars, P. A. et. al. (2013). Evaluation of the CORDEX-Africa multi-RCM hindcast: systematic model errors. Climate Dynamics, 42 (5-6), 1189–1202. doi: https://doi.org/10.1007/s00382-013-1751-7

[16] Pavlova, T. V., Katcov, V. M., Meleshko, V. P., Shkol'nik, I. M., Govorkova, V. A., Nadezhina, E. D. (2014). New generation of climate models. Proceedings of Voeikov Main Geophisical Observatory, 575, 5–64.

[17] Electronic database of climatic data. Available at: https://ceres-tool.larc.nasa.gov/ord-tool/jsp/EBAFSFC4Selection.jsp

[18] Marzol, M. V., Sánchez, J. L., Yanes, A. (2011). Meteorological patterns and fog water collection in Morocco and the Canary Islands. Erdkunde, 65 (3), 291–303. doi: https://doi.org/10.3112/erdkunde.2011.03.06

[19] Alisov, B. P. (1974). Climatology. Moscow, 300.

Original Research Article: full paper

(2019), «EUREKA: Physics and Engineering» Number 2

FORMULATION OF DESIGN TASKS OF TOWED UNDERWATER VEHICLES CREATION FOR SHALLOW WATER AND AUTOMATION OF THEIR MOTION CONTROL

Oleksandr Blintsov
Department of Computer Technologies and Information Security
Admiral Makarov National University of Shipbuilding
9 Heroiv Ukrainy ave., Mykolaiv, Ukraine, 54025
alex_blintsov@ukr.net

Volodymyr Sokolov
Chief Engineer – First Deputy General Director
State Enterprise «Production Association «O. M. Makarov Southern Machinebuilding Plant»
1 Kryvorizka str., Dnipro, Ukraine, 49047
sokolow@yuzhmash.com

Pavel Kucenko
Research Department
Admiral Makarov National University of Shipbuilding
9 Heroiv Ukrainy ave., Mykolaiv, Ukraine, 54025
arcadia.blacksea@gmail.com

Abstract

The towed underwater system is one of the fixed assets of the study of water areas. The effectiveness of its application depends on the characteristics laid at the design stage. The main task of the towed underwater vehicle (TUV) is the motion of technological equipment. Therefore, it is important to ensure the specified dynamic properties of the unit and automate the control of its motion. In the paper the typical forms of the unit are analyzed, the features of their control at small depths are set.

TUV control is carried out in conditions of uncertainty. Therefore, the design of an automatic control system (ACS) for its motion is proposed to be carried out using the appropriate synthesis method – the method of minimizing local functionals.

The control law contains integral components and, under the constraints of control actions, generates the problem of integral saturation. To eliminate the integral saturation in the work, the condition integration method is improved. On its basis, the control law and the structure of the controller of high dynamic accuracy of a second-order nonlinear object are synthesized. It is the basis for the synthesis of ACS controlled degrees of freedom of the underwater vehicle in conditions of uncertainty.

Usually TUVs contain two degrees of mobility. Translational motions of the unit are generated by changing its angular orientation. The paper synthesizes TUV controllers of pitch and roll based on the control law of the second order. Each control signal of the unit can affect both the roll and the pitch of the unit, which leads to decrease in the quality of control in general. To coordinate the work of controllers, a method is proposed, which is based on adjusting the initial conditions of the controller with greater error. On its basis, the automatic control system of the rotational motion of the unit is synthesized. It provides high dynamic precision control of two-dimensional rotational motion of the unit in uncertainty and is the basis for the ACS synthesis of its translational motion in space.

Keywords: towed underwater vehicle, automatic control system, rotational motion, integral saturation.

DOI: 10.21303/2461-4262.2019.00854

1. Introduction

Towed underwater systems (TUS) are among the most common types of underwater technology and are widely used for research and development of the oceans [1]. Currently, they are increasingly being used to carry out research and production work in shallow waters – on rivers and lakes, in coastal marine waters with depths of 30–50 meters [2].

Typical types of work in shallow water are [3–6]:
– hydrological and environmental studies;
– search and documentation of sunken objects;

– survey work and mapping of the bottom surface of navigable waters;

– underwater archaeological research;

– humanitarian demining of the water area;

– work in the interests of the marine mining industry (search and survey of phyllophora fields, places of industrial fish and shellfish, etc.).

The main instruments of the unit for performing the above works are photo and video cameras, side-scan sonars, hydroacoustic profilographs, sensors of hydrophysical and hydrochemical characteristics of water, etc.

The structure of a typical TUS contains a cable winch (CW), which is located on the tugboat (TB), cable-tug (CT), towed underwater vehicle (TUV) and the launch system (LS). CT root end is fixed on the CW, CT suspension end is fixed on TUV (**Fig. 1**) [7].

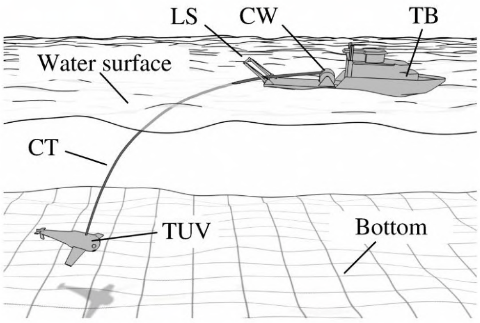

Fig. 1. The main elements of the towed underwater system

The features of the TUV use in shallow water include:

– high requirements for TUV mass-dimensional characteristics, due to the use of small TBs;

– high demands on the accuracy of the TUV spatial motion, due to the limitations of the vertical maneuver due to the small depths of water areas.

This makes the actual task of creating TUS for operation in shallow water areas and the synthesis of high-precision automatic control systems for the spatial motion of their TUVs.

2. Literature review and problem statement

Designing TUS as a maritime mobile object with a high level of automation is a well-known scientific problem [7]. From the standpoint of hydrodynamics and the theory of automatic control, TUS is an essentially nonlinear object, because it contains elements with concentrated (TB and TUV) and distributed (CT) parameters. These elements mechanically interact with each other and work in conditions of uncertainty.

A large number of scientific publications are devoted to research and design of TUS and their control systems.

The main problems that are solved in them include questions:

– calculation of the forces and moments arising at TUV and CT;

– mathematical modeling of the CT steady-state motion and its dynamics in transient modes;

– stabilization of the TUV motion on individual axes under the influence of external disturbances.

Thus, in [8], the general issues of designing and constructing a two-unit TUS are considered. The method of simulation modeling explores their dynamics and control methods using the PID controller. Sea rolling, towing speed and the position of the center of mass of the unit are taken into account.

The work [9] discusses monitoring and control of the towed force for safe TUV operation, methods of measuring and monitoring the towed force, and experimental methodology for obtaining the range of the towed force.

TUV hydrodynamic model is studied in [10]. The authors propose a new method of calculating the ideal towed system based on the calculation of Euler angles and determining the tension force at the CT end point.

In work [11], a three-dimensional dynamic model of a typical TUS is investigated during its operation at a fixed depth of 2.5 m. The features of the control unit in recirculation mode are established.

A three-dimensional hydrodynamic TUS model and a program for its calculation by various numerical methods are presented in [12]. The main advantage of the program is the use of an implicit method of integrating a system of differential equations, which ensures the stability of calculations of long-term transients.

The paper [13] is devoted to the comparison of mathematical models of the TUV CT stationary configuration with their experimental studies. A continuous and discrete 2D model of a stationary towing problem in a vertical plane at various towing speeds is considered. The advantages of using a CT discrete mathematical model are shown.

A new high-performance method for mathematical modeling of CT dynamic modes is described in [14]. The method provides high computational efficiency regardless of the degree of freedom of the TUS.

In [15], the TUV control system based on the state and feedback controllers using observers is investigated. The advantages of controllers based on the concept of observers with a high gain, compared with the use of controllers with a linear gain Kalman filter are shown.

These publications mainly deal with the study of the CT impact on the steady-state motion and the TUV dynamics, as well as questions of stabilizing the TUV motion in depth.

The issues of selecting the TUV hydrodynamic form and the synthesis of automatic control systems in scientific publications are not sufficiently covered.

3. The aim and objectives of research

The aim of research is analysis of the TUV hydrodynamic forms and the synthesis of a two-dimensional automatic control system of the rotational motion to ensure high dynamic accuracy of control of a typical TUV at shallow depths in conditions of uncertainty.

To achieve the goal it is proposed to solve the following objectives:

– perform analysis of the TUV features as a control object;

– improve the method of elimination of integral saturation for the ACS synthesis with limitations of control signals;

– synthesize the law of control of high dynamic accuracy of a non-linear object of the second order;

– synthesize controllers of TUV roll and pitch;

– synthesize the ACS with a TUV two-dimensional rotational motion.

4. Research results

4. 1. Features of TUV rotational and translational motions control

The majority of the TUV is a cylindrical body, elongated in the direction of motion, with a streamlined shape with bearing surfaces (wings) and with tail feathers – a system of vertical and horizontal rudders and stabilizers [2]. For effective work of stabilizers, the center of mass of the TUV during the design is shifted to the maximum forward, and the tail part is designed from light materials and lengthened.

Two other hydrodynamic TUV forms, “flying wing” and “frame”, are much less commonly used. To control the motion of the front armor of the first form, traditional wings are deepened from the elevons, and the second form is deepened wings and tail rudders.

The towed underwater vehicles used to study the bottom and underwater objects at shallow depths (up to 50 m) have their own characteristics. Working conditions are characterized by the commensurability of the hydrodynamic forces arising on the CT with the hydrodynamic forces on the TUV body. This must be taken into account when designing its bearing surfaces and tail assembly, as well as their actuating actuators. In addition, due to the small CT length, external disturbances from the rolling of the TB direction are transmitted to the TUV body, which significantly impairs the quality of work of its main devices (sonars, photo and video equipment). This requires the development of high-precision automatic control systems for TUV depth, roll and pitch.

"Planer-2" project TUV is considered [16, 17]. Its body has a cylindrical shape with streamlined ends and is equipped with bearing surfaces (BS) and tail feathers in the form of control wings (CW). BSs are arranged so that the resultant forces that it creates, compensate for the vertical component of the disturbing force from the CT. CWs are located in the aft part of the TUV, which makes it possible to create controllable differentiate and roll moments. The control action for the "Planer-2" project TUV is a vector-row $\bar{u}$:

$$\bar{u} = \{u_{left}, u_{right}\}; \; u_{left} \in [-1, 1]; \; u_{right} \in [-1, 1],$$

where u_{left} – the control signal for the left control wing; u_{right} – the control signal of the right control wing.

At the same time, when $u_{left}=u_{right}$, TUV roll is zero and only the TUV depth controlled is controlled by changing the TUV pitch. The latter, in this case, is guided by a synchronous change of control actions for the left and right wings. If $u_{left} \neq u_{right}$, then there will be a roll and TUV shift to the side. Thus, the control of rotating degrees of freedom (roll and pitch) is the basis for controlling the translational degrees of freedom (vertical and lateral motion) of the TUV.

For turning each CW, an automated electric drive is used, which is modeled using a first-order intensity setter:

$$\dot{u}_{out} = T_{int}^{-1} \mathrm{sat}(\varepsilon, \varepsilon_s);$$

$$\varepsilon = u_{in} - u_{out}; \quad \mathrm{sat}(\varepsilon, \varepsilon_s) = \begin{cases} \varepsilon_s, \text{ at } \varepsilon > \varepsilon_s; \\ -\varepsilon_s, \text{ at } \varepsilon < -\varepsilon_s; \\ \varepsilon, \text{ otherwise}; \end{cases}$$

$$\alpha_{left, right} = K u_{out(left), out(right)}; \; T_{int} = 0{,}01 \, s; \; \varepsilon_s = 0{,}08; \; K = -15°,$$

where u_{in} – the intensity setter input, u_{out} – the intensity setter output, the dot indicates the time derivative; ε – the error signal of the parameters u_{in} and u_{out}; ε_s – the parameter that determines the saturation threshold of the error signal ε; T_{int} – the time constant, which determines the dynamics of the transition process when the parameter ε leaves the saturation mode; sat(ε, ε_s) – a function that implements a nonlinear element with a characteristic of the "saturation" type; $\alpha_{left, right}$ – respectively, the angles of rotation of the left and right CW relative to the TUV body; K – the scaling factor of the control action, since the parameters $u_{left, right}$ are dimensionless, then the coefficient K has an angular dimension; $u_{out(left), out(right)}$ – the outputs of intensity controls, respectively, for the left and right CWs.

For negative values of $u_{left, right}$ the angles of rotation of the left α_{left} and right α_{right} control wings have positive values, create a pitch on the TUV nose and make it go deeper. Accordingly, at positive values of the TUV control actions, the pitch will be received at the stern and will float. The choice of the negative sign of the coefficient K is made taking into account the fact that the final controlled parameter is the TUV translational motion along the vertical axis of the base coordinate system directed upwards [18]. Therefore, the signs of control actions (with the equality of their absolute values) correspond to the direction of TUV motion along the vertical axis of the base coordinate system.

If $u_{left} > u_{right}$, then $\alpha_{left} < \alpha_{right}$, in connection with this TUV get a roll on the left side. This, accordingly, will cause it to move to the right, and vice versa, if $u_{left} < u_{right}$, then $\alpha_{left} > \alpha_{right}$, in connection with this, TUV will receive a roll on the starboard. This, accordingly, will cause it to move to the left. Such motions are explained by the fact that the "lifting force" of the bearing surface is directed downwards.

Automation of TUV rotational motion control is the basis for automating the control of its translational motion.

4. 2. Synthesis of TUV pitch control law

Transients in the CWs are much faster for transients when TUV rotational motion, so let's assume that the dynamics of the TUV rotational motion is subject to the second order of differential equations [16].

As a control object, TUV is a non-linear object that operates under uncertainty. Therefore, to synthesize the control law, let's use a method based on the concept of inverse dynamics together with minimization of local functionals [19].

When controlling a one-dimensional second-order object, the functional G(u), which is the normalized energy of the second derivative of the controlled variable, is subject to minimization [19]:

$$G(u)=\frac{1}{2}\left[\ddot{y}_d(y_g,t)-\ddot{y}(t,u)\right]^2,\ \ t\geq 0,$$

where y – the controlled variable; y_d – the desired value of the controlled variable obtained from the ACS reference model; y_g – specified value of the controlled variable (control problem); u – control signal (control action); t – time. Dots denote time derivatives.

The control action is obtained by minimizing the functional G(u) using the second order gradient search method [19]:

$$\ddot{u}+h\dot{u}=-\lambda\frac{\partial G(u)}{\partial u};\ h,\lambda=\text{const}>0,$$

where h and λ – the parameters of the gradient search.

The partial derivative of the functional G(u) with respect to the variable u is determined on the basis that the parameter u directly affects only the highest derivative of the controlled parameter y:

$$\frac{\partial G(u)}{\partial u}=-\left(\ddot{y}_d-\ddot{y}\right)\frac{\partial \ddot{y}}{\partial u}.$$

Differential control law takes the following form:

$$\ddot{u}+h\dot{u}=\sigma k(\ddot{y}_d-\ddot{y});\ \ k>0;\ \ \sigma=\operatorname{sign}\left(\frac{\partial \ddot{y}}{\partial u}\right), \tag{1}$$

where k – the gain in the contour of the control function; sign(·) – Signum function; σ – a parameter that ensures the fulfillment of the sign rule [19].

To ensure high dynamic control accuracy, let's set the reference model in the following form:

$$T_r^2\ddot{e}=Ke_g-2\zeta_r T_r\dot{e}-e;$$

$$e=y_g-y;\quad K=1;\quad \zeta_r=1;\quad e_g=0,$$

where e – the control error, e_g – the specified value of the control error; y_g – the specified value of the controlled variable; T_r – the time constant of the reference model, K – the gain of the reference model, ζ_r – the damping coefficient of the reference model.

Let's single out from the reference model the highest derivative of the controlled parameter, which will be the desired acceleration of the controlled variable $\ddot{y}_d$:

$$\ddot{y}_d=\ddot{y}_g+\frac{2}{T_r}\dot{e}+\frac{1}{T_r^2}e.$$

The parameter $\ddot{y}_d$ is substituted into the control law equation (1).

To select the controller parameters k and h, it is necessary to estimate the time constant of the control function loop. The speed of the control loop u must be significantly higher than the speed of the reference model [19]:

$$\frac{T_r}{T_u} = c >> 1,$$

where T_u – the time constant of the contour of the control function; c – the parameter that determines the relationship between T_r and T_u.

Based on the recommendations of [19], let's construct the differential equation of the contour of the control function:

$$\left.\begin{aligned} & T_u^2\ddot{u} = u_{opt} - 2\zeta T_u\dot{u} - u; \\ & T_u^2 = \frac{|\alpha|}{k};\ 2\zeta T_u = \frac{|\alpha|h}{k};\ \zeta = 1;\ \alpha = \left(\frac{\partial\ddot{y}}{\partial u}\right)^{-1}, \end{aligned}\right\} \tag{2}$$

where α – a parameter characterizing the inertia of the control object; ζ – the damping coefficient; u_{opt} – a control action that delivers the absolute minimum of the functional G(u). The sign of the parameter α corresponds to the sign of the parameter σ, so it declined and the absolute value of α remained in the equation.

If it is impossible to estimate the parameter α of the control object, then it is proposed to adjust the controller as follows. First, set the time constant of the reference model T_r and the coefficient c. On the basis of them by combining expressions with the participation of T_u with (2) determine the parameter h:

$$h = 2T_r^{-1}c.$$

Further increase the value of the parameter *k* until the controller will not provide the desired dynamic characteristics of the ACS.

The control law in the form (1) permits a reduction of the order to *u*, that is, two orders of magnitude. Let's substitute $\ddot{y}_d$ in the control law and integrate it twice and obtain [20]

$$\left.\begin{aligned} & u = \sigma k\left(e + \frac{2}{T_r}e_i\right) + \chi_i;\ \chi_i = \int_0^t \chi dt + C_2;\ e = y_g - y; \\ & e_i = \int_0^t e dt + C_1;\ \chi = \frac{\sigma k}{T_r^2}e_i - hu;\ k > 0;\ \sigma = \mathrm{sign}\left(\frac{\partial\ddot{y}}{\partial u}\right), \end{aligned}\right\} \tag{3}$$

where $C_{1,2}$ – the integration constant, their value is usually taken to be zero.

The control law (3) makes it possible to ensure a high dynamic accuracy of controlling a second-order nonlinear object under uncertainty conditions without using information about derivatives of a controlled quantity.

4. 3. Improvement of the method of eliminating integral saturation and controller synthesis for controlling a second-order object

When controlling real objects, the ACS should take into account the constraints of control actions that lead to integral saturation and a decrease in the quality of control. A well-known method for eliminating integral saturation is the integration method according to the condition [21], which provides for the termination of integration when the control action is out of allowable limits. After the control action enters the allowable range, the integration will continue from the value that was before the moment of entering the saturation.

With a step change in the control task y_g or with its rapid increase, an overshoot is observed, due to the following. When the ACS is in the saturation zone, the law of control can produce the value of an unlimited control action $\hat{u}$ that is much higher than the limit values: $|\hat{u}| >> 1$. For large k integrators go out of saturation as y approaches y_g, that is, for small $|e|$. Not having had time to work out the minimization of the functional G(u), the ACS again enters the saturation zone.

It is proposed to improve the ACS performance by adjusting the initial integration conditions after the ACS has entered the saturation zone. Let's adjust the initial condition of the integrator for the parameter e. The value of the initial condition will be formulated so that when a controller $\hat{u}$ drops into the saturation zone, the controller transfers it to the edge of this zone. Since the value of χ_ι depends on e_i, and the value of e_i will be changed artificially, the value of χ_ι obtained by integration loses its meaning. Therefore, the initial condition of the integrator for the parameter χ_ι is set equal to zero. The expression for the initial condition of the parameter e_i is obtained on the basis of the control law:

$$e_{iIC} = \frac{T_r}{2\sigma k}\left(\operatorname{sign}(\hat{u}) - \sigma k e - \chi_{iIC}\right); \;\; \chi_{iIC} = 0, \tag{4}$$

where χ_{iIC} – the initial condition of the integrator for the parameter χ_ι.

At the next iteration of the calculation of the control action, the equation for the control action as the value of e_i will only get the calculated value of e_{iIC} and the resulting value $\hat{u}$ will fall into the vicinity of the saturation limit.

Resetting the integrator of the parameter e_i to the value of e_{iIC} will allow the ACS to leave the saturation zone faster and work out the minimization of the functional G(u), thereby improving the quality of the ACS operation.

The effect of high-frequency switching control is observed when the computer implementation of the control law (3) with the adjustment of the initial conditions. It is due to the fact that resetting the integrator of the parameter e_i to the value of e_{iIC} causes the ACS to operate at the saturation limit. The amplitude of such a switch can be either imperceptible or reach large values depending on the parameters of the object, the controller and the integration step. To reduce this effect, it is proposed to expand the zone $\hat{u}$ when determining signs of saturation s. In addition, in order to avoid incorrect values of u in the saturation mode, it is proposed to replace $\operatorname{sign}(\hat{u})$ with $\operatorname{sign}(e)$.

The control law, taking into account the constraints of the control action and with the adjustment of the initial conditions of integration, takes the following form:

$$\left.\begin{aligned}
& u(\hat{u}) = \begin{cases} \hat{u}, \text{at } \hat{u} \in [-1, 1]; \\ \operatorname{sign}(e), \text{otherwise}, \end{cases} \\
& s(\hat{u}) = \begin{cases} \text{false, at } \hat{u} \in [-K_s, K_s]; \\ \text{true, otherwise}; \end{cases} \\
& \hat{u} := \sigma k\left(e + \frac{2}{T_r} e_i\right) + X(\chi, s, 0, t); \\
& e_i := X(e, s, e_{iIC}, t); \;\; \chi = \frac{\sigma k}{T_r^2} e_i - hu; \\
& e_{iIC} = \frac{T_r}{2\sigma k}\left[K_s \operatorname{sign}(e) - \sigma k e - X(\chi, s, 0, t)\right]; \\
& k > 0; \;\;\; \sigma = \operatorname{sign}\left(\frac{\partial \ddot{y}}{\partial u}\right); \;\; K_s \geq 1,
\end{aligned}\right\} \tag{5}$$

where K_s – the coefficient of expansion of the zone of allowable values $\hat{u}$; $X(\cdot)$ – the integrator model, the integrand is specified as the first argument, the sign of saturation is given as the second argument, the initial condition of integration is entered as the third argument, and time is the fourth argument.

The block diagram of the controller built on its basis is shown in **Fig. 2**.

The "Sat" block in the controller structure (**Fig. 2**) calculates the parameter s and the limited control action u, which is applied to the object, based on its unlimited value $\hat{u}$.

As a result of improving the method of eliminating integral saturation, a controller of high dynamic accuracy is obtained by a second-order object, able to work in conditions of uncertainty.

The controller input receives the difference between the given y_g and the actual y values of the controlled parameter, that is, the control error e. The output is a control action u.

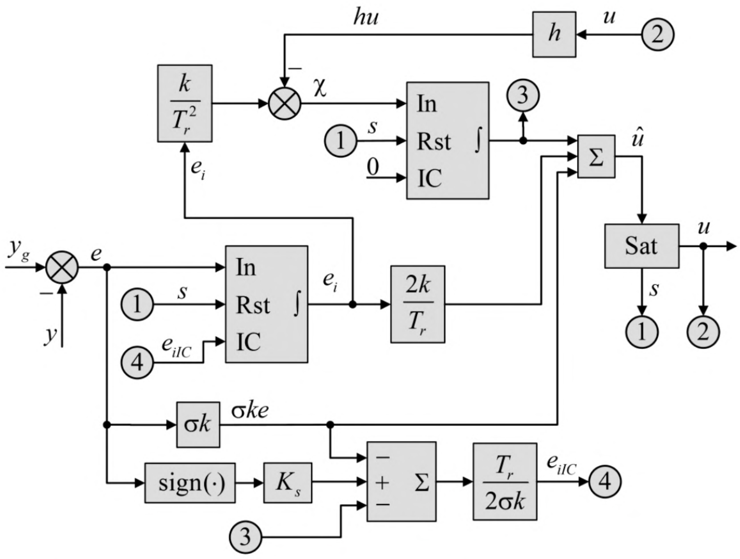

Fig. 2. Block diagram of the controller with the adjustment of the initial conditions

4. 4. Synthesis and investigation of the automatic control system of TUV rotational motion

The synthesis of a multidimensional ACS by the TUV rotational motion provides for controller adjustments of the TUV roll and pitch and the coordination of their work.

Based on the results of simulation modeling, the controller parameters of the roll and pitch are selected (**Table 1**).

Table 1
Parameters of roll and pitch controllers

Parameter	Roll controller	Pitch controller
T_r, s	0,5	0,5
s	5	5
k, deg^{-1}	1	2
h, s^{-1}	20	20
σ	1	1
K_s	1,06	1,06
u_{left}	$-u_\theta$	u_ψ
u_{right}	$+u_\theta$	u_ψ

In **Table 1**: u_θ – the output of the roll controller, u_ψ – the output of the pitch controller.

Such a choice of parameters provides high dynamic control accuracy with a sinusoidal control task and a small overshoot with a step change in the control task. It was possible to reduce the overshoot due to the adjustment of the initial conditions of integration in the control process. **Fig. 3, 4** show the ACS simulation results by the TUV pitch with a step change in the control task.

In **Fig. 4, 5**: ψ_g – the set value of the pitch, ψ – the actual value of the pitch (controlled quantity).

TUV depth was reduced to 19.5 m at ψ>0 (pitch at the stern) and increased to 20.5 m at ψ<0 (pitch to the bow).

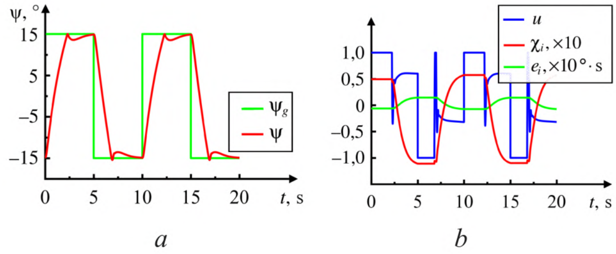

Fig. 3. ACS simulation results by the TUV pitch with an algorithmic prohibition of integration at a towing speed of 1 m/s: *a* – control task and controlled parameter; *b* – control signal and the values of the integrated parameters

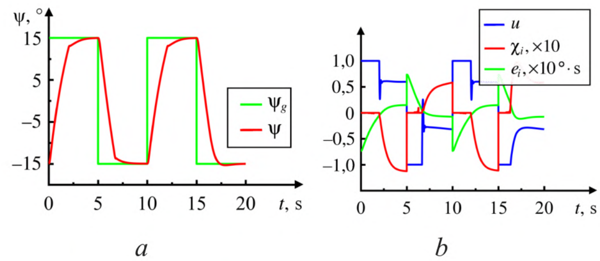

Fig. 4. ACS simulation results by TUV pitch with the adjustment of the initial conditions at a towing speed of 1 m/s: *a* – control task and controlled parameter; *b* – control signal and the values of the integrated parameters

As it is possible to see, the use of an improved method for eliminating integral saturation (**Fig. 4**) provides a reduced overshoot compared to the classical method of integrating the condition (**Fig. 3**).

Fig. 5, 6 show the results of ACS simulation with the TUV roll with a harmonious change in the control task and various towing speeds.

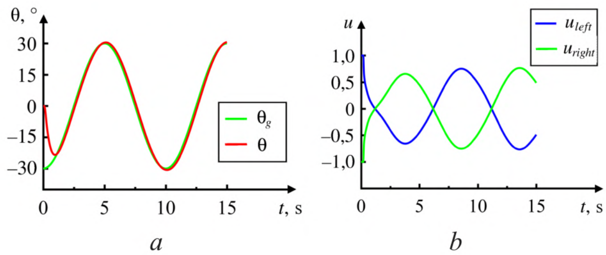

Fig. 5. ACS simulation results by TUV roll at a towing speed of 1 m/s: *a* – set and controlled values, *b* – control actions

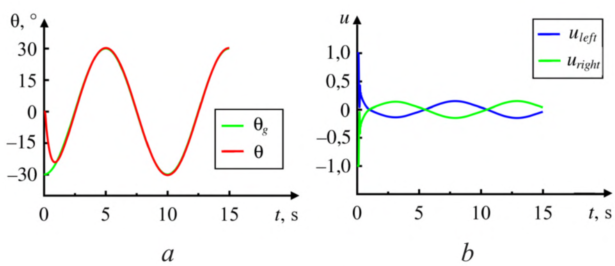

Fig. 6. ACS Simulation results by TUV roll at a towing speed of 3 m/s: *a* – set and controlled values, *b* – control actions

In **Fig. 5, 6**: θ_g – the given value of the roll, θ – the actual value of the roll (controlled quantity).

The control task changes in such a way that the ACS enters saturation only at the beginning of the simulation, when the control error is of great importance. Such parameters of the control task are selected in order to assess the controller accuracy.

The simulation results show a high dynamic accuracy of the controllers of the TUV angular orientation at different towing speeds (from 1 to 3 m/s) and various forms of the control task. But these results were obtained when controllers were working separately from each other.

For automatic control of the TUV multidimensional rotational motion it is necessary to coordinate the operation of the roll and pitch controllers. First of all, let's coordinate the outputs of the roll u_θ and pitch controllers u_ψ:

$$u_{left} = u_\psi - u_\theta; \;\; u_{right} = u_\psi + u_\theta.$$

Each control wing can influence both the roll and the pitch of TUV. The main problem with the coordination of controlled actions is the saturation of control loops. For example, the control action u_{left} or u_{right} can get into saturation even if the outputs of the controllers u_θ and u_ψ are within acceptable limits. This leads to deterioration in the control quality. The sign of saturation can be formed by the variables u_{left} and u_{right}. But this will not improve the control quality, since the integrators of all control circuits are reset. This will lead to additional deviations of the controlled values from their specified values.

To coordinate the controller operation, a method is proposed, which is based on adjusting the initial conditions of the controller with greater error. Its essence is as follows. First, to determine the sign of ACS saturation with the TUV angular position *s* on the basis of the outputs of the roll and pitch controllers:

$$s(u_\theta, u_\psi) = \begin{cases} \text{true, at } |u_\psi| + |u_\theta| > 1; \\ \text{false, otherwise.} \end{cases}$$

Let's note that the qualities u_θ and u_ψ are taken to limit the outputs of the roll and pitch controllers.

Next, let's determine how much it is necessary to reduce the output of one of the controllers in order to derive the ACS from the saturation zone; let's denote this value by u_Δ:

$$u_\Delta = |u_\psi| + |u_\theta| - 1.$$

The main feature that will determine which of the controllers should be reset is the difference between roll control errors e_θ and pitch e_ψ. If the absolute value of the pitch error e_ψ exceeds the absolute value of the roll error e_θ, then reset the pitch control integrators. If the absolute value of roll error e_θ exceeds the absolute value of pitch error e_ψ, then reset the roll controller integrators. If the errors are the same, then reset both controllers:

$$s_\theta(e_\psi, e_\theta, s) = \begin{cases} \text{true, at } s \wedge |e_\psi| \le |e_\theta|; \\ \text{false, otherwise;} \end{cases}$$

$$s_\psi(e_\psi, e_\theta, s) = \begin{cases} \text{true, at } s \wedge |e_\psi| \ge |e_\theta|; \\ \text{false, otherwise;} \end{cases}$$

$$e_\theta = \theta_g - \theta,$$

$$e_\psi = \psi_g - \psi,$$

where $s_{\theta,\psi}$ – the dump flags of integrators of roll and pitch controllers, respectively.

The initial integration conditions after the reset also need to be adjusted to the fact that due to the output of which is removed from the ACS controllers from the saturation zone:

$$u_{\psi.IC}=\begin{cases}\operatorname{sign}(u_\psi)\left(\left|u_\psi\right|-u_\Delta\right), \text{at} \left|e_\psi\right|>\left|e_\theta\right|;\\ u_\psi, \text{at} \left|e_\psi\right|<\left|e_\theta\right|;\\ u'_\psi, \text{at} \left|e_\psi\right|=\left|e_\theta\right|.\end{cases}$$

$$u_{\theta.IC}=\begin{cases}u_\theta, \text{at} \left|e_\psi\right|>\left|e_\theta\right|;\\ \operatorname{sign}(u_\theta)\left(\left|u_\theta\right|-u_\Delta\right), \text{at} \left|e_\psi\right|<\left|e_\theta\right|;\\ u'_\theta, \text{at} \left|e_\psi\right|=\left|e_\theta\right|.\end{cases}$$

If the absolute values of the error control level than ASC is derived by the means of both controllers. In this case, it is also necessary that the controls u_{left} and u_{right} are within acceptable limits. For this, the normalization factor k_u will be calculated:

$$k_u=\begin{cases}1, \text{at} \max\left(\left|u_{left}\right|,\left|u_{right}\right|\right)<1;\\ \max\left(\left|u_{left}\right|,\left|u_{right}\right|\right), \text{otherwise}.\end{cases}$$

Based on it, the parameters u'_θ and u'_ψ are calculated:

$$u'_\psi=\frac{u_\psi}{k_u};\ u'_\theta=\frac{u_\theta}{k_u}.$$

Initial conditions will be determined similarly to (4):

$$e_{\theta,\psi.iIC}=\frac{T_r}{2\sigma k}\left(u_{\theta,\psi.IC}-\sigma k e_{\theta,\psi}\right).$$

The coefficient K_s of the controllers should be chosen to be slightly less than one, so that after resetting the control loops that are not immediately saturated.

Thus, the ACS of TUV rotational motion consists of matched controllers of the TUV roll and pitch. These controllers are synthesized on the basis of the control law (5) and agreed upon on the basis of the proposed method for adjusting the initial conditions of the controller with greater error.

Let's perform simulation of synthesized ACS of TUV rotational motion. With a harmonious change of the control task, the ACS provides high dynamic control accuracy if it does not fall within the saturation zone.

Fig. 7 shows the ACS transient processes by TUV rotational motion in conditions of uncertainty.

The parameters of the control task are chosen so that after the completion of the transition process, one of the controlled variables starts the transition process on the other controlled quantity. This made it possible to assess the influence of the control circuits on each other.

As it is possible to see, when operating without coordination, transients for eliminating errors affect other control loops and cause a deterioration in quality (**Fig. 7, *a, c***). And when using the ACS with the coordination of control actions based on the proposed method of adjusting the initial conditions, the quality of control almost does not deteriorate (**Fig. 7, *b, d***).

The synthesized ACS provides high precision control of the TUV two-dimensional rotational motion in conditions of uncertainty. It is the basis for the synthesis of ACS of TUV transitional motion in space.

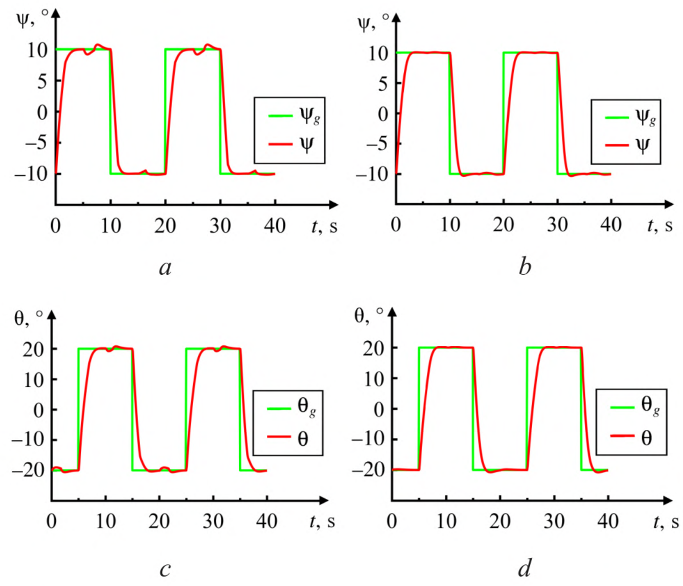

Fig. 7. ACS simulation results by the TUV rotational motion: *a* –TUV pitch, ACS without matching; *b* – TUV pitch, ACS with matching; *c* – TUV roll, ACS without matching; *d* – TUV roll, ACS with matching

5. Conclusions

1. Based on the analysis of the most common hydrodynamic forms of towed underwater vehicles, features of controlling them at shallow depths for the synthesis of automatic control systems for their motion have been established.

2. The integration-by-condition method has been improved to eliminate the integral saturation of the automatic control system by forming the initial integration conditions so that when a control hits the saturation zone, the reset of the controller integrators will transfer it to the edge of this zone.

3. On the basis of the improved integration-by-condition method and the method of minimizing local functionals, the control law and the structure of the high dynamic precision controller have been synthesized for a second-order nonlinear object as the theoretical basis for the synthesis of automatic control systems for underwater vehicle controlled degrees of freedom in conditions of uncertainty.

4. Roll and pitch controllers of the towed underwater vehicle have been synthesized based on the second order control law and improved integration-by-condition method as the basis for the synthesis of a two-dimensional automatic control system of the towed underwater vehicle.

5. The automatic control system for the rotational motion of a towed underwater vehicle has been synthesized based on synthesized roll and pitch controllers and the proposed method for matching control circuits, which provides high dynamic accuracy of controlling the two-dimensional rotational motion of a towed underwater vehicle under conditions of uncertainty and is the basis for the synthesis of an automatic control system for its translational motion in space.

References

[1] Podvodnye tekhnologii i sredstva osvoeniya Mirovogo okeana (2011). Moscow: Oruzhie i tekhnologii, 779.

[2] Rimskiy-Korsakov, N. A. (2017). Tekhnicheskie sredstva dlya issledovaniy dna akvatoriy gidrolokacionnymi metodami. Mezhdunarodniy zhurnal prikladnyh i fundamental'nyh issledovaniy, 10, 205–213.

[3] Blintsov, O. V., Nadtochiy, A. V. (2014). The generalized underwater technics efficiency estimation methodology of deep sea archaeological projects. Eastern-European Journal of Enterprise Technologies, 1 (3 (67)), 25–29. doi: https://doi.org/10.15587/1729-4061.2014.21045

[4] Nadtoshy, A. (2016). Identification of risks in the course of managing the deep sea archeological projects using marine robotics. EUREKA: Physics and Engineering, 6, 59–64. doi: https://doi.org/10.21303/2461-4262.2016.00244

[5] Blintsov, V., Hrytsaienko, M. (2016). Improvement of the management of material and technical resources of water cleaning projects from explosive objects. Technology Audit and Production Reserves, 6 (2 (32)), 51–56. doi: https://doi.org/10.15587/2312-8372.2016.86768

[6] Mohamed, H., Nadaoka, K., Nakamura, T. (2018). Assessment of Machine Learning Algorithms for Automatic Benthic Cover Monitoring and Mapping Using Towed Underwater Video Camera and High-Resolution Satellite Images. Remote Sensing, 10 (5), 773. doi: https://doi.org/10.3390/rs10050773

[7] Dudykevych, V., Oleksandr, B. (2016). Tasks statement for modern automatic control theory of underwater complexes with flexible tethers. EUREKA: Physics and Engineering, 5, 25–36. doi: https://doi.org/10.21303/2461-4262.2016.00158

[8] Linklater, A. (2005). Design and Simulation of a Towed Underwater Vehicle. Thesis submitted to the Faculty of the Virginia Polytechnic Institute and State University in partial fulfillment of the requirements for the degree of Master of Science In Aerospace Engineering. Blacksburg. Virginia, 170.

[9] Choi, J.-K., Shiraishi, T., Tanaka, T., Kondo, H. (2011). Safe operation of an autonomous underwater towed vehicle: Towed force monitoring and control. Automation in Construction, 20 (8), 1012–1019. doi: https://doi.org/10.1016/j.autcon.2011.04.002

[10] Feng, D. K., Zhao, W. W., Pei, W. B., Ma, Y. C. (2011). A New Method of Designing Underwater Towed System. Applied Mechanics and Materials, 66-68, 1251–1255. doi: https://doi.org/10.4028/www.scientific.net/amm.66-68.1251

[11] Chuanlong, L., Yuwen, Z., Xulong, Y. (2012). Simulation of Recycling Cable in Underwater Towed System. Proceedings of the 1st International Conference on Mechanical Engineering and Material Science. doi: https://doi.org/10.2991/mems.2012.38

[12] Srivastava, V. K., Tamsir, M. (2011). Dynamic behavior of underwater towed cable in linear profile. International Journal of Scientific & Engineering Research, 2 (7). Available at: https://pdfs.semanticscholar.org/fe04/8af7057476a54f47dbd7c344e6b59d854fcf.pdf

[13] Paifelman, E. (2017). A comparison between mathematical models of stationary configuration of an underwater towed system with experimental validations for oceans'17 MTS/IEEE Aberdeen conferences. Conference: OCEANS 2017 – Aberdeen. doi: https://doi.org/10.1109/oceanse.2017.8084854

[14] Wang, G., Rong, B., Tao, L., Rui, X. (2012). Riccati Discrete Time Transfer Matrix Method for Dynamic Modeling and Simulation of an Underwater Towed System. Journal of Applied Mechanics, 79 (4), 041014. doi: https://doi.org/10.1115/1.4006237

[15] Minowa, A. (2015). System Analyses and motion Control of a Towed Underwater Vehicle. Master's Thesis. Graduate School of Marine Science and Technology. Tokyo University of Marine Science and Technology.

[16] Blintsov, O. V., Sokolov, V. V. (2017). Specialized simulating complex for studying motion dynamics of the towed underwater system. Collection of Scientific Publications NUS, 3. doi: https://doi.org/10.15589/jnn20170308

[17] Blintsov, O. V., Sokolov, V. V. (2018). Imitatsiyna model dynamiky prostorovoho rukhu bezekipazhnoi pidvodnoi buksyruvanoi systemy yak obiekta keruvannia. Innovatsiyi v sudnobuduvanni ta okeanotekhnitsi: mater. IX Mizhnar. nauk.-tekhn. konf., 328–330.

[18] Lukomskiy, Yu. A., Peshekhonov, V. G., Skorohodov, D. A. (2002). Navigaciya i upravlenie dvizheniem sudov. Sankt-Peterburg: Elmor, 360.

[19] Krut'ko, P. D. (2004). Obratnye zadachi dinamiki v teorii avtomaticheskogo upravleniya. Cikl lekciy. Moscow: Mashinostroenie, 576.

[20] Blintsov, O. V., Sokolov, V. V., Korytskyi, V. I. (2018). Avtomatychne keruvannia bezekipazhnym pidvodnym kompleksom systemy monitorynhu akvatoriyi v umovakh nevyznachenosti: mater. VIII Vseukr. nauk.-tekhn. konf. z mizhn. uchastiu. Suchasni problemy informatsiynoi bezpeky na transporti, 19–26.

[21] Denisenko, V. V. (2009). Komp'yuternoe upravlenie tekhnologicheskim processom, eksperimentom, oborudovaniem. Moscow: Goryachaya liniya – Telekom, 608.

Original Research Article: full paper

(2019), «EUREKA: Physics and Engineering» Number 2

GENERALIZED METHOD OF DESIGNING UNMANNED REMOTELY OPERATED COMPLEXES BASED ON THE SYSTEM APPROACH

Volodymyr Blintsov
Department of electrical engineering of ship and robotic complexes
Admiral Makarov National University of Shipbuilding
9 Heroiv Ukrainy ave., Mykolaiv, Ukraine, 54025
volodymyr.blintsov@nuos.edu.ua

Olexandr Klochkov
Department of electrical engineering of ship and robotic complexes
Admiral Makarov National University of Shipbuilding
9 Heroiv Ukrainy ave., Mykolaiv, Ukraine, 54025
oleksandr.klochkov@nuos.edu.ua

Abstract

Self-propelled underwater systems belong to the effective means of marine robotics. The advantages of their use include the ability to perform underwater work in real time with high quality and without risk to the life of a human operator. At present, the design of such complexes is not formalized and is carried out separately for each of the components – a remotely operated vehicle, a tether-cable and cable winch, a cargo device and a control and energy device. As a result, the time spent on design increases and its quality decreases. The system approach to the design of remotely operated complexes ensures that the features of the interaction of the components of the complex are taken into account when performing its main operating modes. In this paper, the system interaction between the components of the complex is proposed to take into account in the form of decomposition of "underwater tasks (mission) – underwater technology of its implementation – underwater work on the selected technology – task for the executive mechanism of the complex" operations. With this approach, an information base is formed for the formation of a list of mechanisms of the complex, the technical appearance of its components is being formed, which is important for the early design stages. Operative, creative and engineering phases of the design of the complex are proposed. For each phase, a set of works has been formulated that cover all the components of the complex and use the author's existence equations for these components as a tool for system analysis of technical solutions.

The perspective of the scientific task of the creative phase to create accurate information models of the functioning of the components of the complex and models to support the adoption of design decisions based on a systematic approach is shown.

The obtained results form the theoretical basis for finding effective technical solutions in the early stages of designing remotely operated complexes and for automating the design with the assistance of modern applied computer research and design packages.

Keywords: remotely operated vehicles, system approach, design phase, equation of existence.

DOI: 10.21303/2461-4262.2019.00878

1. Introduction

A significant part of the search, inspection, environmental protection and other underwater work is traditionally performed with a wide involvement of remotely operated vehicles (ROV) [1, 2]. Such devices are used, as a rule, from the ship's carrier, on which the control and energy device (CED), cargo device (CD), cable winch (CW) with tether cable (TC) are located.

The main advantages of the ROV use in marine practice include performing work under the control or supervision of a human operator in real time. This ensures the high quality and performance of the ROV underwater mission, eliminates the risk to human life in comparison with traditional diving technologies [3].

A promising direction in the ROV development is the creation of unmanned remotely operating complexes (ROC) based on them, when they are equipped with CDs to fully automate the implementation of the underwater mission and is installed on unmanned carrier ships (CS).

The equipment composition of a typical ROC is shown in **Fig. 1.**

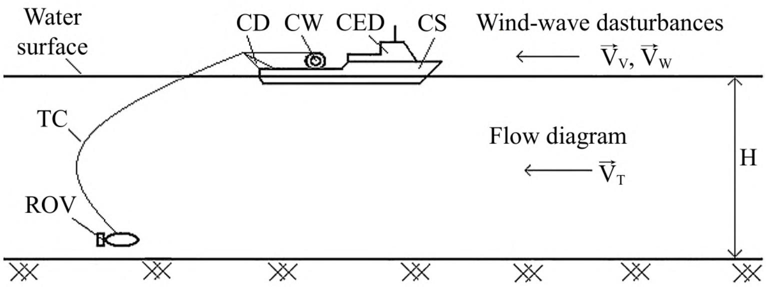

Fig. 1. Equipment composition of a typical ROC

At present, the design and creation of the ROC and ROV is mainly performed as a unique research and engineering activity based on the cognitive approach (that is, not formalized). This increases the duration of the design stage of the creation of such equipment and, ultimately, their cost.

A wide variety of ROV applications and the high relevance of the ROC creation stimulate the development of a generalized methodology for their design as a separate type of marine robotics, based on the achievements of system theory [4].

The main hypothesis of the article is the possibility and expediency of transferring the methodology for the design of the ROVs to the principles of a systems approach as the theoretical basis for automating the processes of their design in the early stages of development.

2. Literature review and problem statement

Modern methods of ROC design cover almost the full range of issues related to the creation of their main component ROVs themselves, their tether cables and control and energy device.

The first scientific papers on this issue were published in the 80s of the last century and quite fundamentally formulated the design tasks of that period and the first technical solutions regarding the ROV and TC as unique oceanographic equipment [5–7].

In further studies, scientists focused on the development and improvement of ROV individual components (engines with electric and hydraulic drives [8], navigation and control systems [9, 10], buoyancy materials [11]), as well as on the creation of attachments and tools for the remote performance of underwater operations [12, 13].

Over the past 10 years, the ROV design has been further developed in the following areas:

– improvement of their manual and automated control systems;

– development of methods for creating cheap ROVs, including for shallow water;

– creation of training ROVs.

For example, in [14], a modular approach to the creation of hardware and software controls for ROV based on the open source platform Visor3 is described. This shortens the development time of the ROV software control systems and simplifies the implementation of their diagnostics and repair modes. The work [15] describes the use of the built-in operating system μC/OS-II, which software gateway ensures the operation and stability of work in real time. The work [16] presents the constructions of controllers used to control the ROV depth control system, which involves the use of elements of artificial intelligence – a fuzzy logic controller SIFLC, an adaptive neuro-fuzzy inference system ANFIS), a controller of fuzzy logic Mamdani and a traditional controller based on the PID controller. The work [17] is devoted to the development of underwater video surveillance systems with the service function of scaling an underwater object.

Recently, in connection with the intensification of underwater operations in shallow water (depths of up to 50–100 meters), there has been a tendency to create cheap ROV, which had high operational properties, in particular, in terms of automation of control and information processing. For example, in [18], an easy-to-use, portable, safe, and reliable ROV is developed that is capable of performing scientific research under the guidance of students. University Teknologi Malaysia scientists have developed and built low cost ROV based on the use of cheap materials (polyvinyl chloride, etc.) [19]. In [20], the mechanical design, propulsion properties, electrical systems, as well as the software architecture of the graphical user interface for creating a shallow-purpose ROV are explained in detail. The work [21] is devoted to the design and development of low-cost miniature ROV for work at shallow depths with complex trajectories of movement.

In [22], a prototype ROV with three degrees of freedom is developed and tested, which is connected to the fuel and energy complex by unshielded twisted pairs of conductors, where a microcontroller is used to transfer data between the joystick and the ROV.

In addition to these areas, scientists are working on issues of an integrated approach to the ROV creation.

Thus, in [23], designs of naval ROV, which provide reliable visual information for the observation and maintenance of ship hulls and underwater structures of Columbia port equipment, are presented. The design is presented as a complex of four main subsystems: mechanical naval, computer hardware and software, navigation and control. The most responsible design solutions are evaluated taking into account environmental conditions, size limitations, hydrostatics, hydrodynamics, degrees of freedom, the availability of instruments and control equipment. The CAD-CAE and CFD (Computational Fluid Dynamics) computing tools are used as design and research tools.

Significant results are obtained in the direction of the practical creation and application of the ROV. For example, in [24], the design and creation of the ROV Ariana-I created at the University of Shiraz (IR Iran) is described. This system is equipped with sensors of rotation, pitch, roll and depth, which provide a sufficient number of feedback signals, giving the system six degrees of freedom. The video system is based on the Ethernet equipment, the control and feedback of the sensors are transmitted via the RS485 bus, and the video signal, the signaling of water flow and the battery charging wire on one multicore cable.

Research [25, 26] focuses on the ROV development, which use experimental data transmission systems through the acoustic channel, inertial sensors, numerical simulation in Matlab (Simulink), etc.

Research [27] presents the concept of the ROV design for the inspection of underwater oil and gas fields, in which the control of spatial motion is performed using vectorized propellers.

Important ROV variants are created for the inspection of underwater pipelines [28], for remote investigation of the underwater environment with the transmission of information via cable to the coast station [29].

A number of ROVs are designed and created for educational tasks, in particular, for preparing students of colleges and universities [30–33].

The most thorough studies in the areas of the ROV design and their control systems in recent years have been performed in [34–36]. Thus, the work [34] presents the ROV development and construction, which differ conceptually depending on their application – micro, mini, light, heavy classes of ROV, etc. The paper [35] addresses the issues of ROV and ROC classification, while the paper [36] proposes the concept of representing the ROC as a maritime object with flexible connections.

These and other scientific work in the direction of the ROC design are associated with the research of their individual components – ROV, TC, control systems and the like. However, the issue of creating a unified methodology for the ROC design in the composition of the ROV, TC, CW, CD and CED as a marine complex, designed to function as a single system, is not covered in modern scientific literature. The urgency for the maritime practice of creating such complexes is due to the need to perform a wide range of underwater missions in automatic mode, including from the unmanned CS.

The creation of such complexes is a complex applied scientific task; therefore, their design should be carried out on the basis of a system approach.

The aim of research is development of a generalized ROC design methodology based on a systematic approach as a theoretical basis for finding technical solutions in the early stages of their design.

To achieve the aim it is proposed to solve the following tasks:

– to establish the features of the application of a systematic approach to the ROC design;

– to develop the substantive part of the design procedure for ROC, which implements the principles of the system approach.

3. The results of the development of a generalized methodology for the ROC design

3. 1. Features of the application of a systematic approach to the ROC design

The essence of the system approach *S* to design a modern high-tech and market competitive product is considering the functioning of the components of the product, taking into account their interaction [37]. Such interaction between the ROC components (**Fig. 1**) should be analyzed in the following sequence of operations:

– underwater tasks U_Z, which should accomplish the ROC;

– underwater technology U_T, which should be implemented by the ROC to perform the task U_Z;

– a lot of underwater work U_J, which must be performed using this technology U_T;

– a lot of tasks U_V for Y_{ROC} actuators that implement the U_J.

Thus, there is the following sequence of operations of the designer-systems engineering for the ROC design:

$$S=U_Z \to U_T \to U_J \to U_F. \quad (1)$$

The set of tasks U_F forms the information base for the formation of a list of Y_{ROC} mechanisms and can be used to form the technical appearance of future ROC components – ROV, CW, CD, CED, as well as to form requirements for the TC operational properties.

The ROC design based on the principles of a systematic approach (analysis of the functioning of the ROC components, taking into account their interaction and taking into account the influence of the environment) can be represented by the following phases:

– formulation of the main factors of its future application X_P (production phase, the final product of which is the development of technical requirements (technical specifications) G to the future of the product;

– product design (creative phase, the end result of which P_P is the overall structure and composition of product K, its previous material M, energy E, informational I and operational J characteristics) [38];

– technical design of the product C_P (the engineering phase, the end result of which is the technical design – a set of drawings and other technical documentation, in general, meet the technical requirements G).

Thus, in the general case, from the standpoint of a systematic approach to the design of a modern high-tech and market competitive product, it is possible to present a variety of basic operations:

$$S=\{X_P;\ P_P;\ C_P\}|_G. \quad (2)$$

Let's consider these design phases in more detail.

3. 2. Development of the content part of the ROC design methodology

In the case of ROC creation as a whole market product, the components of a systematic approach can be formulated as follows.

The formulation of the main factors of the ROC use X_P (production phase – external design):

– definition and preliminary analysis of information about the basic underwater task $A=\{A_1,\ldots A_N\}$, which should be carried out by the ROC;

– determination of the characteristics of the aquatic environment Z, in which the ROC should work (characteristics of the working area (depth H, wind $\vec{V}_V$ and wave $\vec{V}_W$ disturbances, diagrams of the underwater flow $\vec{V}_T$, hydrophysical X_{HF} and hydrochemical X_{HC} characteristics of the aquatic environment, etc.).

Thus, the staged phase of the ROC creation can be described by the following sets of design works:

$$X_P=\{A;\ Z\}; \quad (3)$$

$$A=\{A_1,\ldots A_N\};\tag{4}$$

$$Z=\left\{H;\vec{V}_V;\vec{V}_W;\vec{V}_T;X_{HF};X_{HC}\right\},\tag{5}$$

where N – the number of basic underwater tasks for the created ROC.

ROC design P_P (creative phase – internal design):

– definition and analysis of design constraints on the created ROC O_{ROC} – mass-dimensional O_M, energy O_E, information O_I, operational O_J, cost O_{Ek};

– determination of preliminary information on the structure and composition of K_{ROC} equipment of ROC components (underwater vehicle K_{ROV}, cable K_{TC}, cable winch K_{CW}, cargo device K_{CD} and control and energy device K_{CED}), which are necessary for underwater tasks A;

– substantiation of the ROV architectural-constructive type Q_{ROV} as the central task of the creative phase – the hydrodynamic type of the ROV case, the arrangement of the propulsive-steering devices and the external replaceable tool, etc.;

– development of virtual 3D-models of VM ROC components (VM_{ROV}, VM_{TC}, VM_{CW}, VM_{CED} та VM_{CD});

– development of mathematical models MM as an instrumental basis for the ROC analysis – models of ROC operation in quasi-stationary and dynamic modes MM_F, necessary to verify the compliance of the complex being created with the technical requirements G, and economic-mathematical models MM_E (models of the cost of creating ROC with a certain structure and composition K) to verify compliance with the requirements of value constraints O_{Ek};

– a preliminary analysis of the possibility of ROC creation according to specified technical requirements G on the basis of solving the equations of the ROC existence R_{ROC} [38] This analysis is performed by compiling and solving the equations of the material characteristics of the ROC components R_M (ROC mass and volume balance equations, etc.), the energy balance equations of the ROC components R_E, the equations of their information support R_I, and the equations providing the ROC performance characteristics R_J; the numerical values of these equations are formed using data on the characteristics of the ROC components contained in the database DB of previously created ROV, TC, CW, CD and CED, as well as market-accessible nodes and systems of the specified equipment;

– in the case of a positive result of the preliminary analysis, the database of the component parts DB_K and the construction materials DB_M for the ROC components are generated, based on information from the DB;

– in the case of a negative result of the preliminary analysis, a search is made for solutions to adjust the structure and/or replace equipment K of ROC components or an order is created for designing and creating new equipment.

Thus, the implementation of a systems approach in the ROC design provides for the implementation of the following set of design works (creative phase):

$$P_P=\{O_{ROC};\ K;\ Q_{ROV};\ VM;\ MM;\ R_{ROC};\ (M;\ E;\ I;\ J)|_{DB}\};\tag{6}$$

$$O_{ROC}=\{O_M;\ O_E;\ O_I;\ O_J;\ O_{Ek}\};\tag{7}$$

$$K_{ROC}=\{K_{ROV};\ K_{TC};\ K_{CW};\ K_{CED};\ K_{CD}\};\tag{8}$$

$$VM=\{VM_{ROV};\ VM_{TC};\ VM_{CW};\ VM_{CED};\ VM_{CD}\};\tag{9}$$

$$MM=\left\{MM_F\big|_G;\ MM_E\big|_{O_E}\right\};\tag{10}$$

$$R_{ROC}=\{R_M;\ R_E;\ R_I;\ R_J\}|_G;\tag{11}$$

$$M=\{M_{ROV};\ M_{TC};\ M_{CW};\ M_{CED};\ M_{CD}\}|_{DB};\tag{12}$$

$$E=\{E_{ROV}; E_{TC}; E_{CW}; E_{CED}; E_{CD}\}|_{DB}; \tag{13}$$

$$I=\{I_{ROV}; I_{TC}; I_{CW}; I_{CED}; I_{CD}\}|_{DB}; \tag{14}$$

$$J=\{J_{ROV}; J_{TC}; J_{CW}; J_{CED}; J_{CD}\}|_{DB}. \tag{15}$$

Obviously, a promising scientific task of the creative phase is the automation of the ROC design processes based on the creation of accurate information models of their operation in specified modes *A* and models to support the adoption of design decisions based on a systems approach.

ROC technical design C_P (engineering phase – internal design):

– execution of design calculations B_{ROC}, confirming the performance and reliability of the ROC components, confirming compliance with the technical requirements of G to it and the implementation of design constraints O_{ROC} on its creation;

– development of project documentation (drawings) D_{ROC}, necessary for the manufacture of new components and systems for ROC components;

– development of documentation D_M and D_K for the purchase, respectively, of materials and ROC components and systems, which are included in the project from the databases DB_M and DB_K;

– development of documentation on the preliminary feasibility study for the ROC creation D_{TEO}.

Thus, the implementation of a systems approach in the ROC technical design provides for the implementation of the following set of design and engineering works (engineering phase):

$$C_P=\{B_{ROC}; D_{ROC}; DB_M; DB_K; D_{TEO}\}; \tag{16}$$

$$B_{ROC}=\{B_{ROV}; B_{TC}; B_{TW}; B_{CED}; B_{CD}\}\big|_{G,O_{ROC}}; \tag{17}$$

$$D_{ROC}=\{D_{ROV}; D_{TC}; D_{CW}; D_{CED}; D_{CD}\}|_{BD}; \tag{18}$$

$$D_M=\{D_{MROV}; D_{MTC}; D_{MCW}; D_{MCED}; D_{MCD}\}|_{BD}; \tag{19}$$

$$D_K=\{D_{KROV}; D_{KTC}; D_{KCW}; D_{KCED}; D_{KCD}\}|_{BD}; \tag{20}$$

The relation (1)–(20) form the basis of the methodology of ROC design based on the system approach methodology. The formed list of design works of the production phase and design and construction phases of the ROC can be easily formalized by mathematical and computer modeling methods, makes it possible to involve modern CAD/CAM/CAE software packages in design, and CFD packages to study their operation.

4. Discussion of the generalized methodology for ROC design

ROCs form a large class of underwater robotics facilities. The significant advantages of their use include the ability to remotely perform underwater work in real time and without risk to the life of a human operator. Modern methods of designing such complexes are poorly systematized and relate to the design of their individual components – remotely operated vehicles, their tether cables and control systems. This increases the duration of the design work and reduces their quality.

Unmanned technologies for the implementation of underwater work require a systematic approach to the process of ROC design, which involves taking into account the peculiarities of the interaction of the components of the complex when performing its main operating modes. This allows to create complexes, the individual components of which are designed from a unified position of system engineers and most fully correspond to the ROC underwater missions.

It is proposed to implement a systematic approach to the ROC design in the form of decomposition of the offshore operation as "underwater tasks (mission) – underwater technology of its implementation – underwater work using the selected technology – a task for the executive mechanism of the complex" chain. This creates an information base for the formation of the list of executive mechanisms of the complex and forms the technical appearance of its components in the early stages of design.

The proposed production, creative, and engineering phases of the ROC design allow to clearly formulate the set of works that cover the design of all components of the complex. An important component of the creative design phase is the use of the developed system of existence of equations of the existence of the system, which allow to systematically evaluate design solutions for material, energy, information and operational characteristics. This allows already in the early stages of design to establish the possibility of ROC creation with specified characteristics.

Obtained for each phase of the set of design works include, in particular, the development of mathematical and virtual 3D-models of the ROC components. This allows to further transfer the design of such complexes on a fully computer technology using modern application software packages.

5. Conclusions

Modern approaches to the ROC and ROV design cover the study of their individual components – ROV, TC and control systems. Approaches to the design of these components as elements of a single automatic underwater complex are not covered in the literature.

The expediency is shown and features of application of the system approach to the unmanned ROC design are established. A system interaction between the components of the complex has been proposed to take into account both the decomposition of "underwater tasks (mission) – underwater technology of its implementation – underwater work according to the chosen technology – the task for the executive mechanism of the complex" operations.

It is proposed to perform the ROC design as a sequential implementation of the staging, creative and engineering phases. For each phase, a number of papers were formulated that cover all the components of the complex (ROV, TC, CW, CD and CED) and use the existence equations for these components as a tool for system analysis of technical solutions.

A promising scientific task of the creative phase is the automation of the ROC design processes based on the creation of accurate information models of their operation in specified modes A and models to support the adoption of design decisions based on a systems approach.

The obtained results form the theoretical basis for finding effective technical solutions in the early stages of ROC design and for automating the design with the involvement of modern applied CAD/CAM/CAE applications and CFD packages.

References

[1] Milne, P. H. (1980). Underwater Engineering Surveys. Gulf Publishing Company, 366.

[2] Yastrebov, V. S., Sobolev, G. P., Smirnov, A. V. et. al. (1981). Sistemy i elementy glubokovodnoy tekhniki podvodnyh issledovaniy. Leningrad: Sudostroenie, 304.

[3] Button, R. W., Kamp, J., Curtin. T. B., Dryden, J. (2009). Unmanned Undersea Vehicles. RAND Corporation, 220.

[4] Luhmann, N. (2012). Introduction to Systems Theory. Polity, 300.

[5] Smrcina, K. L., Fish, J. P. (1989). Remotely Operated Vehicle. Reliability Study. Phase II Final Report. Arlington, 124. Available at: https://apps.dtic.mil/dtic/tr/fulltext/u2/a240672.pdf

[6] Yastrebov, V. S., Gorlov, A. A., Siminskiy, V. V. (1986). Elektroenergeticheskie ustanovki podvodnyh apparatov. Leningrad: Sudostroenie, 208.

[7] Last, G., Williams, P. (1991). An introduction to ROV operations. Oilfield Publications Ltd, 232.

[8] Templeton, J. S. (2006). Offshore Technology in Civil Engineering: Hall of Fame Papers from the Early Years. American Society of Civil Engineers, 160.

[9] Jacak, W. (1999). Intelligent robotic Systems: design, planning, and control. International Federation for Systems Research International Series on Systems Science and Engineering. Vol. 14. Kluwer Academic Publishers, 310.

[10] Triantafyllou, M. S., Hover, F. S. (2003). Maneuvering and Control of Marine Vehicles. Massachusetts, 145.

[11] Molloy, P. (2000). Smart Materials for Subsea Buoyancy Control. Glasgow Theses Service, 369.

[12] Gianluca, A. (2006). Underwater Robots. Motion and Force Control of Vehicle-Manipulator Systems. Springer, 268. doi: http://doi.org/10.1007/11540199

[13] Shostak, V. P. (2011). Podvodnye apparaty-roboty i ih manipulyatory. Moscow: GEOS, 134.

[14] Aristizábal, L. M., Rúa, S., Gaviria, C. E., Osorio, S. P., Zuluaga, C. A., Posada, N. L., Vásquez, R. E. (2016). Design of an open source-based control platform for an underwater remotely operated vehicle. DYNA, 83 (195), 198–205. doi: http://doi.org/10.15446/dyna.v83n195.49828

[15] Liu, W. D., Li, X. Y., Gao, L. (2012). Design of a Gateway for Remotely Underwater Vehicles. Applied Mechanics and Materials, 209-211, 2138–2141. doi: http://doi.org/10.4028/www.scientific.net/amm.209-211.2138

[16] Azmi, M. W. N., Aras, M. S. M., Zambri, M. K. M., Harun, M. H. (2018). Comparison of Controllers Design Performance for Underwater Remotely Operated Vehicle (ROV) Depth Control. International Journal of Engineering & Technology, 7, 419–423.

[17] Girgin, S. (2013). A Design Project of a Remotelyoperated Underwater Vehicle. Izmir.

[18] Guerra, J., Heinevetter, R., Tristan, M., Killian, P., Waschura, A. (2014). Proteus: Mini underwater remotely operated vehicle. Santa Clara University, 115. Available at: https://www.researchgate.net/publication/274698477_Proteus_Mini_Underwater_Remotely_Operated_Vehicle_ROV_Mechanical_Engineering_Thesis

[19] Ahmed, Y. M., Yaakob, O., Sun, B. K. (2014). Design of a New Low Cost ROV Vehicle. Jurnal Teknologi, 69 (7). doi: http://doi.org/10.11113/jt.v69.3262

[20] Anwar, I., Mohsin, M. O., Iqbal, S., Abideen, Z. U., Rehman, A. U., Ahmed, N. (2016). Design and fabrication of an underwater remotely operated vehicle (Single thruster configuration). 2016 13th International Bhurban Conference on Applied Sciences and Technology (IBCAST). doi: http://doi.org/10.1109/ibcast.2016.7429932

[21] Nguyen, D. A., Cao, Q. H., Nguyen, P. H. (2016). Research, Design and Control of a Remotely Operated Underwater Vehicle. 5-th World Conference on Applied Sciences, Engineering & Technology. Available at: https://pdfs.semanticscholar.org/0974/e8a5b7460ee4009cac1f772b0a66ab3726d4.pdf

[22] Wiryadinata, R., Nurliany, A. S., Muttakin, I., Firmansyah, T. (2017). Design of a Low Cost Remotely Operated Vehicle with 3 DoF Navigation. Bulletin of Electrical Engineering and Informatics, 6 (1), 13–23. Available at: https://media.neliti.com/media/publications/61851-EN-design-of-a-low-cost-remotly-operated-ve.pdf

[23] Ramírez, J. A., Vásquez, R. E., Gutiérrez, L. B., Flórez, D. A. (2007). Mechanical/Naval Design of an Underwater Remotely Operated Vehicle (ROV) for Surveillance and Inspection of Port Facilities. Volume 16: Transportation Systems. doi: http://doi.org/10.1115/imece2007-41706

[24] Marzbanrad, A., Sharafi, J., Eghtesad, M., Kamali, R. (2011). Design, Construction and Control of a Remotely Operated Vehicle (ROV). Volume 7: Dynamic Systems and Control; Mechatronics and Intelligent Machines, Parts A and B. doi: http://doi.org/10.1115/imece2011-65645

[25] Wang, Y.-L., Lu, C.-Y. (2012). Design and parameter estimation of a remotely operated underwater vehicle. Design and parameter estimation of a remotely operated underwater vehicle. Journal of Marine Engineering & Technology, 11 (2), 39–48. Available at: https://www.tandfonline.com/doi/pdf/10.1080/20464177.2012.11020265?needAccess=true

[26] García-Valdovinos, L. G., Salgado-Jiménez, T., Bandala-Sánchez, M., Nava-Balanzar, L., Hernández-Alvarado, R., Cruz-Ledesma, J. A. (2014). Modelling, Design and Robust Control of a Remotely Operated Underwater Vehicle. International Journal of Advanced Robotic Systems, 11 (1). doi: http://doi.org/10.5772/56810

[27] Vasantharaj, R., Paravastu, V., Shobana, M., Loganayaki, S. (2014). Remotely Piloted Unmanned Underwater Vehicle Design and Control for Pipeline Maintenance. Proceedings of National Conference on Man Machine Interaction, 40–43.

[28] Joochim, C., Phadungthin, R., Srikitsuwan, S. (2015). Design and development of a Remotely Operated Underwater Vehicle. 2015 16th International Conference on Research and Education in Mechatronics (REM). doi: http://doi.org/10.1109/rem.2015.7380385

[29] Rahimuddin, Hasan, H., Rivai, H. A., Iskandar, Y., Claudio, P. (2018). Design of Omni Directional Remotely Operated Vehicle (ROV). Journal of Physics: Conference Series, 962, 012017. doi: http://doi.org/10.1088/1742-6596/962/1/012017

[30] Lien, B. (2009). Design Your Own Underwater Remotely Operated Vehicle (ROV). Technology Teacher, 68 (7), 22–25. Available at: https://eric.ed.gov/?id=EJ838392

[31] ROV PROGRAM – TEAM MANUAL. Underwater Robotics for High School Students (2010). Eastern Edge Robotics, 63. Available at: https://www.marinetech.org/files/marine/files/Curriculum/Other%20Curriculum%20Resources/MIROV2MANUAL.pdf

[32] Harsh, S., Vignesh, P. (2013). Design, Fabrication & Testing of Underwater Remotely Operated Vehicle. LAP Lambert Academic Publishing, 72. Available at: https://www.amazon.in/Fabrication-Testing-Underwater-Remotely-Operated/dp/3659314099

[33] Bernier, M., Foley, R. T., Rioux, P., Stech, A. (2010). Latis II Underwater Remotely Operated Vehicle Technical Report. The University of MAINE, 20. Available at: http://www.mickpeterson.org/Classes/Design/2009_10/Projects/Website-ROV-Amy/UMaine%20ROV%20Final%20Report.pdf

[34] Roslan, I. S., Muhamad Said, M. F., Abu Bakar, S.A. (2015). Conceptual Design of Remotely Operated Underwater Vehicle. Journal of Transport System Engineering, 1 (2), 15–19.

[35] Certification and Classification of Unmanned Submersibles. Unmanned Submersibles (ROV, AUV) and Underwater Working Machines (2009). Germanishcer Lloyd.

[36] Dudykevych, V., Oleksandr, B. (2016). Tasks statement for modern automatic control theory of underwater complexes with flexible tethers. EUREKA: Physics and Engineering, 5, 25–36. doi: https://doi.org/10.21303/2461-4262.2016.00158

[37] Blanchard, B. S., Fabrycky, W. J. (2006). Systems Engineering and Analysis. Prentice Hall International Series in Industrial & Systems Engineering. Upper Saddle River: Pearson Prentice Hall, 804.

[38] Blintsov, V., Klochkov, O. (2016). Equations of existence selfpropelled underwater system as assessment of the possibility of its creation. Pidvodni tekhnolohiyi, 3, 25–30.

DEVELOPMENT OF THE METAL RHEOLOGY MODEL OF HIGH-TEMPERATURE DEFORMATION FOR MODELING BY FINITE ELEMENT METHOD

Oleg Markov
Department of Computational Design and Modeling Processes and Machines
Donbass State Engineering Academy
72 Akademicheskaya str., Kramatorck, Ukraine, 84313
oleg.markov.omd@gmail.com

Oleksiy Gerasimenko
Department of Computational Design and Modeling Processes and Machines
Donbass State Engineering Academy
72 Akademicheskaya str., Kramatorck, Ukraine, 84313
profalliance@i.ua

Leila Aliieva
Metal working by pressure
Donbass State Engineering Academy
72 Akademicheskaya str., Kramatorck, Ukraine, 84313
leyliali2017@gmail.com

Alexander Shapoval
Department of Manufacturing Engineering
Kremenchuk Mykhailo Ostohradskyi National University
20 Pershotravneva str., Kremenchug, Ukraine, 39600
shapoval_a@kdu.edu.ua

Abstract

It is shown that when modeling the processes of forging and stamping, it is necessary to take into account not only the hardening of the material, but also softening, which occurs during hot processing. Otherwise, the power parameters of the deformation processes are precisely determined, which leads to the choice of more powerful equipment. Softening accounting (processes of stress relaxation) will allow to accurately determine the stress and strain state (SSS) of the workpiece, as well as the power parameters of the processes of deformation. This will expand the technological capabilities of these processes. Existing commercial software systems for modeling hot plastic deformations based on the finite element method (FEM) do not allow this. This is due to the absence in these software products of the communication model of the component deformation rates and stresses, which would take into account stress relaxation. As a result, on the basis of the Maxwell visco-elastic model, a relationship is established between deformation rates and stresses. The developed model allows to take into account the metal softening during a pause after hot deformation. The resulting mathematical model is tested by experiment on different steels at different temperatures of deformation. The process of steels softening is determined using plastometers. It is established experimentally that the model developed by 89...93 % describes the rheology of the metal during hot deformation. The relationship between the components of the deformation rates and stresses is established, which allows to obtain a direct numerical solution of plastic deformation problems without FED iterative procedures, taking into account the real properties of the metal during deformation. As a result, the number of iterations and calculations has significantly decreased.

Keywords: hot deformation, hardening, softening, stress relaxation, FEM, hardening curve, pause, energy-power parameters, forging and stamping.

DOI: 10.21303/2461-4262.2019.00877

1. Introduction

In the FEM study of the hot stamping and forging operations, difficulties arise due to the nonlinearity of the properties of the material during high-temperature deformation [1, 2]. The main idea of the existing methods for taking into account the nonlinearity of these properties is solving the problem in an elastic formulation and use additional iterations (successive approximations) to switch to the plastic properties of a deformable metal [3]. As a result, the total computation time increases, which makes the FEM method less efficient compared to other numerical methods [4]. A more complete account of the mechanical characteristics of the deformable metal is one of the most important reserves of intensification and increasing the efficiency of modeling forging and stamping operations [5].

In the process of hot deformation, the metal is strengthened, at the same time dynamic processes of return, polonium saturation and recrystallization occur, leading to relaxation of stresses (softening) in the material at forging and stamping temperatures [6]. Accounting for the phenomenon of thermal softening of metals and alloys allows to improve the technical and economic indicators of the production of metal products produced by hot deformation [7]. Practice shows that during hot deformation with pauses, it is possible to carry out operations with lower energy consumption for deformation [8]. Therefore, the establishment of a valid metal rheology, which is strengthened and rooted out during hot deformation to establish a stress-strain state is an important task in mechanical engineering [9]. The aim of the work is to develop a mathematical model that would repeat the rheology of the material during the implementation of forging and stamping operations, which will improve the accuracy of FEM and power parameters determination when forging large-sized forgings.

To achieve the aim, the following objectives are set:

– establish an analytical model of stress relaxation in the alloy during hot deformation;

– check the installed model with the actual behavior of the metal during the implementation of hot deformation.

2. Establishment of an analytical model of stress relaxation

When solving FEM problems, it is advisable to establish and set a real relationship between deformation rates $\{\dot{\varepsilon}\}$ and stresses when varying temperature and rate regimes during hot deformation, when viscosity appears in the alloy [10]. This ratio is necessary for setting the plasticity matrix [K] for the FE modeling and determination of stress components [11]

$$\{\sigma\}=[D]\cdot\{\dot{\varepsilon}\}. \tag{1}$$

The main difference between irreversible (viscous) deformations and plastic solids is that the latter depend on the deformation rate, especially at elevated temperatures [12]. The alloy has a viscosity when the deformation rate affects the stress $\sigma=\sigma(\dot{\varepsilon})$. The viscosity of the metal is manifested in the fact that after deformation the internal stresses change with time. For the operations of forging and stamping, when the material is rotated with hardening, the Maxwell relaxing model is an exact model that takes into account the rheology.

The deformation degree, according to this model, consists of elastic $\overline{\varepsilon^e}$ and viscous $\overline{\varepsilon^v}$ components.

$$\bar{\varepsilon}=\overline{\varepsilon^e}+\overline{\varepsilon^v}. \tag{2}$$

Differentiating expression (2), let's obtain:

$$\frac{d\bar{\varepsilon}}{dt}=\dot{\varepsilon}_{xx}=\dot{\varepsilon}_{xx}^{e}+\dot{\varepsilon}_{xx}^{v}; \tag{3}$$

$$\dot{\varepsilon}_{xx}^{e}=\frac{d\bar{\varepsilon}^{e}}{dt}=\frac{d\left(\sigma_{xx}/E\right)}{dt}=\frac{\left(d\sigma_{xx}/dt\right)}{E}; \tag{4}$$

$$\dot{\varepsilon}_{xx}^{v}=\frac{d\overline{\varepsilon^{v}}}{dt}=\frac{\sigma_{xx}}{\nu}. \tag{5}$$

So

$$\frac{d\bar{\varepsilon}}{dt}=\frac{1}{E}\frac{d\sigma_{xx}}{dt}+\frac{\sigma_{xx}}{\nu}, \tag{6}$$

where ν – dynamic viscosity, MPa×s; E – Young modulus, MPa.

Accounting for the stresses σ(0) at the time t=0 and fixed deformation $\left(\frac{d\bar{\varepsilon}}{dt}=0\right)$ of equation (6) takes the form

$$\frac{1}{E}\frac{d\sigma_{xx}}{dt}+\frac{\sigma_{xx}}{\nu}=0$$

from where

$$\sigma=\sigma(0)\exp\left[-t/T\right],$$

where T – the pause time, s.

$$T=\nu/E, \tag{7}$$

represents the time for which the initial stress decreases by a factor of $e=2{,}718$.

Thus, it can be assumed that Maxwell's environment takes into account the real behavior of the metal during high-temperature plastic deformation (hardening, as well as softening). The minimization provides a reduction in the resistance to deformation (in this case, by an exponential dependence) with constant deformation [13].

After introducing the notation T (7), let's rewrite Eq. (6)

$$\frac{d\sigma_{xx}}{dt}+\frac{\sigma_{xx}}{T}=E\cdot\frac{d\bar{\varepsilon}}{dt}. \tag{8}$$

Regarding σ_{xx}, expression (8) under the initial condition, when the time t=0 and $\sigma_{xx}=\sigma_{xx}^{0}$ has the form

$$\sigma_{xx}=e^{\left(-t/T\right)}\cdot\left\{E\cdot\int_{0}^{t}\frac{d\bar{\varepsilon}}{dt}\cdot e^{\left(t/T\right)}\cdot dt+\sigma_{xx}^{0}\right\}.$$

If $\sigma_{xx}^{0}=0$ and the body also deforms at a constant rate, then the stresses change in time according to the law

$$\sigma_{xx}=E\cdot\bar{\varepsilon}\cdot\left(1-e^{\left(-t/T\right)}\right).$$

In real deformation processes, the rate is not constant [14]; therefore, to solve equation (8), let's define a function of the deformation degree. This function must be growing, as in the process of deformation the deformation degree increases. As such a function, it is possible to choose a monotonically increasing exponential function, which corresponds to the actual deformation processes (**Fig. 1**)

$$\bar{\varepsilon}=\frac{T}{A}\cdot\dot{\varepsilon}_{xx}\left(1-e^{-\frac{At}{T}}\right). \tag{9}$$

Deformation rate in this case

$$\dot{\varepsilon}=\frac{d\bar{\varepsilon}}{dt}=\frac{T}{A}\cdot\dot{\varepsilon}_{xx}\left(-e^{-\frac{At}{T}}\right)\cdot\left(-\frac{A}{T}\right)=\dot{\varepsilon}_{xx}\cdot e^{-\frac{At}{T}}. \tag{10}$$

Using the above functions (8) and (9), graphs of changes in the degree (ε) and velocity ($\dot{\varepsilon}$) of deformation in time are plotted (**Fig. 1**). The initial data for the calculations are: the pause time (T) is 2.0 s; deformation rate ($\dot{\varepsilon}$) is 0.002 s^{-1}; the deformation time (t) varies from 0 to 6 seconds. These output parameters correspond to the actual deformation processes (stamping or one press during forging).

These exponential dependencies correspond to the forging and stamping operations. In particular, with an increase in the degree of deformation, a hardening of the material and an increase in the size of the deformation zone occur, which leads to an increase in the deformation force [15]. As a result, the deformation rate exponentially decreases [16].

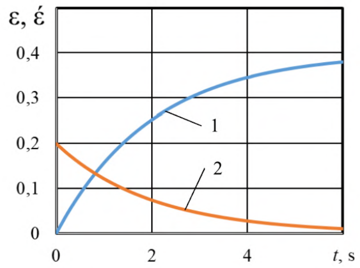

Fig. 1. Dependences of degree ε and deformation rate $\dot{\varepsilon}$ on time:
1 – deformation degree; 2 – deformation rate

Substituting the deformation rate $\frac{d\bar{\varepsilon}}{dt}$ (10) into the desired equation (8), let's obtain the following differential equation

$$\frac{d\sigma_{xx}}{dt}+\frac{\sigma_{xx}}{T}=E\cdot\dot{\varepsilon}_{xx}\cdot e^{-\frac{At}{T}}. \tag{11}$$

The resulting equation is solved by the variation method of a constant; for this, the homogeneous differential equation is first considered

$$\frac{d\sigma_X}{dt}+\frac{\sigma_X}{T}=0;\quad \frac{d\sigma_X}{\sigma_X}=-\int\frac{dt}{T};\quad \ln\frac{\sigma_X}{C}=-\int\frac{dt}{T},$$

so

$$\sigma_X(t)=Ce^{-\int\frac{dt}{T}}.$$

To solve the inhomogeneous equation (8), let's apply the method of variation by a constant, replacing C with an unknown function $\varphi(t)$, then

$$\sigma_X(t)=\phi(t)e^{-\int\frac{dt}{T}}. \tag{12}$$

Differentiate (12) and obtain

$$\frac{d\sigma_X}{dt}=\frac{d\phi}{dt}\cdot e^{-\int\frac{dt}{T}}-\frac{\phi(t)}{T}\cdot e^{-\int\frac{dt}{T}}. \tag{13}$$

After substitution (13) into equation (8)

$$\frac{d\phi}{dt}\cdot e^{-\int\frac{dt}{T}}-\frac{\phi(t)}{T}\cdot e^{-\int\frac{dt}{T}}+\frac{\phi(t)}{T}\cdot e^{-\int\frac{dt}{T}}=E\cdot\frac{d\varepsilon}{dt}.$$

So,

$$\frac{d\phi}{dt}=E\cdot\frac{d\varepsilon}{dt}\cdot e^{\int\frac{dt}{T}}.$$

Integrating, let's define

$$\phi(t)=\int E\cdot\frac{d\varepsilon}{dt}\cdot e^{\int\frac{dt}{T}}dt+C_1. \tag{14}$$

After substitution (14) in (12) let's obtain

$$\sigma_X(t)=e^{-\int_{t_0}^{t}\frac{dt}{T}}\left[C_1+\int_{t_0}^{t}E\frac{d\varepsilon}{dt}\cdot e^{\int_{t_0}^{t}\frac{dt}{T}}dt\right],$$

where t_0 and t – the integration limits: t_0 – the beginning of the pause, and t – the end of the pause.

Assuming that

$$\bar{\varepsilon}=\frac{T}{A}\cdot\varepsilon_{XX}(1-e^{-\frac{At}{T}}) \text{ and } \sigma_{xx}^0=0$$

let's obtain

$$\frac{d\bar{\varepsilon}}{dt}=\dot{\varepsilon}_{XX}\cdot e^{-\frac{At}{T}}.$$

If $t_0=0$, then

$$\sigma_X(t)=e^{-\frac{t}{T}}\left[C_1+\int_0^t E\dot{\varepsilon}_{XX}e^{-\frac{At}{T}}\cdot e^{\frac{t}{T}}dt\right].$$

After appropriate transformations and using the initial condition $\sigma_{xx}^0=0$, let's obtain

$$C=-E\cdot\dot{\varepsilon}_{xx}\cdot\frac{T}{1-A}.$$

So,

$$\sigma_X(t)=e^{-\frac{t}{T}}\left[-E\cdot\dot{\varepsilon}_{XX}\cdot\frac{T}{1-A}+\frac{T}{1-A}E\cdot\dot{\varepsilon}_{XX}\cdot e^{\frac{t}{T}(1-A)}\right]$$

or

$$\sigma_X(t)=E\cdot\dot{\varepsilon}_{XX}\cdot\frac{T}{1-A}\cdot\left[e^{-\frac{tA}{T}}-e^{-\frac{t}{T}}\right].$$

When A=1, one should reveal the uncertainty of the form $\left\{\frac{0}{0}\right\}$ and come to a particular case of the solution. Let's consider separately the case when A→1

$$\sigma_{XX}=\lim_{A\to1}\left[E\cdot\dot{\varepsilon}_{XX}\cdot\frac{T}{1-A}\left(e^{-\frac{tA}{T}}-e^{-\frac{t}{T}}\right)\right]=E\cdot\dot{\varepsilon}_{XX}\cdot T\cdot\lim_{A\to1}\frac{e^{-\frac{tA}{T}}-e^{-\frac{t}{T}}}{1-A}=\left\{\frac{0}{0}\right\}=$$

$$=E\cdot\dot{\varepsilon}_{XX}\cdot T\cdot\lim_{A\to1}\frac{e^{-\frac{t}{T}}\left(e^{-\frac{t}{T}(A-1)}-1\right)}{1-A}=\left[e^{-\frac{t}{T}(A-1)}-1\infty-\frac{t}{T}(A-1)\text{ at }A\to1\right]=$$

$$=E\cdot\dot{\varepsilon}_{XX}\cdot T\cdot\lim_{A\to1}\frac{e^{-\frac{t}{T}}\left(-\frac{t}{T}(A-1)\right)}{1-A}=E\cdot\dot{\varepsilon}_{XX}\cdot T\cdot e^{-\frac{t}{T}}\cdot\frac{t}{T}=E\cdot\dot{\varepsilon}_{XX}\cdot t\cdot e^{-\frac{t}{T}}.$$

Therefore, when A=1, let's obtain

$$\sigma_{XX} = E \cdot \dot{\varepsilon}_{XX} \cdot t \cdot e^{-\frac{t}{T}}. \tag{15}$$

Taking into account the above, with A=1, it is possible to simplify the functions describing the degree and rate of deformation (10) to the form:

$$\overline{\varepsilon} = T \cdot \dot{\varepsilon}_{xx} \cdot (1 - e^{-\frac{t}{T}}),\ \ \frac{d\overline{\varepsilon}}{dt} = \dot{\varepsilon}_{xx} \cdot e^{-\frac{t}{T}}.$$

A mathematical procedure is carried out to solve the limit as A→1 does not change the appearance of the functions for describing degrees and deformation rates; they are similar to those shown in **Fig. 1**. Analysis of the established model (15) allows to determine the results important for materials science:

– the maximum stress affects the Young's modulus at certain temperatures of deformation and rate of deformation;

– the peak of the function (15) corresponds to the time equal to T=ν/E, that is, this is the moment when the pause (metal unloading) comes, does not contradict the mechanics of the deformation process. This time T can be calculated with a certain degree and rate of deformation, it is the initial data for solving the problem.

In addition, this model allows to determine the viscosity ν of a material from relation (7) through the product T·E or by fitting. According to the known deformation time, rate and degree of deformation, let's change the Young's modulus to match the values of the function (15) with the experiment. Thus, taking into account the viscous properties of the body is reduced to establishing the exact value of the Young's modulus, depending on the temperature level.

The solution to this problem is not difficult with a known material tensile diagram or in the presence of a hardening curve for different temperatures. Also, to determine the Young's modulus, it is possible to use the reference literature. Young's modulus with increasing temperature decreases exponentially.

The obtained model does not exclude the determination of the Young's modulus by the method of selection to the coincidence of the obtained dependence with the hardening-softening curve. Reducing the level of stress in the material after deformation (during a pause), according to the obtained model, occurs exponentially, does not contradict the actual behavior of the material after the load is removed. It does not require the specification of additional factors.

3. Results of experimental studies of steel rheology during hot deformation

To test the developed model of steel rheology during hot deformation, it is necessary to conduct experimental studies and compare them with the analytical model. In this case, it is necessary to establish the mechanical properties of the material that is deformed. The main factors affecting the mechanical properties of the material under study: temperature, degree and rate of deformation. Investigated steel: 40Х, 9ХФ, ХВГ, 10Х16Н8. The temperature of steel samples varied in the range from 800 to 1200 °C with steps of 100 °C. The deformation degree varies from 0 to 0.4, the deformation rate in the range $(2...6)\times10^{-3}s^{-1}$, covers the deformation and high-speed mode of technological processes of forging and stamping. Experimental planning is carried out using type 3^3 PFE plan. The high-temperature mechanical properties of steels are studied jointly with Czestochowa University of Technology (Poland) on the Gleeble 3800 unit for physical modeling of thermomechanical compression and tension tests. After conducting experimental studies and processing the results obtained using the experiment planning theory, the coefficients of the regression equations are determined, which determine the dependence of the deformation resistance on the degree, deformation rate and temperature. After exclusion of non-significant coefficients:

$$\begin{aligned}\sigma_s(\varepsilon, \xi, T) = 38 + 38 \cdot X_1 + 18 \cdot X_2 - 46 \cdot X_3 + 21 \cdot X_2^{\ 2} + 29 \cdot X_3^{\ 2} + \\ +39 \cdot X_1^{\ 2} \cdot X_2^{\ 2} \cdot X_3^{\ 2} - 26 \cdot X_1^{\ 2} \cdot X_2^{\ 2} - 39 \cdot X_2^{\ 2} \cdot X_3^{\ 2} - 19 \cdot X_1^{\ 2} \cdot X_3^{\ 2},\end{aligned} \tag{16}$$

where

$$X_1 = \frac{\varepsilon - 0{,}1}{0{,}1},\ X_2 = \frac{\xi - 6\times10^{-3}}{4\times10^{-3}},\ X_3 = \frac{T - 1000}{200}.$$

For comparison and verification of the theoretical and experimental results, equations (15) and (16) are used to construct the dependences of the deformation resistance during deformation with a pause at hot pressure treatment temperatures (**Fig. 2**). The experimental data are shown by the dashed line, and the theoretical ones by the solid line.

Graphically developed in the work dependence (15) is shown in **Fig. 2** as a function, has areas of hardening and relaxation of stresses (softening) when removing the load. **Fig. 2** shows experimental data of flow curves (curves 1 and 3) for various steels at a deformation rate $\dot{\varepsilon} = 7\times10^{-3}\ s^{-1}$ and heating temperatures of 900 °C and 1000 °C, function (15) is shown by curves 2 and 4.

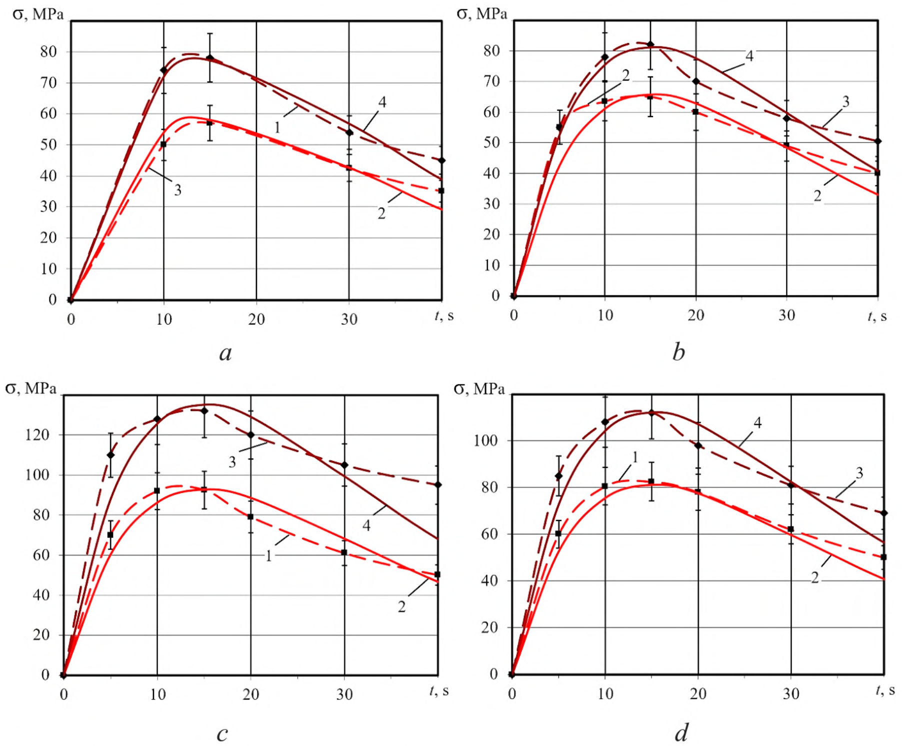

Fig. 2. Comparison of experimental data for hardening – softening with dependent (15) for steel: *a* – 40X; *b* – 9XФ; *c* – XBГ; *d* – 10X16H8; 1 – T=1000 °C (experiment); 2 – T=1000 °C (calculations); 3 – T=900 °C (experiment); 4 – T=900 °C (calculations)

Comparison of the obtained theoretical data with the results of experiments shows their qualitative and quantitative correspondence. In the areas of hardening and relaxation, the difference is 7...11 %.

4. Discussion of the results obtained using the developed model of the visco-elastic behavior of steel at pressure treatment temperatures

The analysis of the obtained results makes it possible to establish that a developed rheological model describes the physical processes occurring in hot-deformed steels – material hardening and stress relaxation. Based on the developed mathematical model, it is found that the maximum stress is determined by the Young's modulus for certain temperatures and material and deformation rate at the acoustic time of deformation. The peak of the function corresponds to the time T=ν/E. The analytical dependence asymptotically approaches the state when the stress is zero, and the experimental data asymptotically approach a certain stress, which is the yield strength of the material. This difference is explained by the fact that during the experimental study, the specimen remained under load after deformation, due to the research method and the design of the cam plastometer. As a result, the stress can't be reduced to zero, since the load seems to act after the deformation process stops, so that it is possible to set a change in relaxation in the material after deformation is stopped. The difference between the experimental and calculated stress values at the relaxation site is the value of the yield strength of the material at a given temperature. Taking into account in the resulting model the effect of the load on the sample with a value equal to the yield strength of the material (σ_T), let's obtain the coincidence of dependencies with a deviation of 7...11 %. Thus, the reason for the discrepancy between the experimental data and the theoretical values of hardening and softening is established, which gives reason to consider the developed model to be reliable, since it describes the rheology of the metal during hot deformation by 89...93 %.

In contrast to the existing methods for taking into account the mechanical properties of a material when FEM modeling, an analytical model is developed, which allows not to carry out iterative procedures. A feature of the developed model of the connection component of the deformation rate and stress during hot deformation is that it takes into account the mechanism of stress relaxation in the metal (alloy) after deformation. This opens up broad prospects for its use in FE modeling.

A limitation of this approach is the need to specify a Young's modulus for a certain material depending on temperature. This information is not enough in the literature today. Moreover, it is advisable to check the resulting model on other metals and alloys.

5. Conclusions

1. Based on Maxwell's viscoelastic rheological model, the relationship between the components of deformation rates and stresses is established. This makes it possible to obtain a direct numerical solution of nonlinear problems of hot plastic deformation in the course of modeling by the finite element method taking into account the real properties of the metal at high temperatures. As a result of using the developed model of the material rheology during deformation in the hot state in the calculation decreases by 4 times compared with the use of elastic and elastic-plastic models of materials used in commercial software products based on FEM. This is due to the exception of carrying out additional iterative procedures to establish the real resistance of the material for certain thermo-speed deformation conditions. The developed model takes into account not only the processes of material hardening during deformation, but also softening (stress relaxation) in the pause after deformation.

2. Resistance to hot deformation and stress relaxation after deformation of steels at different temperatures, degrees and deformation rates is experimentally established. Stress relaxation after hot deformation is explained by recrystallization processes. The obtained results are compared with theoretical data established on the basis of the developed model of material rheology during hot deformation. It is experimentally proved that the developed model is 89...93 % describing the steel rheology during hot deformation.

References

[1] Markov, O., Zlygoriev, V., Gerasimenko, O., Hrudkina, N., Shevtsov, S. (2018). Improving the quality of forgings based on upsetting the workpieces with concave facets. Eastern-European Journal of Enterprise Technologies, 5 (1 (95)), 16–24. doi: https://doi.org/10.15587/1729-4061.2018.142674

[2] Buckingham, R. C., Argyrakis, C., Hardy, M. C., Birosca, S. (2016). The effect of strain distribution on microstructural developments during forging in a newly developed nickel base superalloy. Materials Science and Engineering: A, 654, 317–328. doi: https://doi.org/10.1016/j.msea.2015.12.042

[3] Ma, F., Lu, W., Qin, J., Zhang, D., Ji, B. (2007). The effect of forging temperature on microstructure and mechanical properties of in situ TiC/Ti composites. Materials & Design, 28 (4), 1339–1342. doi: https://doi.org/10.1016/j.matdes.2006.02.004

[4] Ma, Q., Lin, Z., Yu, Z. (2009). Prediction of deformation behavior and microstructure evolution in heavy forging by FEM. The International Journal of Advanced Manufacturing Technology, 40 (3-4), 253–260. doi: https://doi.org/10.1007/s00170-007-1337-9

[5] Pantalé, O., Gueye, B. (2013). Influence of the Constitutive Flow Law in FEM Simulation of the Radial Forging Process. Journal of Engineering, 2013, 1–8. doi: https://doi.org/10.1155/2013/231847

[6] Wu, Y., Dong, X., Yu, Q. (2015). Upper bound analysis of axial metal flow inhomogeneity in radial forging process. International Journal of Mechanical Sciences, 93, 102–110. doi: https://doi.org/10.1016/j.ijmecsci.2015.01.012

[7] Kukhar, V., Burko, V., Prysiazhnyi, A., Balalayeva, E., Nyhnibeda, M. (2016). Development of alternative technology of dual forming of profiled workpiece obtained by buckling. Eastern-European Journal of Enterprise Technologies, 3 (7 (81)), 53–61. doi: https://doi.org/10.15587/1729-4061.2016.72063

[8] Dobrzański, L. A., Grajcar, A., Borek, W. (2008). Influence of hot-working conditions on a structure of high-manganese austenitic steels. Journal of Achievements in Materials and Manufacturing Engineering, 29 (2), 139–142.

[9] Weides, G., Blaes, N., Bokelmann, D. (2008). Optimisation of the forging process of profiled discs for low pressure turbine rotors by FEM simulation. 17 International Forgeмasters Meeting, Santander.

[10] Erman, E., Medei, N. M., Roesch, A. R., Shah, D. C. (1989). Physical modeling of the upsetting process in open-die press forging. Journal of Mechanical Working Technology, 19 (2), 195–210. doi: https://doi.org/10.1016/0378-3804(89)90004-1

[11] Markov, O. E., Perig, A. V., Markova, M. A., Zlygoriev, V. N. (2015). Development of a new process for forging plates using intensive plastic deformation. The International Journal of Advanced Manufacturing Technology, 83 (9-12), 2159–2174. doi: https://doi.org/10.1007/s00170-015-8217-5

[12] Kitamura, K., Terano, M. (2014). Determination of local properties of plastic anisotropy in thick plate by small-cube compression test for precise simulation of plate forging. CIRP Annals, 63 (1), 293–296. doi: https://doi.org/10.1016/j.cirp.2014.03.038

[13] Markov, O. E. (2012). Forging of large pieces by tapered faces. Steel in Translation, 42 (12), 808–810. doi: https://doi.org/10.3103/s0967091212120054

[14] Mitani, Y., Mendoza, V., Osakada, K. (1991). Analysis of rotor shaft forging by rigid-plastic finite element method. Journal of Materials Processing Technology, 27 (1-3), 137–149. doi: https://doi.org/10.1016/0924-0136(91)90049-k

[15] Markov, O. E., Perig, A. V., Zlygoriev, V. N., Markova, M. A., Grin, A. G. (2016). A new process for forging shafts with convex dies. Research into the stressed state. The International Journal of Advanced Manufacturing Technology, 90 (1-4), 801–818. doi: https://doi.org/10.1007/s00170-016-9378-6

[16] Dragobetskii, V., Zagirnyak, M., Naumova, O., Shlyk, S., Shapoval, A. (2018). Method of Determination of Technological Durabilityof Plastically Deformed Sheet Parts of Vehicles. International Journal of Engineering & Technology, 7 (4.3), 92–99. doi: https://doi.org/10.14419/ijet.v7i4.3.19558

ANALYSIS OF DYNAMIC LOADING OF IMPROVED CONSTRUCTION OF A TANK CONTAINER UNDER OPERATIONAL LOAD MODES

Oleksij Fomin
Department of Wagons and Wagonriage Facilities
State University of Infrastructure and Technology
9 Kyrylivska str., Kyiv, Ukraine, 04071
fomin1985@ukr.net

Alyona Lovska
Department of Wagons
Ukrainian State University of Railway Transport
7 Feierbakh sq., Kharkiv, Ukraine, 61050
alyonaLovskaya.vagons@gmail.com

Oleksandr Gorobchenko
Department of traction rolling stock of railways
State University of Infrastructure and Technology
9 Kyrylivska str., Kyiv, Ukraine, 04071
gorobchenko.a.n@gmail.com

Serhii Turpak
Department of transport technologies
Zaporizhzhya National Technical University
64 Zhukovsky str., Zaporizhzhia, Ukraine, 69093
sergeyturpak@gmail.com

Iryna Kyrychenko
Department of Electrical Engineering
East Ukrainian National University named after V. Dal
59-a Central ave., Severodonetsk, Ukraine, 93400
i_kir@ukr.net

Oleksii Burlutski
Department of Mechanics and Designing Machines
Ukrainian State University of Railway Transport
7 Feierbakh sq., Kharkiv, Ukraine, 61050
leha2006181@gmail.com

Abstract

An increase in the volume of bulk cargo transportation through international transport corridors necessitates the commissioning of tank containers. Intermodalization of a tank container predetermines its load in various operating conditions depending on the type of vehicle on which it is carried: aviation, sea, air or rail. The analysis of the operating conditions of tank containers, as well as the regulatory documents governing their workload, led to the conclusion that the most dynamic loads acting on the supporting structures during transportation by rail. Namely, during the maneuvering collision of a wagon-platform, on which there are tank containers. In this case, it is stipulated that for a loaded tank container, the dynamic load is assumed to be 4g, and for an empty (for the purpose of checking the reinforcement) – 5g. It is important to note that when the tank container is underfilled with bulk cargo and taking into account movements of fittings relative to fittings, the maximum value of dynamic load can reach significantly larger values. Therefore, in order to ensure the strength of tank containers, an improvement of their structures has been proposed by introducing elastic-viscous bonds into the fittings.

To determine the dynamic loading of the tank container, taking into account the improvement measures, mathematical models have been compiled, taking into account the presence of elastic, viscous and elastic-viscous bonds between the fittings, stops and fittings. It is established that the elastic bond does not fully compensate for the dynamic loads acting on the tank container. The results of mathematical modeling of dynamic loading, taking into account the presence of viscous and elastic-viscous coupling in the fittings, made it possible to conclude that the maximum accelerations per tank container do not exceed the normalized values.

The determination of the dynamic loading of the tank container is also carried out by computer simulation using the finite element method. The calculation takes place in the software package CosmosWorks. The maximum values of accelerations are obtained, as well as their distribution fields relative to the supporting structure of the tank container.

The developed models are verified by the Fisher criterion. The research will contribute to the creation of tank containers with improved technical, operational, as well as environmental characteristics and an increase in the efficiency of the liquid cargo transportation process through international transport corridors.

Keywords: tank container, supporting structure, fittings, dynamic loading, maneuvering collisions.

DOI: 10.21303/2461-4262.2019.00876

1. Introduction

Improving the efficiency of the transportation process through international transport corridors makes it necessary to introduce intermodal means into the transport process. It is known that the most common among these are containers or tank containers. Transportation of containers can be carried out by almost all types of transport - rail, road, air or sea. This results in the workload of their structures under various operating conditions.

The study of regulatory documents [1] on the loading of containers in operation led to the conclusion that the greatest force on their design is carried out during carriage on flatcars, namely during a maneuvering collision. It is important to note that the degree of dynamic loading of containers in operation can reach significant values [2–5]. This is due not only to the action on the wagon-platform with tank containers during a maneuvering impact load of 3.5 MN [6–8]. Also, there may be a load arising from the impact of the tank-container fittings with the fittings by the platform-wagon stops [9]. In addition, the movement of bulk cargo in the tank container boiler also causes additional force on the supporting structure [10]. All these factors can contribute to damage to the structural elements of tank containers and wagons.

Therefore, to ensure the strength of tank containers, as well as reducing the cost of manufacture and operation, it is necessary to improve their supporting structures. It will also allow to increase the efficiency of operation of tank containers and to develop recommendations for the creation of new alternative designs with improved technical, economic and environmental characteristics. The aim of research is analysis of the dynamic loading of the improved design of tank containers under operating conditions of load.

To achieve the aim, the following objectives are set:

– to carry out mathematical modeling of the loading of the tank container placed on the wagon-platform during a maneuvering collision;

– to conduct a computer simulation of the loading of the tank container placed on the wagon-platform during a maneuvering collision;

– to verify the proposed container loading models.

2. Mathematical modeling of the loading of the tank container placed on the wagon-platform during a maneuvering collision

To reduce the dynamic loading of the tank container in operation, it is proposed to install in the fittings (**Fig. 1, *a***) elastic or viscous elements (**Fig. 1, *b***). The occurrence of a shock load between fittings and fitting stops can occur in the case when the dynamic load P_d exceeds the friction force F_f between their horizontal planes.

To determine the dynamic loading of the tank container during a maneuvering collision, taking into account improvement measures, a mathematical model (1) is compiled, which takes into account the movement of the tank container placed on the wagon-platform. The design scheme is shown in **Fig. 2.**

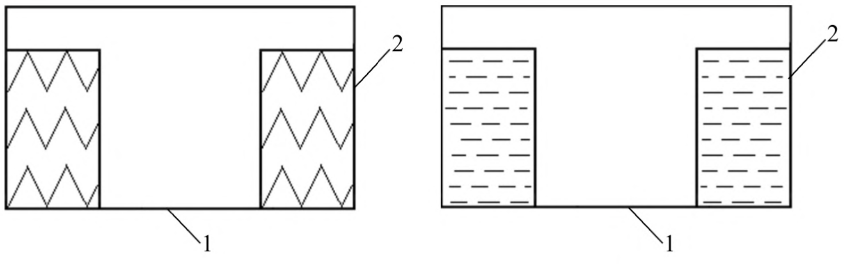

Fig. 1. Improved design of container fittings: *a* – elastic bond; *b* – viscous bond; 1 – fittings; 2 – elastic (a), viscous (b) element

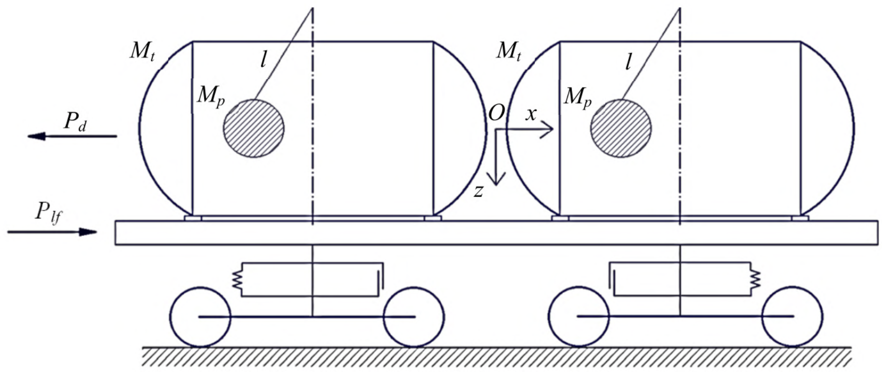

Fig. 2. Diagram of the action of the longitudinal force on the wagon-platform with tank containers placed on it

The wagon-platform model 13-4012M was chosen as the prototype wagon. Investigations were carried out in relation to a tank container of size 1CC.

The model takes into account the dry friction force that occurs when moving the fittings of tank containers relative to the horizontal planes of fitting stops and the elastic bond between fittings stops and fittings [11, 12]. The study of the dynamic loading of the tank container was carried out in a flat coordinate system. The movement of the bulk cargo was described by a set of mathematical pendulums.

As a bulk cargo gasoline is accepted. Determination of the hydrodynamic characteristics of the bulk cargo was carried out taking into account 95 % of the loading of the boiler in bulk. In this case, the value M_P=6.6 t and I_{BC}=250 t·m^2 was obtained.

The solution of the mathematical model (1) is implemented in the MathCad software environment [13]. At the same time, it was reduced to the normal Cauchy form $\dot{y}(t)=Q(t,y)$. Where $q_1=y_1$; $q_2=y_2$; $\dot{q}_1=y_3$; $\dot{q}_2=y_4$.

The solution of the system of differential equations (1) in normal form was carried out by integrating according to the Runge-Kutta method. The initial conditions are assumed to be zero.

$$\begin{cases} M_{PC}^{gw}\cdot\ddot{q}_1=P_{lf}-\sum\limits_{i=1}^{n}\left(F_f\cdot \mathrm{sign}(\dot{q}_1-\dot{q}_2)+S_f(q_1-q_2)\right), \\ M_t\cdot\ddot{q}_2=\sum\limits_{i=1}^{n}\left(F_f\cdot \mathrm{sign}(\dot{q}_1-\dot{q}_2)+S_f\cdot(q_1-q_2)+M_p\cdot l\cdot q_3\right), \\ I_{BC}\cdot\ddot{q}_3=M_p\cdot l\cdot\ddot{q}_2-g\cdot M_p\cdot l\cdot q_3, \end{cases} \tag{1}$$

where M_{PC}^{gw}– gross weight of wagon-platform; P_{lf} – the value of the longitudinal force acting on the coupler; F_f– friction force between fittings stops and fittings; M_t – tank container mass; S_f– stiffness of elastic elements in tank container fittings; M_P – the mass of a pendulum that simulates the movement of a bulk cargo in a tank container; l – the length of the pendulum suspension; I_{BC} – the moment of pendulum inertia; q_1, q_2, q_3 – coordinates that determine the movement, respectively, of the wagon-platform, tank container and bulk cargo relative to the longitudinal axis.

The transition from the system of differential equations of the second order (1) to the system of differential equations of the first order (2) was carried out to apply standard algorithms for solving the system in Mathcad:

$$Q(t,y)=\begin{bmatrix} y_4 \\ y_5 \\ y_6 \\ \dfrac{P_{lf}-\sum\limits_{i=1}^{n}\left(F_f\cdot \text{sign}(y_4-y_5)+S_f(y_1-y_2)\right)}{M_{PC}^{gw}} \\ \dfrac{\sum\limits_{i=1}^{n}\left(F_f\cdot \text{sign}(y_4-y_5)+S_f\cdot(y_1-y_2)+M_p\cdot l\cdot y_3\right)}{M_t} \\ \dfrac{M_p\cdot l\cdot \dot{y}_5-g\cdot M_p\cdot l\cdot y_3}{I_{BC}} \end{bmatrix}, \tag{2}$$

$$Z=\text{rkfixed}\,(Y0, tn, tk, n, Q),$$

where Y0 – a vector containing the initial conditions, tn, tk – the quantities that define the initial and final integration variables, n – a fixed number of steps, Q – a symbol vector.

Based on the calculations made, the acceleration is obtained, which act on the improved design of the tank container placed on the wagon-platform during a maneuvering collision (**Fig. 3**). This acceleration value was about 50 m/s^2 (≈5g), that is, it exceeds the allowable value [1].

The total stiffness of the elastic elements per tank container was in the range of 420–530 kN/m.

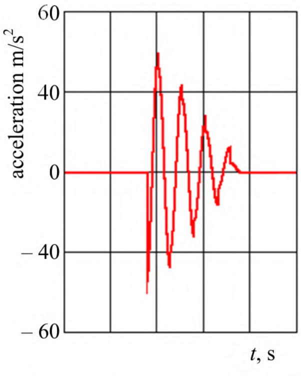

Fig. 3. Acceleration, acting on a tank container with elastic bonds in the fittings, placed on the wagon-platform during a maneuvering collision

To reduce the dynamic loading of the tank container placed on the wagon-platform during a maneuvering collision, a variant of the execution of fittings with viscous bonds was also considered.

A mathematical model of the dynamic loading of a tank container during a maneuvering collision with regard to the presence of a viscous bond in the fittings is given below.

$$\begin{cases} M_{PC}^{gw} \cdot \ddot{q}_1 = P_{lf} - \sum\limits_{i=1}^{n} \left(F_f \cdot \mathrm{sign}(\dot{q}_1 - \dot{q}_2) + \beta_f (\dot{q}_1 - \dot{q}_2)\right), \\ M_t \cdot \ddot{q}_2 = \sum\limits_{i=1}^{n} \left(F_f \cdot \mathrm{sign}(\dot{q}_1 - \dot{q}_2) + \beta_f (\dot{q}_1 - \dot{q}_2) + M_p \cdot l \cdot q_3\right), \\ I_{BC} \cdot \ddot{q}_3 = M_p \cdot l \cdot \ddot{q}_2 - g \cdot M_p \cdot l \cdot q_3. \end{cases} \quad (3)$$

The acceleration acting on a tank container with viscous bonds in the fittings placed on the wagon-platform during a maneuvering collision is shown in **Fig. 4**. When the value of viscous resistance in the tank container fittings is inflicted, the acceleration is about 40 m/s^2 ($\approx$4g) and does not exceed the normalized value [1].

$$Q(t, y) = \begin{bmatrix} y_4 \\ y_5 \\ y_6 \\ \dfrac{P_{lf} - \sum\limits_{i=1}^{n} \left(F_F \cdot \mathrm{sign}(y_4 - y_5) + \beta_f (y_4 - y_5)\right)}{M_{PC}^{gw}} \\ \dfrac{\sum\limits_{i=1}^{n} \left(F_F \cdot \mathrm{sign}(y_4 - y_5) + \beta_f (y_4 - y_5) + M_P \cdot l \cdot y_3\right)}{M_c} \\ \dfrac{M_P \cdot l \cdot \dot{y}_5 - g \cdot M_P \cdot l \cdot y_3}{I_{BC}} \end{bmatrix}, \quad (4)$$

$$Z = \mathrm{rkfixed}\,(Y0, tn, tk, n, Q).$$

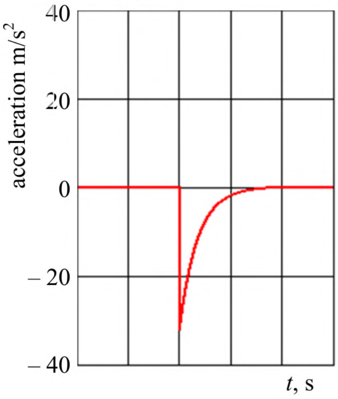

Fig. 4. Acceleration acting on a tank container with viscous bonds in the fittings, placed on the wagon-platform during a maneuvering collision

In this case, the total viscous resistance to the movement of one tank container should be in the range of 9–54 kN s/m.

The case of elastic-viscous bond between fittings and fittings stops is also considered. The mathematical model will look like this:

$$\begin{cases} M_{PC}^{gw} \cdot \ddot{q}_1 = P_{lf} - \sum\limits_{i=1}^{n} \left(F_f \cdot \mathrm{sign}(\dot{q}_1 - \dot{q}_2) + c(q_1 - q_2) + \beta_f (\dot{q}_1 - \dot{q}_2)\right), \\ M_t \cdot \ddot{q}_2 = \sum\limits_{i=1}^{n} \left(F_f \cdot \mathrm{sign}(\dot{q}_1 - \dot{q}_2) + c(q_1 - q_2) + \beta_f (\dot{q}_1 - \dot{q}_2) + M_P \cdot l \cdot q_3\right), \\ I_{BC} \cdot \ddot{q}_3 = M_P \cdot l \cdot \ddot{q}_2 - g \cdot M_P \cdot l \cdot q_3. \end{cases} \quad (5)$$

The solution of equation (5) was sought in the form:

$$Q(t,y)=\begin{bmatrix} y_4 \\ y_5 \\ y_6 \\ \dfrac{P_{lf}-\sum\limits_{i=1}^{n}\left(F_f\cdot \text{sign}(y_4-y_5)+c(q_1-q_2)+\beta_f(y_4-y_5)\right)}{M_{PC}^{gw}} \\ \dfrac{\sum\limits_{i=1}^{n}\left(F_f\cdot \text{sign}(y_4-y_5)+c(q_1-q_2)+\beta_f(y_4-y_5)+M_p\cdot l\cdot y_3\right)}{M_t} \\ \dfrac{M_P\cdot l\cdot \dot{y}_5-g\cdot M_P\cdot l\cdot y_3}{I_{BC}} \end{bmatrix}, \tag{6}$$

$$Z=\text{rkfixed}\,(Y0,tn,tk,n,Q).$$

The acceleration acting on the tank container, taking into account the elastic-viscous bond in the fittings, is shown in **Fig. 5.**

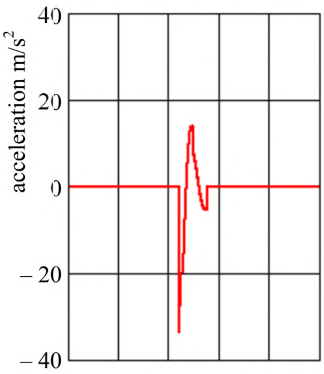

Fig. 5. Acceleration acting on a tank container with viscous and elastic bond in fittings, placed on a wagon-platform during a maneuvering collision

The stiffness of the elastic element is assumed to be 480 kN/m and the viscous resistance coefficient is 30 kN·s/m. The maximum acceleration value is about 40 m/s^2 (≈4g) and does not exceed the normalized value [1].

3. The research results of the loading of the tank container placed on the wagon-platform during a maneuvering collision

3. 1. Computer simulation of the loading of the tank container placed on the wagon-platform during a maneuvering collision

To study the dynamic loading of a tank container with regard to improvement measures, computer simulation was carried out using the finite element method [14, 15] implemented in the CosmosWorks software package (France) [16, 17].

The model for determining the dynamic loading of a wagon-platform with tank containers during a maneuvering collision is shown in **Fig. 6**. The model takes into account that the tank container fittings are affected by the horizontal load P_h, due to the impact of the P_f shock load on the vertical surface of the rear stop of the automatic coupling. Also taken into account are vertical reactions in the supporting areas of the fittings on the fitting stops P_h. It is taken into account that the tank container is affected by pressure from the bulk cargo R_{BC}. On the tank bottom, pressure R_b is applied, due to a longitudinal impact on the rear stop of the automatic coupling of the wagon-platform and movement of the fittings relative to the fitting stops. Fixing the tank container was carried out in the areas of its support on the wagon-platform. It is taken into account that when a dynamic load is applied to the fittings, it is moved relative to the initial position by 30 mm. In the tank container fittings were installed elastic elements, hardness 420 kN/m.

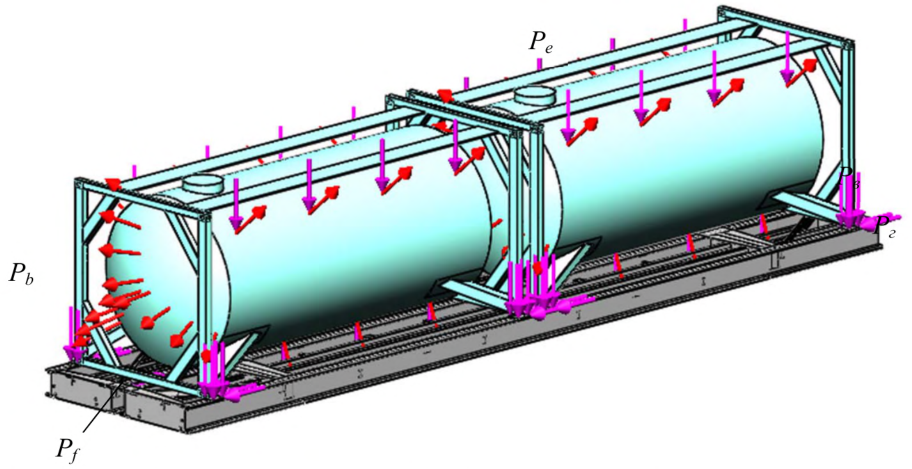

Fig. 6. Model for determining the dynamic loading of a wagon-platform with tank containers during a maneuvering collision

Steel grade 09G2S with the corresponding numerical values of strength and yield strength was used as a construction material [18–20]. The calculation results are shown in **Fig. 7**.

When modeling the dynamic loading of a tank container, taking into account the presence in the fittings of a viscous bond, the total viscous resistance to movement of one tank container should be in the range of 9–54 kN·s/m.

The results of modeling the dynamic loading of the tank container, taking into account the viscous bond between the fittings and the fitting stops, made it possible to conclude that the maximum accelerations acting on the supporting structure of the tank container are 41.4 m/s^2.

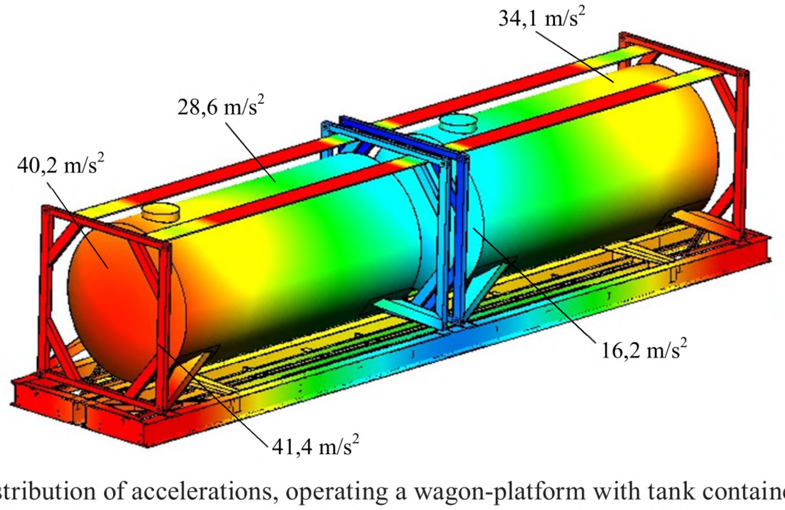

Fig. 7. Distribution of accelerations, operating a wagon-platform with tank containers during a maneuvering collision

So, the maximum accelerations acting on the tank container, taking into account the elastic bond between the fittings and fitting stops do not exceed the permissible [1].

On the basis of the compiled strength model, the values of the critical oscillation frequencies of the tank container were determined (**Table 1**).

Table 1
Numerical values of the critical oscillation frequencies of the tank container of an improved design

Oscillation form	Frequency, rad/s	Frequency, Hz
1	52.25	8.32
2	53.65	8.53
3	57.18	9.1
4	145.6	23.17
5	146.81	23.37
6	150.07	23.88
7	202.65	32.25
8	221.87	35.31
9	278.06	44.25
10	286.44	45.6

The research results show that the values of the critical oscillation frequencies are within the allowable limits [18–20].

3. 2. Verification of loading models of containers placed on a wagon-platform during a maneuvering collision

In order to verify the developed models, the F-criterion was applied [21, 22]. The input parameter of the mathematical and computer model of the dynamic loading of the container is the impact force in the automatic coupling of the wagon-platform, and the output parameter is the acceleration acting on the tank container placed on the wagon-platform (**Table 2**).

The required number of static data was recognized by Student's criterion [23].

When the value of the mathematical expectation is 33.6, the variance is 31.7, the standard deviation is 5.63, it has been established that the optimal number of measurements is 6 and the number of measurements made is sufficient to obtain a reliable assessment of the results.

Table 2
The results of modeling the dynamic loading of the tank container

Impact force, MN	2.8	2.9	3.0	3.1	3.2	3.3	3.4	3.5
Mathematical model	30	31	32.1	33	34.2	35.2	36	37.4
Computer model	33.1	34.2	35.5	36.7	37.9	39	40.2	41.4

The calculation results show that for the case of viscous interaction of fittings from fittings with dispersion of reproducibility S_y=6.5 and dispersion of adequacy S_{ad2}=8.4, the actual value of the F-criterion F_r=1.3, which is less than the table value of the criterion F_t=3, 07 So the hypothesis about the adequacy of the developed model is not disputed.

The discrepancy between the results of mathematical and computer modeling of the dynamic loading of the tank container is shown in **Fig. 8.**

At the same time, the maximum value of the discrepancy is 10.4 % with the impact force at the automatic coupling of the wagon-platform 3.4 MN, and the smallest – about 9.3 %, respectively, with 2.8 MN.

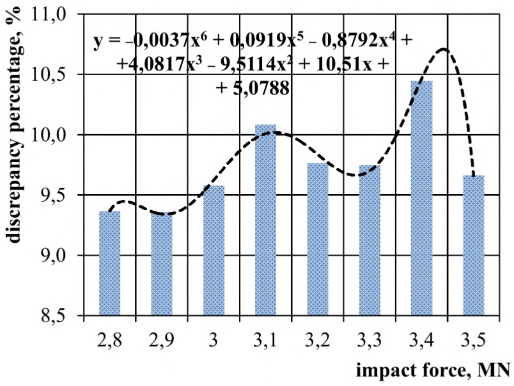

Fig. 8. The discrepancy between the results of mathematical and computer modeling

4. Discussion of the results of the improvement of the supporting structures of tank containers to reduce the dynamic loading in operation

Measures to improve the supporting structures of tank containers to reduce their dynamic loading in operating conditions are proposed. The reduction of dynamic loads is achieved by introducing viscous or elastic-viscous bonds into the tank container fittings.

The peculiarity of the conducted research is that, in contrast to the known solutions, the reduction of the dynamic loading of the tank container is achieved by introducing viscous and elastic-viscous bonds into the design of fittings, rather than by improving the metal structure itself.

It is important to note that in modeling the dynamic loading of a tank container placed on a wagon-platform, it was assumed that there was no oscillation by galloping. That is, the design scheme takes into account only the translational movement of the tank container relative to the longitudinal axis (the equivalent of twitching oscillations in the dynamics of the cars). In addition, the possible eccentricity of the body of the automatic coupling when the impact of shock load on the wagon-platform is not taken into account.

In further studies in this direction, it is necessary to take into account these limitations in order to obtain a more accurate estimate of the dynamic loading of the tank container.

Also an important stage of this research is the experimental determination of the dynamic loading of the tank container of an improved design. Due to the complexity of carrying out a full-scale experiment at the primary stage, it is possible to use the method of similarity theory.

5. Conclusions

A simulation of the loading of the tank container placed on the wagon-platform during a maneuvering collision is carried out. The maximum values of the accelerations acting on the tank container taking into account the improvement measures are determined. It is established that the presence of elastic coupling in the container fittings does not fully compensate for the magnitude of the dynamic load acting on the tank container placed on the wagon-platform during a maneuvering collision. In the presence of a viscous bond in the fittings, the maximum accelerations are about 40 m/s^2 ($\approx$4 g), that is, do not exceed the allowable values. In this case, the total viscous resistance to the movement of one tank container should be in the range of 9–54 kN·s/m.

The case of elastic-viscous bond between fittings and fitting stops is also considered. It is established that with a stiffness of an elastic element of 480 kN/m and a coefficient of viscous resistance of 30 kN s/m, the maximum acceleration value is about 40 m/s^2 ($\approx$4g) and does not exceed the normalized value.

A computer simulation of the loading of the tank container placed on the wagon-platform during a maneuvering collision is carried out. It is established that the maximum accelerations acting on the supporting structure of the tank container are 41.4 m/s^2 and are concentrated in the frame from the cantilever parts of the wagon-platform. The critical oscillation frequency of the tank container is determined. The numerical values of the frequencies do not exceed the permissible.

The proposed tank container loading models are verified. F-criterion are used as a calculated. The optimal number of measurements is determined and the dispersion of adequacy and reproducibility is calculated. The research results show that the hypothesis of adequacy does not deviate. In this case, the calculated value of the criterion below the table is almost 60 %.

References

[1] GOST 31232-2004. Konteynery dlya perevozki opasnyh gruzov. Trebovaniya po ekspluatacionnoy bezopasnosti (2005). Minsk: Belorus. gos. in-t standartizacii i sertifikacii, 6.

[2] Bhattacharyya, R., Hazra, A. (2013). A study on stress analysis of ISO tank container. 58th Congress of The Indian Society of Theoretical and Applied Mechanics, 1–5.

[3] Lisowski, E., Czyzycki, W. (2011). Transport and storage of LNG in container tanks. Journal of KONES Powertrain and Transport, 18 (3), 193–201.

[4] Trejo-Escandón, J. O., Leyva-Díaz, A., Tamayo-Meza, P. A., Flores-Herrera, L. A., Sandoval-Pineda, J. M. (2015). Study of the effect of liquid level on the static behavior of a tank wagon. International Journal of Engineering Research and Science and Technology, 4 (1), 18–25.

[5] Talu, M. (2017). The Influence of the Corrosion and Temperature on the Von Mises Stress in the Lateral Cover of a Pressurized Fuel Tank. Hidraulica, 4, 89–97.

[6] Fomin, O. V., Lovska, A. O., Plakhtii, O. A., Nerubatskyi, V. P. (2017). The influence of implementation of circular pipes in load-bearing structures of bodies of freight cars on their physico-mechanical properties. Scientific Bulletin of National Mining University, 6, 89–96.

[7] Fomin, O., Kulbovsky, I., Sorochinska, E., Sapronova, S., Bambura, O. (2017). Experimental confirmation of the theory of implementation of the coupled design of center girder of the hopper wagons for iron ore pellets. Eastern-European Journal of Enterprise Technologies, 5 (1 (89)), 11–18. doi: https://doi.org/10.15587/1729-4061.2017.109588

[8] Tretiakov, A. V., Tretiakov, O. A., Zimakova, M. V., Petrov, A. A. (2017). Experimental evaluation of shock spectrum response of rolling stock. Science and Transport Progress. Bulletin of Dnipropetrovsk National University of Railway Transport, 3 (69), 147–159. doi: https://doi.org/10.15802/stp2017/103898

[9] Lovska, A. (2018). Simulation of loads on the carrying structure of an articulated flat car in combined transportation. International Journal of Engineering & Technology, 7 (4.3), 140–146. Available at: https://www.sciencepubco.com/index.php/ijet/article/view/19724/9151

[10] Makeev, S. V., Buylenkov, P. M. (2018). Osobennosti rascheta napryazhenno-deformirovannogo sostoyaniya tanka-konteynera s uchetom real'nogo nagruzheniya v ekspluatacii. Nauka-obrazovanie-proizvodstvo: Opyt i perspektivy razvitiya: sbornik materialov XIV Mezhdunarodnoy nauchno-tekhnicheskoy konferencii, posvyashchennoy pamyati doktora tekhnicheskih nauk, professora E. G. Zudova. Vol. 1: Gorno-metallurgicheskoe proizvodstvo. Mashinostroenie i metalloobrabotka. Nizhniy Tagil: NTI (filial) UrFU, 174–184.

[11] Fomin, O., Gerlici, J., Lovskaya, A., Kravchenko, K., Burlutski, O., Hauser, V. (2019). Peculiarities of the mathematical modelling of dynamic loading on containers in flat wagons transportation. MATEC Web of Conferences, 254, 02039. doi: https://doi.org/10.1051/matecconf/201925402039

[12] Fomin, O., Gerlici, J., Lovskaya, A., Gorbunov, M., Kravchenko, K., Prokopenko, P., Lack, T. 2018). Dynamic loading of the tank container on a flat wagon considering fittings displacement relating to the stops. MATEC Web of Conferences, 234, 05002. doi: https://doi.org/10.1051/matecconf/201823405002

[13] Kir'yanov, D. V. (2012). Mathcad 15 / Mathcad Prime 1.0. Sankt-Peterburg: BHV-Peterburg, 432.

[14] Makovkin, G. A., Lihacheva, S. Yu. (2012). Primenenie MKE k resheniyu zadach mekhaniki deformiruemogo tverdogo tela. Ch. 1. Nizhniy Novgorod: Izd-vo NNGASU, 71.

[15] Sokolov, S. A. (2011). Stroitel'naya mekhanika i metallicheskie konstrukcii mashin. Sankt-Peterburg: Politekhnika, 422.

[16] Alyamovskiy, A. A. (2015). SolidWorks Simulation. Inzhenerniy analiz dlya professionalov: zadachi, metody, rekomendacii. Moscow: DMK Press, 562.

[17] Alyamovskiy, A. A. (2010). COSMOSWorks. Osnovy rascheta konstrukciy na prochnost' v srede SolidWorks. Moscow: DMK Press, 784.

[18] DSTU 7598:2014. Vahony vantazhni. Zahalni vymohy do rozrakhunkiv ta proektuvannia novykh i modernizovanykh vahoniv koliyi 1520 mm (nesamokhidnykh) (2015). Derzhavnyi Standart Ukrainy, 162.

[19] GOST 33211-2014. Vagony gruzovye. Trebovaniya k prochnosti i dinamicheskim kachestvam (2016). Moscow: Standartinform, 54.

[20] DIN EN 12663-2-2010. Railway applications – Structural requirements of railway vehicle bodies – Part 2: Freight wagons (2010). BSI, 54.

[21] Matalyckiy, M. A., Hackevich, G. A. (2017). Teoriya veroyatnostey i matematicheskaya statistika. Minsk: Vysheyshaya shkola, 591.

[22] Ivchenko, G. I., Medvedev, Yu. I. (2014). Matematicheskaya statistika. Moscow: Knizhnyy dom "LIBROKOM", 352.

[23] Rudenko, V. M. (2012). Matematychna statystyka. Kyiv: Tsentr uchbovoi literatury, 304.